FINAL TECHNICAL REPORT

Award Number G16AP00128 (University of Rhode Island)
and
Award Number G16AP00127 (Columbia University)

NEAR-SHORE EVALUATION OF HOLOCENE FAULTING AND GEOHAZARD IN THE NEW YORK CITY METROPOLITAN REGION: COLLABORATIVE RESEARCH WITH UNIVERSITY OF RHODE ISLAND AND COLUMBIA UNIVERSITY

Marie-Helene Cormier
University of Rhode Island
Graduate School of Oceanography
215 South Ferry Road
Narragansett, RI 02882
Ph.: (401) 874-6494; Fax: (401) 874-6811
E-mail: mhcormier@uri.edu

John W. King
University of Rhode Island
Graduate School of Oceanography
215 South Ferry Road
Narragansett, RI 02882
Ph.: (401) 874-6182; Fax: (401) 874-6811
E-mail: jwking@uri.edu

Leonardo Seeber
Columbia University
Lamont-Doherty Earth Observatory
61 Route 9W
Palisades, NY 10964
Ph.: (845) 365-8385; Fax: (845) 365-8150
E-mail: nano@ldeo.columbia.edu

Term covered by these awards: May 1, 2016 to April 30, 2017

TABLE OF CONTENTS

ABSTRACT

During its relatively short historic period, the Atlantic Seaboard of North America has experienced one M7+ earthquake near Charleston SC in 1886, as well as a M6+ in 1755 north of Boston. This raises the specter of a similar earthquake anywhere along the eastern seaboard. The horrific scenario of a M7+ earthquake centered under a large metropolitan area, such as New York City (NYC), counterbalances the low probability of such an event. Cost-effective reduction of the risk relies on assessing this probability.

Several faults within metropolitan NYC, such as the Dobbs Ferry fault in Westchester and the 125th Street fault in Manhattan, strike NW, at high angle to the Appalachian trend. These structures display small accumulated displacement, and are characterized by anastomosing brittle fractures. All earthquake sequences with well-established fault sources in the New York City seismic zone, including ones along the NE-striking Ramapo border fault of the Newark Basin, originate from NW-striking faults. *Sykes et al*. [2008] propose a 670-year recurrence time for earthquakes M≥6.0 in the NYC seismic zone. These earthquakes are likely to originate in the shallow crust, given the shallow depth range of well-constrained hypocenters in this zone. Surface ruptures have been prevalent for M>6 earthquakes in similar stable continental region (SCR). Maximum potential magnitudes can be inferred from both the length of seismogenic faults and from worldwide statistics on maximum magnitudes in a given SCR settings. Several lines of evidence for metropolitan New York point to a maximum magnitude in the M7 range. Accordingly, the likelihood of a post-glacial surface rupture in the NYC seismic zone seems high.

This project investigated the geologic record of neotectonic activities offshore New York metropolitan area. On July 19 and 20, 2016, we collected 101 km of high-resolution seismic reflection (CHIRP) profiles along the north shore of western Long Island Sound to determine whether sedimentary strata deposited since the Last Glacial Maximum are offset or deformed by past large earthquakes. The offshore survey area is characterized by a smooth 15.5 kyr-old erosional surface and overlying younger strata on which it is expected that fault or fold-related vertical relief as small as 0.5 m can be resolved. No sediment cover on the land portion of the metropolitan area offers such ideal reference surfaces, widespread in both time and space. Seismic profiles were acquired mostly perpendicular to the NW faults mapped on land, with tracks spaced about 200 m apart, in order to test the lateral continuity of possible structural features and to map them. The use of a small, maneuverable boat allowed us to survey in water as shallow as ~4 m. For the interpretation, we benefited from the comparison of our data with approximately co-located single-channel seismic profiles collected by the USGS in 1985 [*Poppe et al., 2002*].

Preliminary interpretation of the collected data did not reveal detectable stratigraphic offsets in the post-glacial sediments with lateral continuity from track to track. If this result is further confirmed by the still on-going analysis, then it will prove a reliable negative result with implications regarding the lateral dimensions and southeastward continuity of the brittle faults in metropolitan New York and/or for their capability of large earthquakes with surface ruptures. All data and results are now being contributed through the Long Island Sound Resource Center (http://www.lisrc.uconn.edu) hosted at University of Connecticut, as well as through the Marine Geoscience Data System (MGDS) hosted at the Lamont-Doherty Earth Observatory (http://www.marine-geo.org). Further results, especially those pertaining to the evolution of glacial Lake Connecticut, will be published in a peer-reviewed journal.

1. INTRODUCTION: SEISMIC HAZARDS IN NEW YORK CITY METROPOLITAN AREA

As in other Stable Continental Regions (SCRs), the estimation of earthquake hazard in the New York City (NYC) metropolitan area is subject to large uncertainties derived primarily from the subjective interpretation of the source zones (Petersen et al., 2008). In tectonically active regions, seismicity can be characterized by several independent measurements, such as geodetic strain, geologic fault-slip rates, prehistoric surface fault ruptures, and historic seismicity. Reasonable convergence between these independent measurements leads to hazard assessments with relatively small and credible uncertainties. In contrast, tectonic rates in SCRs are generally undetectable both geologically and geodetically. SCR seismicity is lower than at typical plate boundaries, but it is nonetheless significant and includes many destructive earthquakes worldwide. Thus, despite the lack of immediately obvious active geologic structures and of measurable deformation, earthquake hazard in SCR can be significant and the risk can be quite high in metropolitan areas with aging building stocks and infrastructures that predate earthquake codes. During its relatively short historic period, the Atlantic Seaboard of North America has experienced a M7+ earthquake near Charleston SC in 1886. No obvious tectonic feature distinguishes that area and a conservative prognosis must consider similar earthquakes possible anywhere along the Atlantic Seaboard. This conclusion is consistent with worldwide studies of passive continental margins [*Johnston et al., 1994*]. This project aims to test this hypothesis from the geologic record in the NYC metropolitan area. The scenario of a M7+ earthquake centered under an unprepared major metropolitan area is a horrific low-probability event. How low a probability, however, is yet poorly determined, though it is critical in risk reduction investments. NYC has wisely adopted a seismic building code for ground motion, despite having experienced only minor damage from historic earthquakes [*Nordenson and Bell, 2000; Tantala et al., 2008*]. Better information about past earthquakes is the most reliable way to constrain the probability of an earthquake disaster and thus either refine or bring about risk-reduction measures.

Lack of data is often given as the reason for large uncertainties on hazard from SCR earthquakes. Even more consequential may be lack of a credible model to account for the data we do have. So, for example, the greater NYC metropolitan area roughly correlates with a seismic zone (NYCSZ), one of several concentrations of earthquake activity that stand out in the field of epicenters over eastern North America [*Seeber 2009*]. This concentration of earthquakes is significant (Sykes et al., 2008) and leads to a higher level of hazard than other areas of the eastern North America in the USGS hazard maps [*Frankel et al., 2005; Petersen et al., 2008*]. These maps are based on the assumption that the NYCSZ is a stable feature of the seismicity. Conversely, however, this regional cluster could be an aftershock sequence, similar to the long-lasting seismicity following the 1811-12 earthquakes in the mid-continent [*Stein et al., 2009*]. Compounding the lack of statistically robust data on the temporal distribution of seismicity [*Seeber and Armbruster, 1991*] is the difficulty of associating SCR earthquakes with specific faults, which has largely prevented the inclusion of geologic data in hazard analysis. This difficulty has been generally ascribed to the tendency of SCR earthquakes, even large and damaging ones, to occur on secondary faults with little accumulated displacement [*Seeber et al., 1998*]. This tendency, in turn leads to the suggestion that SCR seismogenesis stems from many faults, each contributing earthquakes only rarely [*Fenton et al., 2006*].

Although only moderate seismic hazards are estimated for the NYC area [*Petersen et al., 2014*], some of our current understanding of the relationship between Stable Continental Region earthquakes and faults stem from that area. The 1985 M4.0 Ardsley earthquake (Fig. 1) was associated with the Dobbs Ferry "fracture zone" (Hall, 1981). The term "fracture zone" was upgraded to "fault" after the earthquake [*Seeber & Armbruster, 1989*]. This fault trends NW (Fig. 2) across the dominant NE-striking Paleozoic collision structures and subsequent Mesozoic extensional structures of the Appalachians and Atlantic Seaboard [e.g., *Ratcliffe et al., 1986, Hutchinson et al., 1986; Klitgord et al. 1988*]. It was mapped for about 10 km across most of the "Manhattan Prong", the area bounded by the Hudson River and Long Island Sound [*Seeber & Dawers, 1989; Dawers & Seeber, 1991*]. The fault extends southeastward to the Cameron's Line (Fig. 2), a NW-verging suture thrust fault that formed around 450 Ma during the Taconic orogeny. The Dobbs ferry fault may continue further SE, but lack of outcrop in this urbanized area has prevented further mapping. Total accumulated displacement on the Dobbs Ferry fault is < 10m; furthermore it is right-lateral, opposite from the left-lateral displacement in the 1985 earthquake (Fig. 1). The right-lateral displacement is consistent with this and other NW-striking faults dating back to the Mesozoic rifting phase characterized with ~E-W extension. They have been re-activated in the current SCR regime where the maximum horizontal compressive stress axis is ~E-W [*Dawers & Seeber, 1991*].

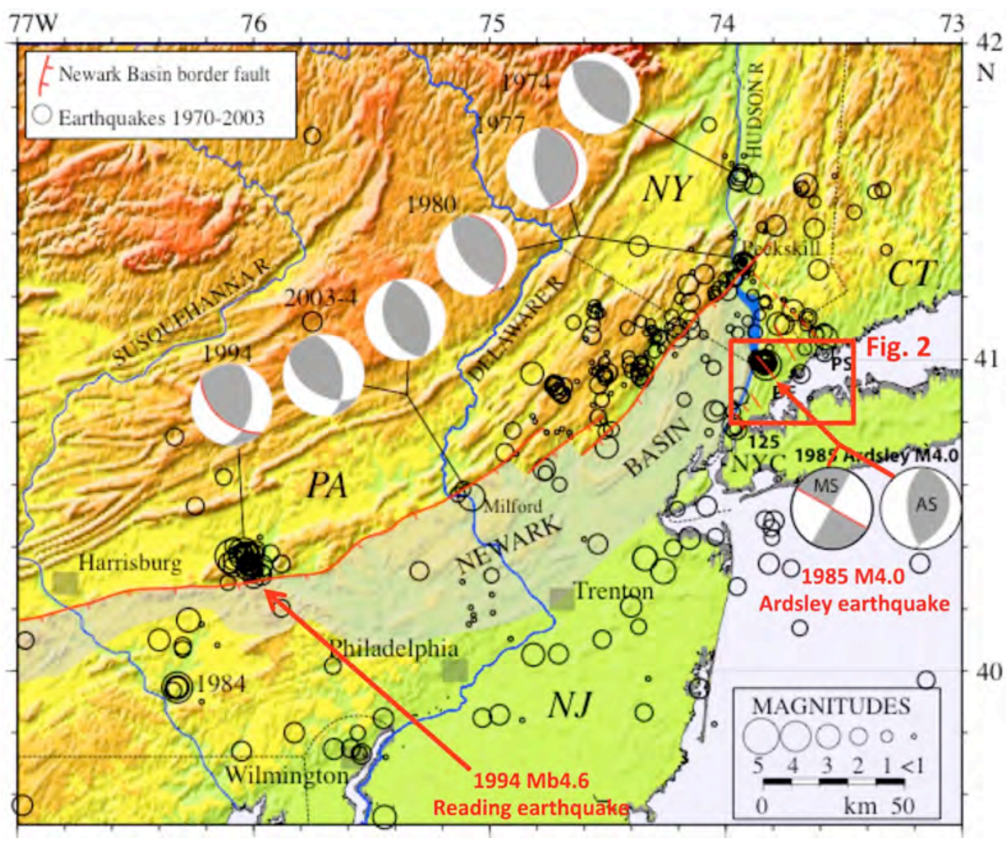

Figure 1. Topography (illumination from the NW) and seismicity detected by a seismic network operated in the greater New York City area by the Lamont-Doherty Earth Observatory since 1970. The < 2.5 km deep 1994 Mb4.6 Cacoosing Valley (Reading) PA earthquake was the largest during that period. A prominent zone of seismicity is spatially associated with the border fault of the Mesozoic Newark basin (gray shading). All known seismogenic faults in this zone, however, strike NW, at high angle to the border fault and to the main structures of the Appalachians, which are highlighted by topography. Focal mechanisms are in lower hemisphere projections.

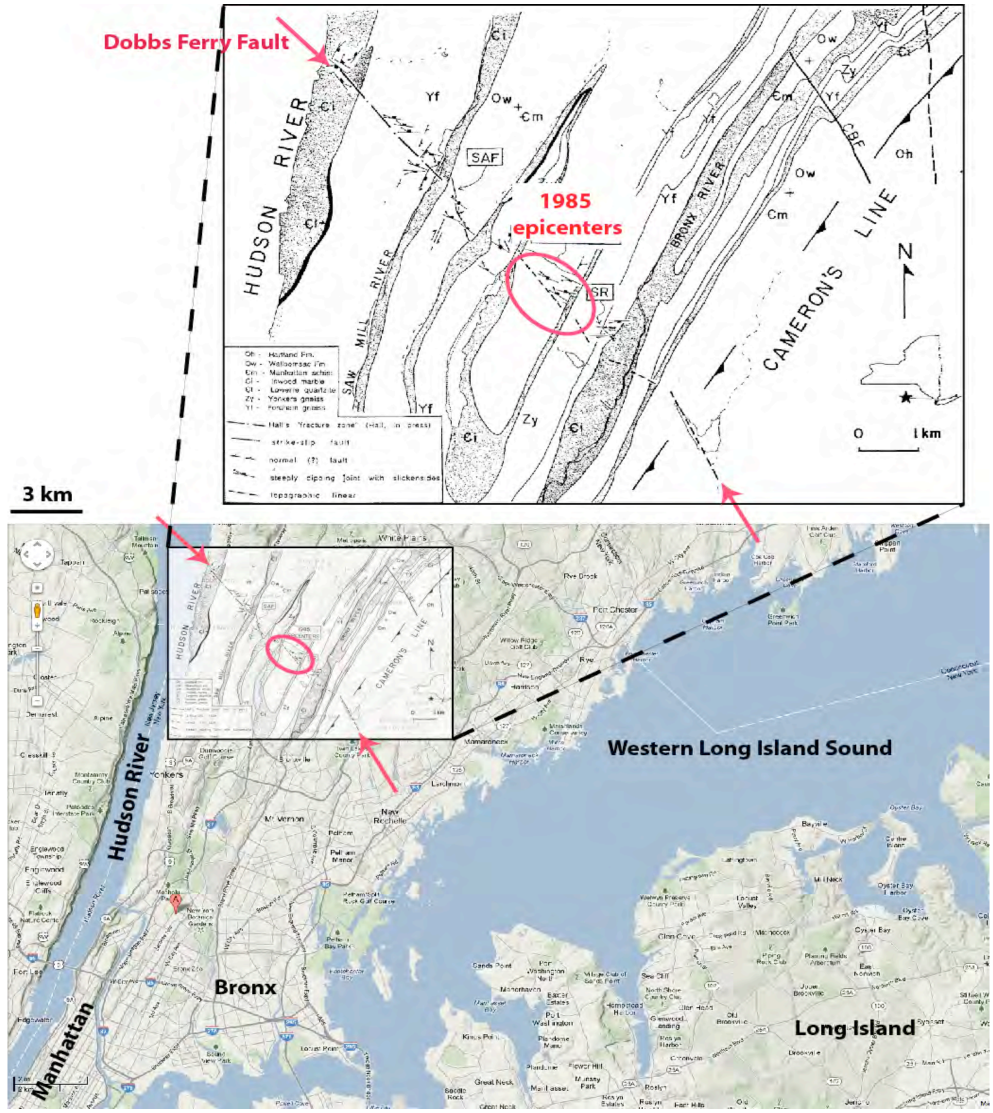

Figure 2. Field mapping of the Dobbs Ferry Fault [*Seeber and Dawers, 1989*] (top) is overlain on a map of the Manhattan Prong (bottom), part of New York metropolitan area. Red arrows point to the NW-striking Dobbs Ferry Fault, and red oval locates the epicenter of the 1985 Ardsley earthquake sequence (Mb = 4.0).

Several other faults across the Manhattan Prong, such as the 125th Street fault in Manhattan (located in Fig. 6), resemble the Dobbs Ferry fault in strike, in having a small accumulated displacement, and in their structural signature characterized by anastomosing brittle fractures and small faults. They are considered a distinct fault set developed in the Mesozoic rifting event (Hall, 1981) and reactivated in the current SCR regime (e.g., Sykes et al., 2008). This pattern is not unique to the Manhattan Prong. All earthquakes with well-established focal mechanisms in the NYC seismic zone, including ones occurring close to the NE-striking Ramapo border fault of the Newark Basin (Ratcliffe et al., 1986; Sykes et al., 2008), originate from small-displacement and thus previously unrecognized NW-striking faults (Seeber et al., 1998). These and other examples worldwide demonstrate that seismotectonics in SCR and along plate boundaries differ fundamentally. This project addresses both the general problem of understanding the role of preexisting faults in SCR seismogenesis as well as specifically the earthquake hazard in the NYC seismic zone.

2. POTENTIAL FOR A LATE QUATERNARY SURFACE RUPTURE IN NYC METROPOLITAN AREA

Historic earthquakes are the main source of information about future SCR seismicity, with the assumption that the rate and magnitude distribution of earthquakes during the historic period are representative of the longer-term seismicity [e.g., *Seeber and Armbruster, 1991*]. *Sykes et al.* [2008] propose a recurrence time of 670 years for earthquakes M≥6.0 in the NYC seismic zone. These earthquakes are likely to originate in the shallow crust, given the shallow depth range of well-constrained hypocenters in this zone [*Klose and Seeber, 2007*]. Based on worldwide data, such SCR earthquakes are likely to rupture the surface [*Coppersmith and Young, 2000*]. Maximum magnitudes can be inferred from both the length of seismogenic faults and from worldwide statistics on maximum magnitudes in a given SCR settings. The rifted margin environment of the NYC seismic zone point to a maximum magnitude in the M7 range [e.g., *Johnston et al., 1994*]. A complete rupture of the 10 km-long Dobbs Ferry fault, as currently mapped, would produce a M>6 earthquake and possibly as large as a M7 if it continues SE below Long Island Sound. Accordingly, the likelihood of a surface rupture in the NYC seismic zone during the post-glacial period seems high. Within this zone, the system of NW-striking brittle faults across the Manhattan Prong (Figs. 1 and 2) is the only one clearly associated with recent instrumental seismicity and is thought to be responsible for the larger historic earthquakes [*Sykes et al., 2008*]. Arguably, it is also the most likely to rupture the surface during the post-glacial period.

The melting of the Laurentide ice sheet from the NYC area between 18-14 ka may also be a contributing factor to seismic hazards. Just as the load of existing continental ice sheets is thought to be responsible for the relatively low seismicity associated with them [e.g., *Johnston, 1989*], the rapid ice unloading of northern America at the end of the Last Glacial period may have triggered a burst of seismicity [e.g., *Stein and Mazzotti, 2007*]. Long Island Sound, located between the large terminal moraines on Long Island and the retreating ice sheet, may have experienced a particularly high transient of differential vertical stresses, possibly raising the probability of large earthquakes and surface ruptures at the end of the Pleistocene. Since then, continuing isostatic rebound and coseismic stress changes may combine to generate further earthquakes on closely spaced faults and cause seismicity to migrate about the region, possibly activating yet-unruptured segments [e.g., *Calais et al., 2010*].

3. RATIONALE FOR AN OFFSHORE SURVEY IN WESTERN LONG ISLAND SOUND

High-resolution subbottom profilers (CHIRP sonars) are now routinely used offshore to image the shallow subsurface with a sub-meter resolution (Fig. 3). CHIRP sonars have a proven record for detection of subtle fault offsets in shallow coastal areas [e.g., *Polonia et al., 2004; Cormier et al., 2006*]. One of the main advantages of conducting an offshore survey for neotectonic activity is that marine sedimentation is generally more continuous in time compared to onshore settings, which are commonly characterized by deposition hiatuses. Marine sedimentation is also more continuous in space, allowing for regional stratigraphic correlations of the Holocene record, another clear advantage for assessment of the spatial extent of ruptures produced by large earthquakes. Lastly, offshore surveys are not impeded by obstacles such as buildings, roads, fences, and dense vegetation, and are acquired more quickly than trenching and field mapping on land. While CHIRP sonars have lower vertical resolution than field outcrops (nominally, 10-20 cm, versus 1-2 cm at field outcrop scale), they quickly image greater horizontal and vertical extents. In fact, CHIRP sonars are typically capable of imaging the entire Holocene and Late Pleistocene sedimentary sequences (Fig. 3), penetrating the upper 5-20 m of the seafloor, an advantage over the limited few meters visible in a typical land outcrop.

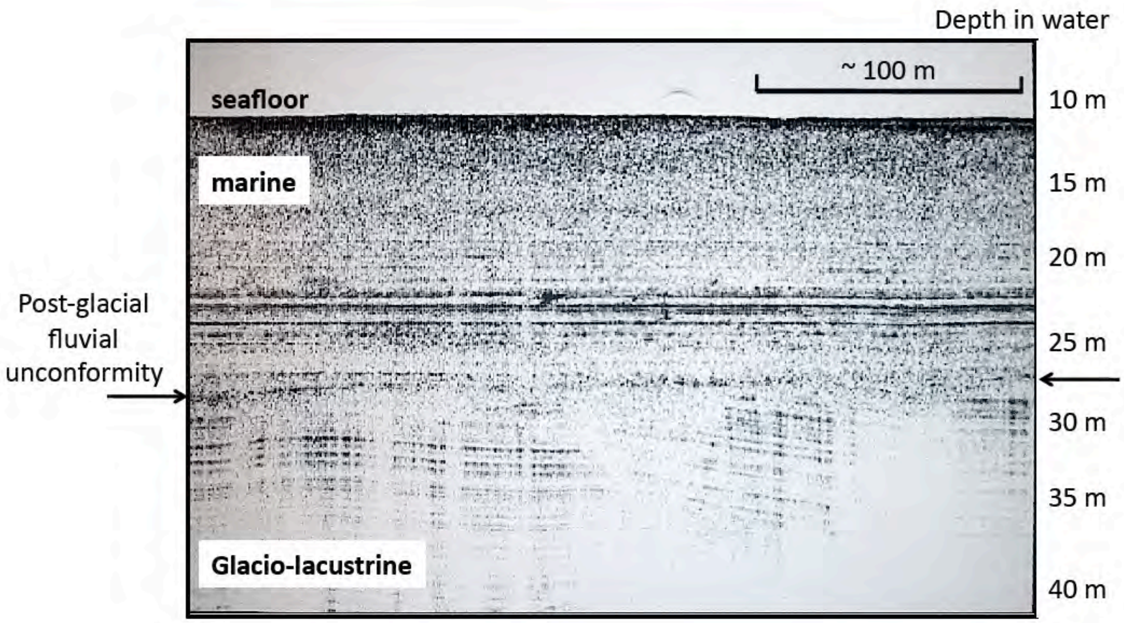

Figure 3. Section of a CHIRP profile acquired in western Long Island Sound on the occasion of an education cruise [*McHugh et al., 2006; Vargas et al., 2007*]. Note how the 15.5 ka post-glacial unconformity is clearly traceable below the sea floor multiple.

Earthquakes in the NYC seismic zone and generally in SCR tend to originate in the shallow upper 5-10 km of the crust [*Klose and Seeber, 2007*]. In these settings, large earthquakes (Mw 6 or higher) are expected to produce some surface ruptures. Given the sub-millennial recurrence time for such earthquakes in the NYC seismic zone [*Sykes et al., 2008*] the probability that a surface rupture would disrupt the sedimentary post-glacial strata of western Long Island Sound is significant. Any fault scarps larger than 50 cm should be clearly imaged in the chirp records. Furthermore, because sedimentation rates in western Long Island Sound have been relatively high since the ice sheet retreated [e.g., *Kim and Bokuniewicz, 1991*], sufficient stratigraphic separation would be expected between different earthquake event horizons if more than one large earthquake did occur in New York metropolitan area during the Holocene. Lastly, large earthquakes may also result in the liquefaction of the shallow strata, an effect that might be detected in chirp profiles as a generally lumpy horizon affected by vertical “pipes” or dikes [e.g., *Cormier et al., 2006*].

4. LATE QUATERNARY STRATIGRAPHY OF LONG ISLAND SOUND

Late Quaternary stratigraphy in Long Island Sound is well constrained by a combination of seismic surveys and core samples [Bertoni et al., 1977; Lewis et al., 1991; Lewis and DiGiacomo-Cohen, 2000; Poppe et al., 2002; 2000a; 2000b]. Lake clay varved sedments were deposited at the bottom of glacial Lake Connecticut as the Laurentide ice sheet retreated. Coalescing delta deposits formed along the northern edge of Lake Connecticut, located south of what is today the Connecticut shore. The lakebed was eventually exposed around 15 ka [*Stone et al., 1986*], when Lake Connecticut drained out via a breach in the terminal moraine that formed its southeastern boundary. Within 500 years, a well-established fluvial drainage system had cut channels through the glacial lake bottom sediment, carrying glacial melt water through the LIS basin and out to sea [*Lewis and DiGiacomo-Cohen, 2000*]. Rising sea level resulted in a marine incursion that first flooded the fluvial system and eventually the entire exposed lakebed. As the sea transgressed westward, wave action further eroded the lakebed surface, producing a ravinement surface [*Lewis and DiGiacomo-Cohen, 2000*]. By 13.5 ka marine deltaic sediment was being deposited on the ravinement surface unconformity and since this time coastal erosion and tidal currents have continuously redistributed sediment within the LIS basin [*Lewis and DiGiacomo-Cohen, 2000*].

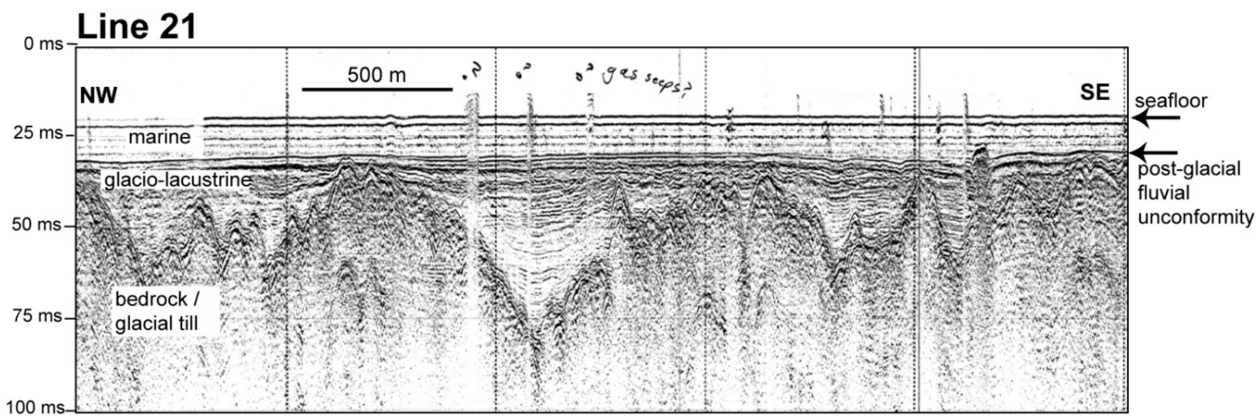

Figure 4. Section of USGS boomer seismic profile A85-821 [*Poppe et al., 2002*], illustrating the main stratigraphic sequences within the study area. A two-way travel-time of 25 ms in sediment corresponds to approximately 25 m in depth. This profile is located in Figure 6. Note how the 15.5 ka post-glacial fluvial unconformity is clearly traceable.

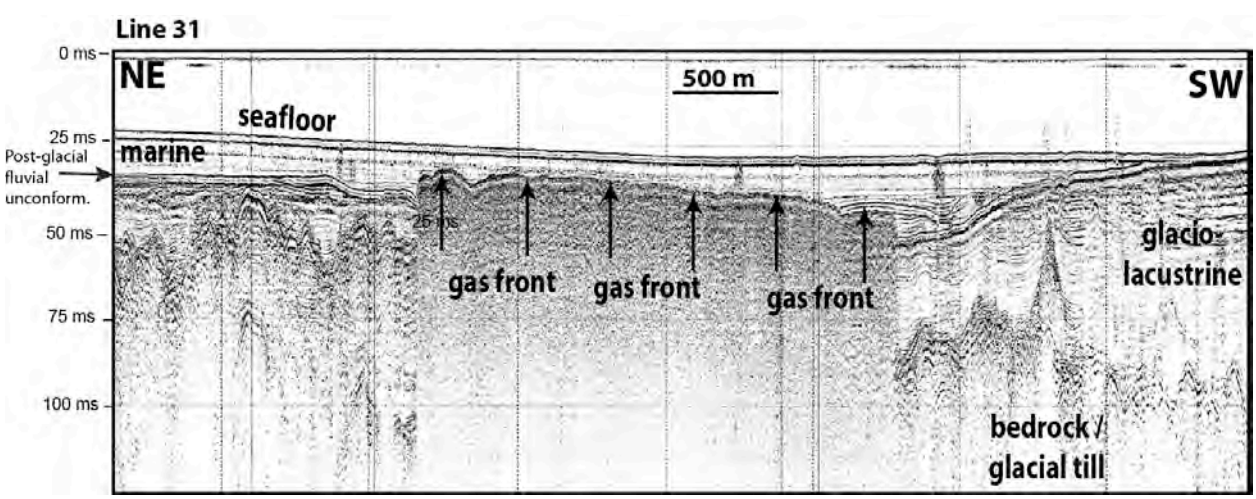

Figure 5. Section of USGS boomer seismic profile A85-831 [*Poppe et al., 2002*] showing a prominent gas-front limited to the deeper, central portion of Long Island Sound. This profile is located in Figure 6.

The glacial lake clay deposits that formed on the Lake Connecticut bottom overlie crystalline bedrock, coastal plain sediment, undifferentiated drift, terminal moraine deposits and lacustrine fan deposits. They are characterized by finely laminated, alternating layers of silt and clay that produce parallel internal reflections in seismic reflection profiles (Figs. 4, 5, and 6) [*Bertoni et al 1977*]. These glacio-lacustrine varved clay deposits drape underlying topography and are commonly 80m thick, and locally >150 m thick in the deep channels west of the Connecticut River [*Lewis and DiGiacomo-Cohen, 2000*]. In the western half of Long Island Sound, separated from the glacio-lacustrine deposits by the unconformity created by marine transgression, are the overlying fine- to coarse-grained marine sediments, including marine deltaic deposits along much of the northern margin [*Lewis and DiGiacomo-Cohen, 2000*]. In the eastern Long Island Sound basin where tidal currents are much stronger, tidal scour has cut through the ravinement surface and redistribution of both glacio-lacustrine and marine sediments has been extensive [*Poppe et al., 2008*]. These late Pleistocene to Holocene stratigraphic sequences are clearly imaged in seismic profiles (both CHIRP and USGS boomer profiles), providing useful markers to date potential neotectonic deformation (Figs. 3, 4, and 5).

5. DATA ACQUISITION

On June 19 and 20, 2016, we collected 101 km of high-resolution subbotom seismic (CHIRP) profiles along the north shore of western Long Island Sound to investigate whether sediments deposited since 15 ka are offset by faulting. The specific goal was to image the relatively smooth unconformity surface that developed after glacial Lake Connecticut drained at ~15.5 ka and the flat-lying marine sequences that started to accumulate between 15 – 9 ka, following the marine transgression of the exposed lakebed [*Lewis and DiGiacomo-Cohen, 2000*]. That unconformity (Figs. 4 and 5) is recognizable in the USGS seismic reflection profiles acquired in Long Island Sound [*Poppe et al., 2002*]. It was equally well imaged in CHIRP sonar profiles acquired in 2006 (Fig. 3) as part of a short educational cruise that embarked 12 students from City University of New York and introduced them to marine geoscience [*McHugh et al., 2006; Vargas et al., 2007*].

5.1 Survey strategy

Field work and seismicity in Metropolitan New York suggest that seismically active faults strike NW (Figs. 1 and 2) [*Seeber & Dawers, 1989; Merguerian, 2004; Sykes et al., 2008*]. While only the Dobbs Ferry fault ruptured recently, other mapped or unmapped NW-striking faults may rupture next. We thus acquired seismic profiles oriented perpendicular to that fault trend, that is, roughly parallel to the north shore of western Long Island Sound (Fig. 6). Our careful analysis of seismic profiles acquired in 1985 by the USGS [*Poppe et al., 2002*] reveals the localized presence of gas-charged sediments that obscure the underlying stratigraphy (Figs. 4 and 5). However, these zones of gassy sediments are clearly limited to the deeper, central part of the sound, as outlined by the yellow segments in Fig. 6. Therefore, the survey tracks have been positioned to hug the shore of the Manhattan Prong, confined to the north by the 4 m bathymetric contour and to the south by the swath of gas-charged sediments. That area is about 1.5-2 km wide and 15 km long. With profiles spaced 200 m apart and encompassing a 1.5-2 km-wide corridor, and with the addition of a few tie lines, we achieved the acquisition of a pseudo 3D seismic dataset (Figs. 7, 8, and 9). In particular, any potential stratigraphic offset resulting from the sea-floor rupture of a NW-striking fault should be traceable from profile to profile, highlighting the strike of the fault. In contrast, stratigraphic offsets that may be produced by erosional scarps, pockmarks, or other non-tectonic features are unlikely to align linearly, and/or to extend further than a few 100 m.

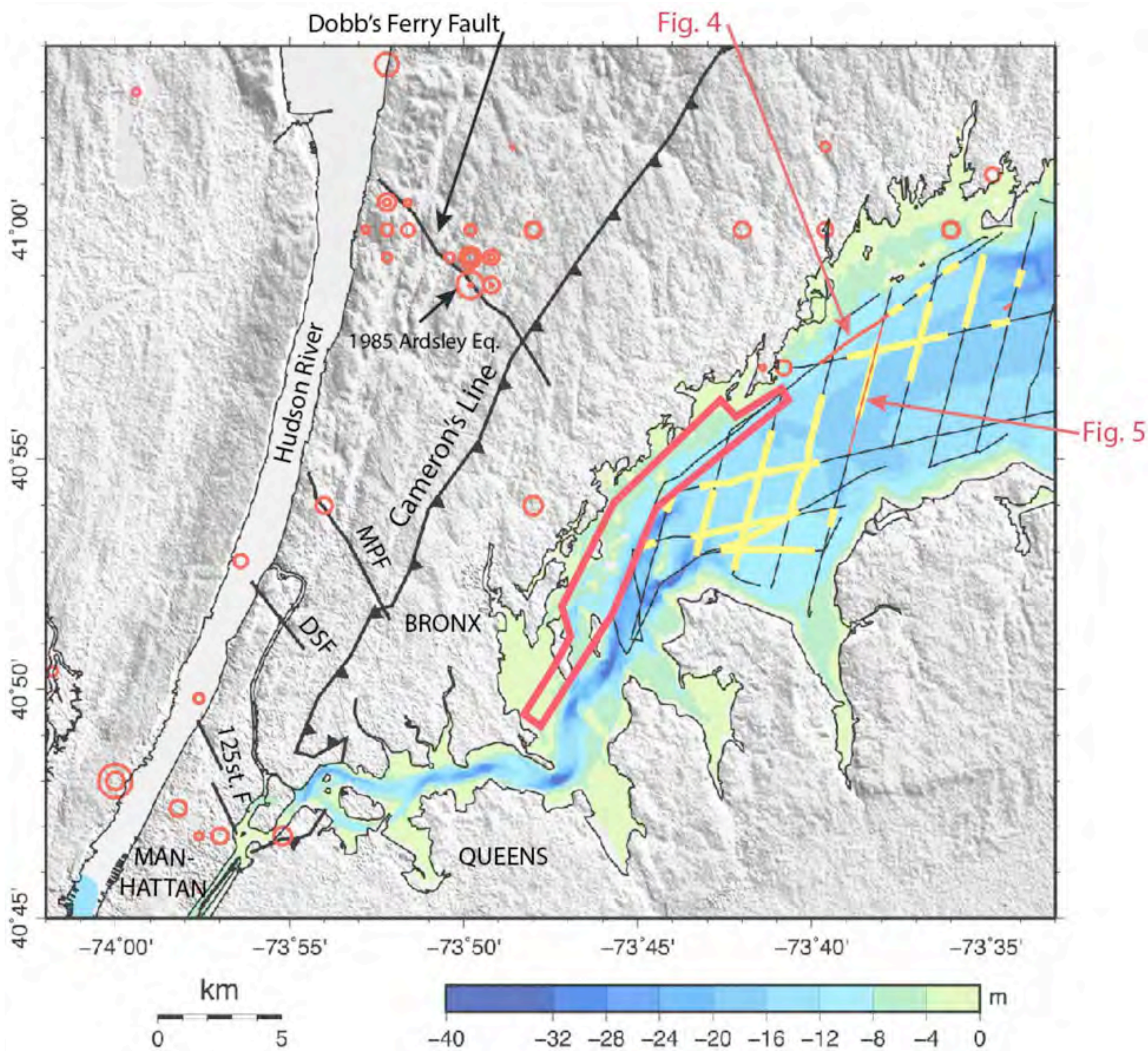

Figure 6. Bathymetry of western Long Island Sound, gridded from NOAA point data, and land topography (gray shades, SRTM). Red circles indicate the locations of known earthquakes [*Sykes et al., 2008*]. Earthquake locations are within +/- 1-2 km; size of circle is proportional to earthquake magnitude. Several known NW-striking faults are indicated: MPF: Mosholu Parkway Fault; DSF: Dickman Street Fault; 125st F: 125th Street fault. Fine black lines indicate the survey tracks of the 1985 USGS seismic reflection survey [*Poppe et al., 2002*]. The two red segments highlight the portions of profiles displayed in Figs. 4 and 5. Yellow segments highlight the portions of these seismic profiles for which a gas front is obscuring underlying reflectors. The red polygon delineates the survey area, which is designed to avoid areas of gas-charged sediments, as well as the deep navigation channel where the 1985 seismic survey showed no penetration.

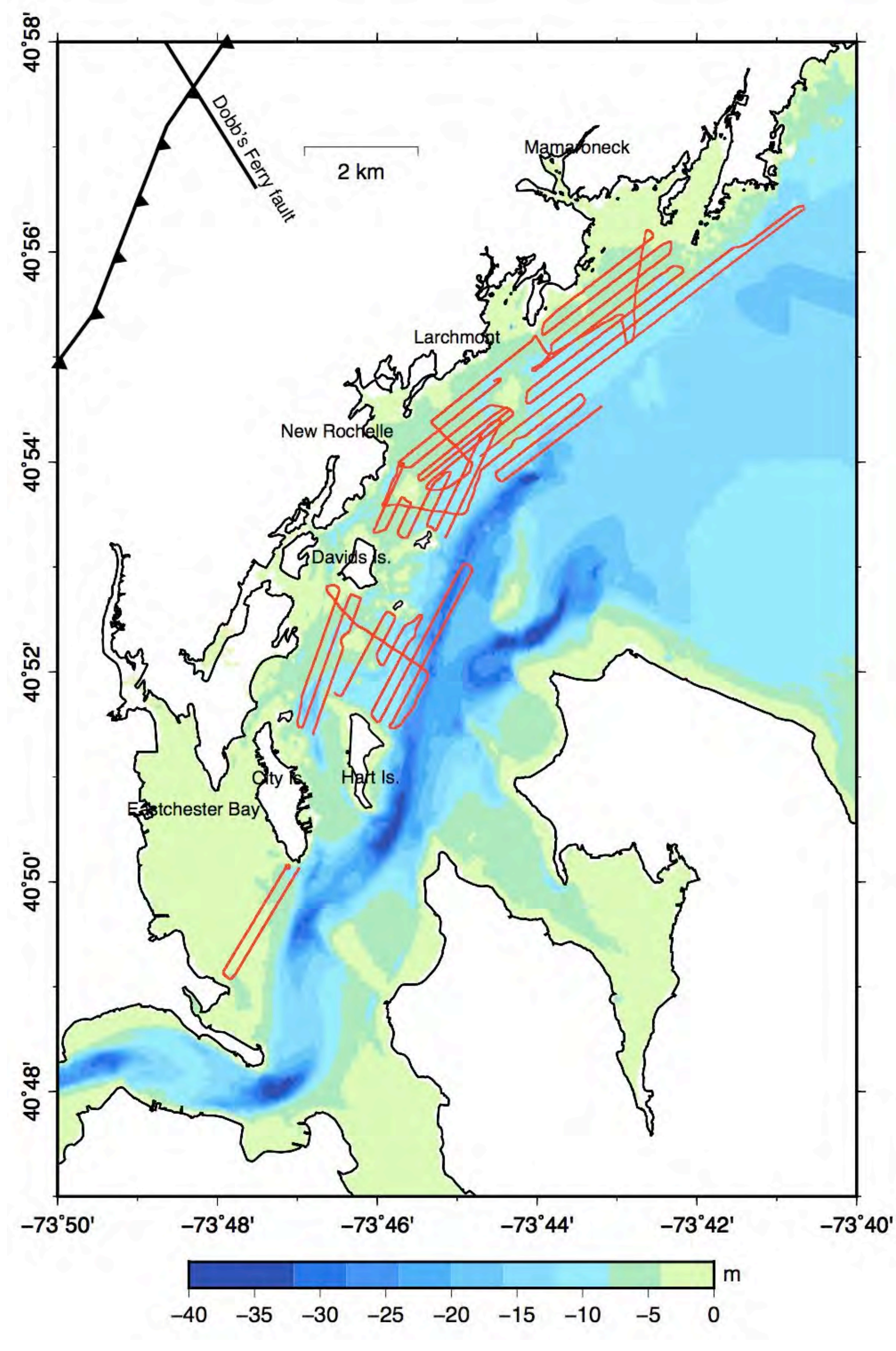

Figure 7. CHIRP tracks collected on June 19 and 20, 2016 with the R/*V SHANNA ROSE* (red lines). Tracks are spaced 200 m apart, except in two locations where they are spaced 100 m apart.

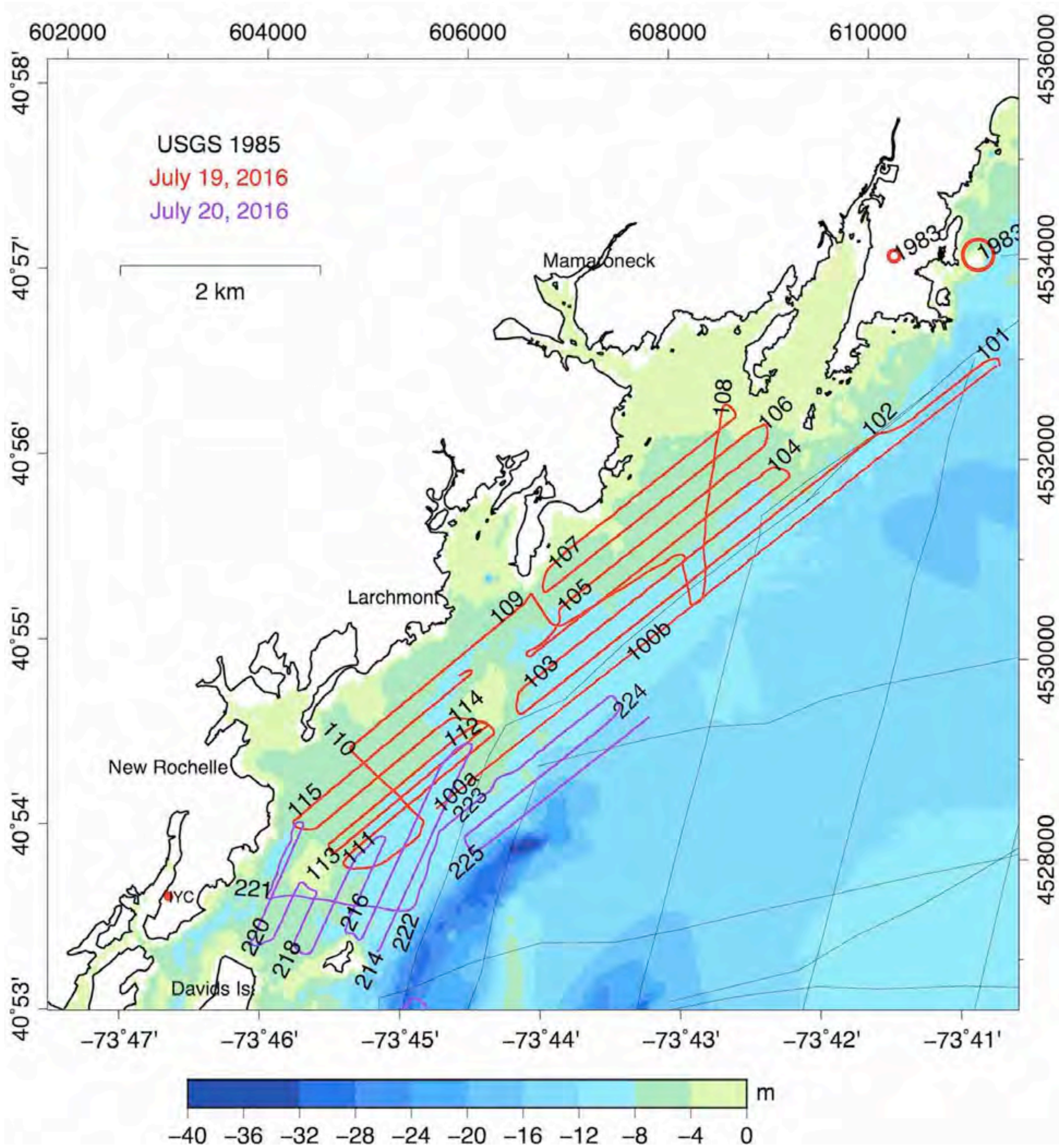

Figure 8. CHIRP profiles collected in the northern section of the survey area. Profile numbers are indicated at their beginning. Profiles acquired on July 19 (red lines) are labeled 100a, 100b, 101 etc. Profiles acquired on July 20 (purple lines) are labeled 200, 201, etc. The faint black lines indicate the single channel seismic profiles acquired by USGS in 1985 [*Poppe et al., 2002*]. Red dot labeled IYC indicates the docking area (Imperial Yacht Club). Top and right axes are labeled in meters, UTM zone 18.

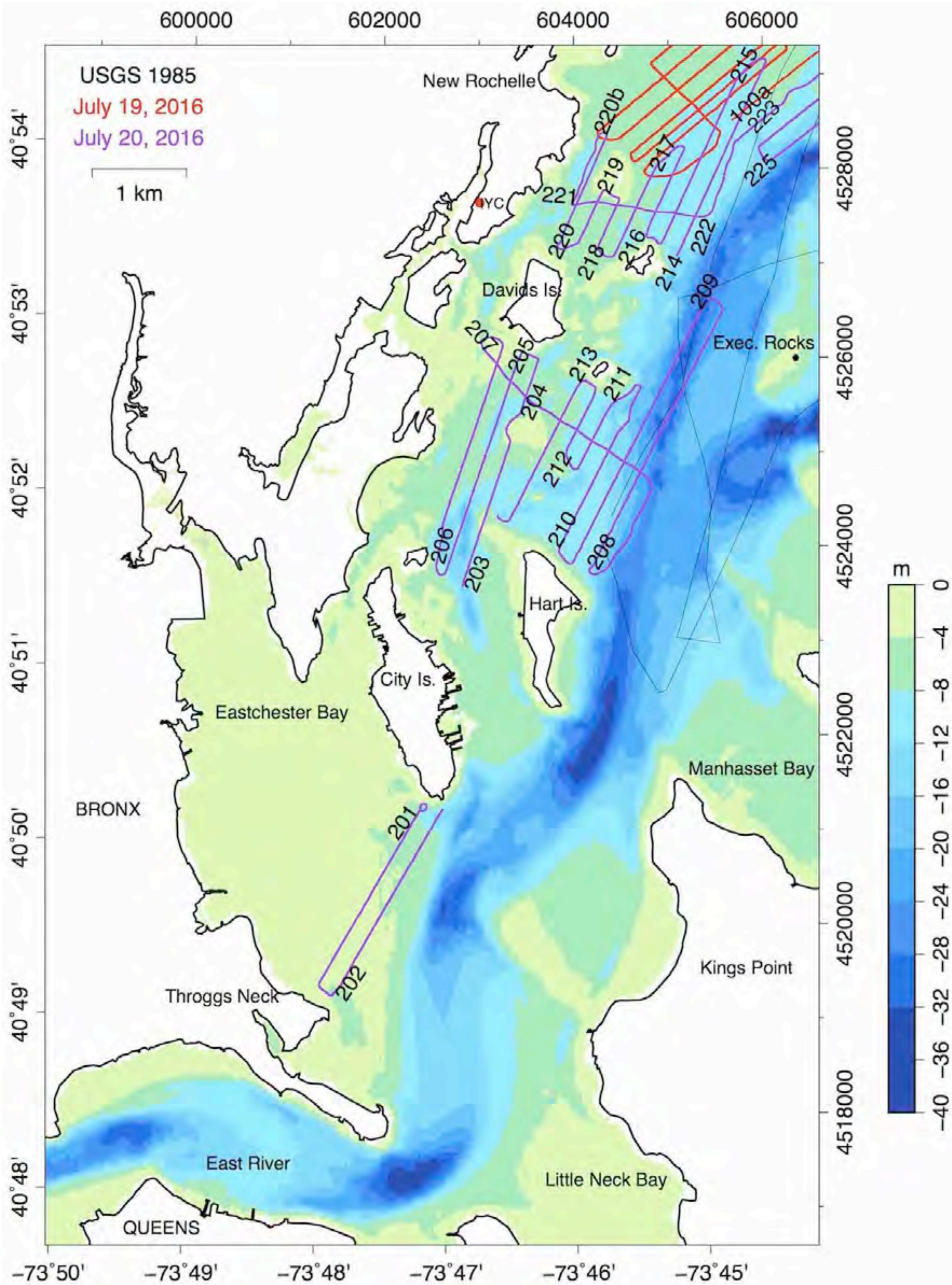

Figure 9. CHIRP profiles collected in the southern section of the survey area. Profile numbers are indicated at their beginning. Profiles acquired on July 19 (red lines) are labeled 100a, 100b, 101 etc. Profiles acquired on July 20 (purple lines) are labeled 200, 201, etc. The faint black lines indicate the single channel seismic profiles acquired by USGS in 1985 [*Poppe et al., 2002*]. Red dot labeled IYC indicates the docking area (Imperial Yacht Club). Top and right axes are labeled in meters, UTM zone 18.

5.2 Survey boat

The boat used for the survey, the *R/V SHANNA ROSE,* is a 42’ Wesmac boat operated by the URI Bay Campus. It is routinely used for geophysical survey offshore Rhode Island and in Long Island Sound (Fig. 10). The 15’ A-frame makes it easy to deploy gear over the stern, and the deckhouse is roomy enough to accommodate all the geophysical electronics and laptops. Overall, the size of that boat makes it relatively inexpensive to operate as well as maneuverable in shallow water, and yet comfortable enough for long daytime operations. A survey speed of 3.7 to 4 knots was maintained during survey to ensure optimum data quality. The boat docked overnight at the nearby Imperial Yacht Club in New Rochelle.

Figure 10. (left) The *R/V SHANNA ROSE* at dock. (top) Acquisition setup inside the deckhouse.

5.3 Positioning

The GPS antenna was mounted 8.42 m forward of the stern of the boat. Output from that antenna was logged in the headers of the CHIRP data and was also fed to the *Hypack* navigation software. All GPS positions are referenced to the customary WGS-84 datum and referred to GMT time. Nautical charts of western Long Island Sound helped with the planning of the survey tracks and provided the background for the *Hypack* navigation software during the survey. In particular, for safety of the towed equipment, survey tracks were designed to remain above the 4 m water depth contour. A laptop displaying the *Hypack* navigation window allowed the pilot to follow the pre-programmed survey tracks, adjusting when needed for unforeseen obstacles such as lobster pots, as well as for ship traffic.

5.4 CHIRP subbottom profiler

The URI’s subbottom profiler used for this project is a *Teledyne-Benthos CHIRP III* that operates in the 2 kHz to 7 kHz band. This relatively low frequency range for a CHIRP sonar was critical to obtain a deeper penetration below seafloor. While the transducers, deck box, and tow cables for that CHIRP system are original to *Teledyne-Benthos*, the transducers have been remounted with a tow float designed by *Falmouth Scientific Inc.* (*FSI*) (Fig. 11). The reason for this reconfiguration is to facilitate the switching back and forth between the CHIRP sonar and the FSI Bubblegun, depending on how the data are looking during acquisition. The Bubblegun offers a more powerful but lower resolution seismic source than the *CHIRP III*; it was available onboard during the survey but was not deployed because the data produced by the *CHIRP III* were consistently of good quality. The FSI tow float is designed to maintain the CHIRP transducers at 1 m below the sea surface regardless of the tow speed. With the boat GPS antenna located forward of the stern by 8.42 m, and 15 meters of cable was let out beyond the aft deck, the layback of the transducer relative to the GPS antenna was 23.4 m during the survey. The ping rate was 1/16 sec most of the time, except when navigating over the deeper channel when the ping rate was decreased to 1/8 sec to allow for returns to be received.

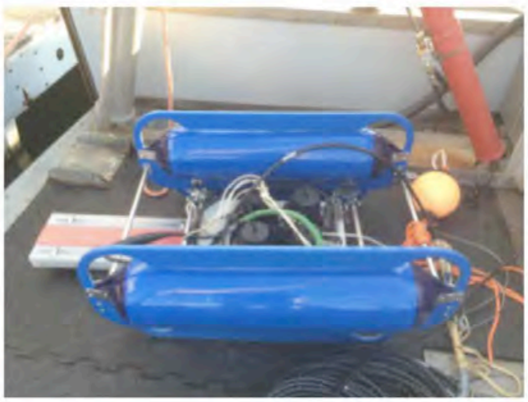

Figure 11.
(*left*) Teledyne-Benthos CHIRP III sonar, mounted with a FSI tow float.
(*below left*) Deploying the CHIRP sonar.
(*below right*) CHIRP sonar under tow, slightly starboard of center beam.

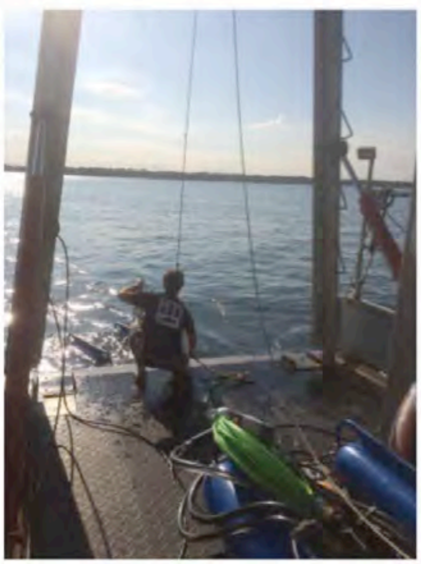

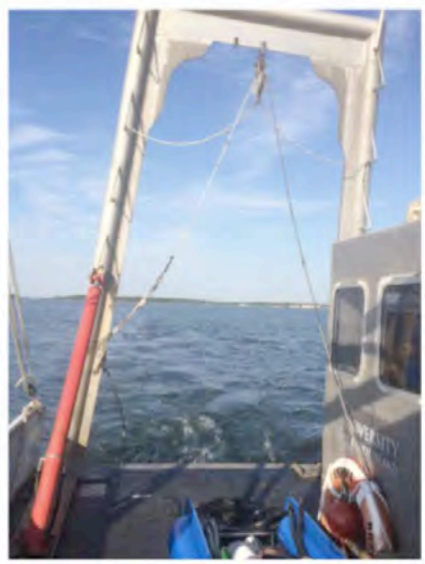

6. DATA PROCESSING

The CHIRP data have been corrected for a constant layback of the sonar behind the GPS antenna (23.4 m), but as of the writing of this report, correction for the depth of the transducer below the sea surface (1 m) and depth corrections for the tidal cycle have not been applied. The tidal range in New Rochelle, as predicted by NOAA/NOS during the survey dates and times, reached 2.56 m:

Date	Time (EDT, GMT-4)	Predicted High/Low ((meters), MLLW datum)
07/19/2016	05:50am	0.01 L
07/19/2016	11:32am	2.27 H
07/19/2016	05:33pm	0.14 L
07/19/2016	11:22pm	2.52 H
07/20/2016	06:15am	-0.04 L
07/20/2016	11:56am	2.35 H
07/20/2016	06:09pm	0.07 L

Standard amplitude corrections have been applied in the form of an AGC filter (Automatic Gain Control) starting at the seafloor. Imagery of each profiles (except for the turns) are provided in Appendix B. The digital data have been saved in the standard industry SEG-Y format and made available in two public databases, as described in section 8.

7. PRELIMINARY RESULTS AND INTERPRETATIONS

This study contributes geophysical data in an area that has not been as well investigated as other parts of the Sound. In fact, the vast majority of publications about the geological history of Long Island Sound provide maps that terminate to the west just short of offshore metropolitan New York City. Hence, this project extends and complements the existing geophysical dataset for Long Island Sound.

Overall, the new CHIRP data confirm our initial inference about areas where gas-charged sediments would be present, and areas with hard bottom/no penetration would occur, based on the examination of the single channel (boomer) data collected in 1985 by USGS [*Poppe et al., 2002*]. Figure 12 further illustrates how the new low frequency CHIRP data have a similar penetration but better resolution than these 1985 data - good news considering the ease with which CHIRP data can be collected in this busy area of Long Island Sound.

Initial data interpretation has been carried out interactively using *OpendTect* (www.opendtect.org), a free seismic reflection interpretation software package (e.g., Fig 13). This software will further be used to produce digital representations of key seismic horizons and corresponding interpolated surfaces. Future work will also involve the interpretation of areas of deposition or non-deposition, bedrock outcrops, dredge channels, gas fronts, and other features of interest.

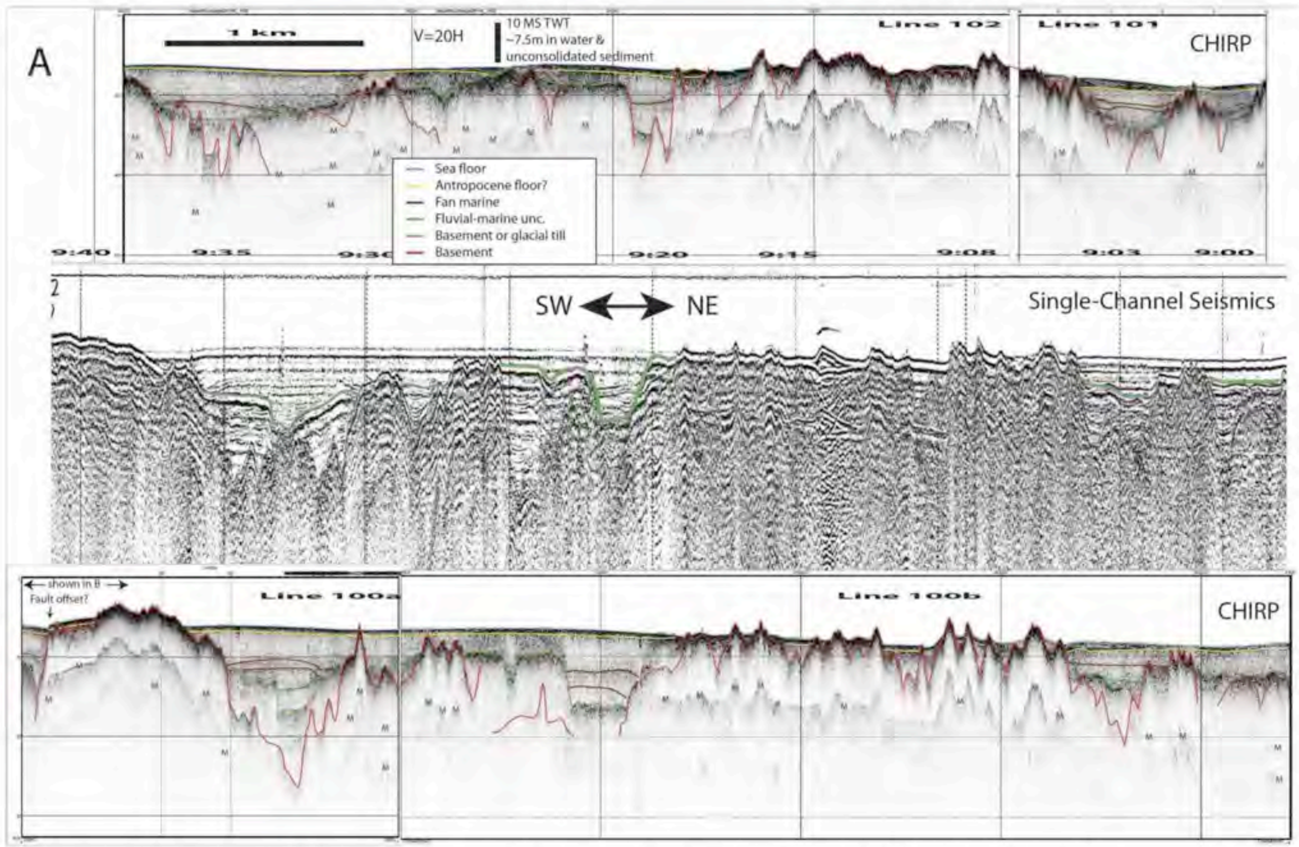

Figure 12. Comparison between a portion of single channel seismic reflection (SCS) profile AST-85-821 collected by USGS in 1985 [Poppe *et al., 2002*] and two adjacent (within ~100 m) CHIRP profiles from our survey – lines 101 and 102 on the north side, and lines 100a and 100b on the south side of the SCS profile (see Fig. 8 for the locations of these profiles). The main features can clearly be correlated across all three profiles and these data are complementary. While the glacio-fluvial unconformity (interpreted as the green horizon) and the basement (interpreted as the red horizon) are easily recognizable in the SCS data, the CHIRP data generally display more reflectors and at a higher resolution. A prominent example is the 1-2 m-thick surficial layer (yellow horizon) which we tentatively interpret as the signature of industrial activity in new York harbor. The label "Fault Offset?" at bottom left (SW end of profile 100a) turned out to be an artifact of the 2-x vertical exaggeration. See Fig. 13 for its appearance with a vertical exaggeration of x3.

Preliminary interpretation of the CHIRP profiles revealed a few instances of step-like features at the seafloor and beneath it. So far, we found all such features to be local erosional scarps and not fault offsets on the basis lack of lateral continuity on adjacent parallel lines (Fig. 13) and/or lack of offset of the subsurface stratigraphy. If this result is further confirmed by the on-going analysis, then it will prove a reliable negative result with implications regarding the lateral dimensions and southeastward continuity of the seismogenic brittle faults in metropolitan New York and/or for their capacity to generate large earthquakes with surface ruptures.

In addition, this project contributes new useful data to investigate the evolution of glacial Lake Connecticut, and in particular, about the timing of its' draining and of the marine transgression that followed. The new data should prove useful for updating the version of the USGS map of the thickness of the Holocene marine layer in western Long Island Sound [*Stone et al., 2005*], as well as that of the system of post-glacial fluvial channels that developed in western Long Island Sound on the exposed lakebed at around 15.5 ka [*Lewis and DiGioacomo-Cohen, 2000*].

As noted by previous authors, the marine uncomformity is marked by tendency for layers below it to be warped and to mimic the acoustic basement (glacial till or bedrock), while those above it are sub-horizontal. We further note that in places, the marine layers are upwardly convex (such as would be expected for fans) over the basement lows (as may be produced by river erosion), so there seems to be an inversion of erosional/depositional style which implies a continuity of the river location. Potentially, these data could be used to calculate the volume (and rate) of sediment transported by early post-glacial rivers in western Long Island Sound.

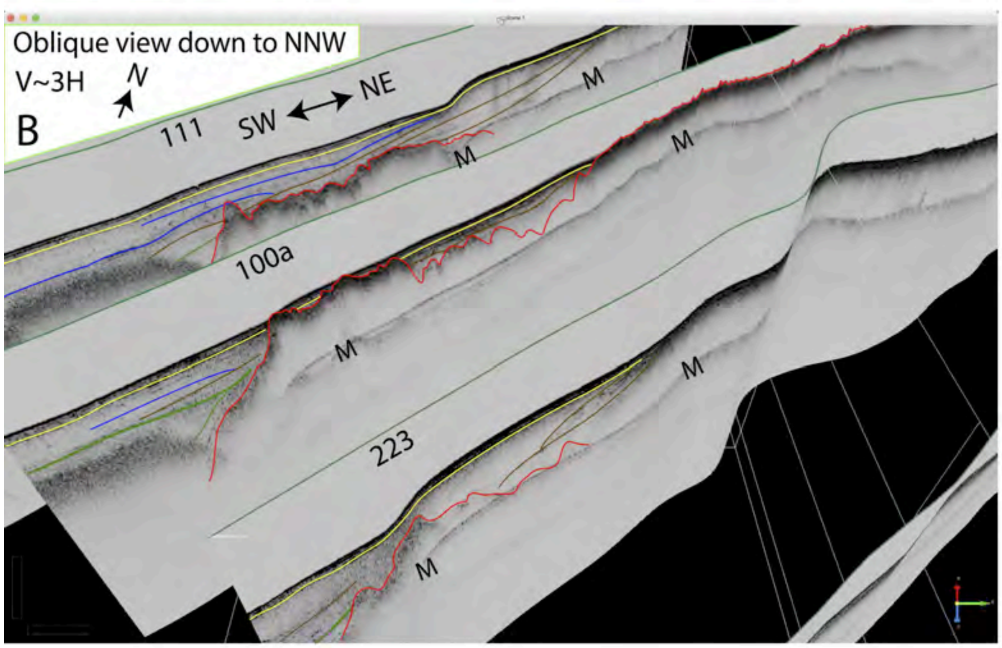

Figure 13. Oblique view of CHIRP profiles 111, 100a, and 223. See Fig. 8 for their locations. Data are displayed with the software OpendTect with a vertical exaggeration of ~ x3. At this scale, the feature labeled “fault offset?” on profile 100a in Fig. 12 is revealed to simply be a bedrock outcrop. Furthermore, the same bedrock surface is draped by sediment in the two adjacent profiles (223 and 111), which display clearly continuous reflectors.

8. DATA DISSEMINATION

As of writing of this report, steps are being taken to provide all raw and processed data to two online databases. The first one is the *Long Island Sound Resource Center* (LISRC; http://www.lisrc.uconn.edu/lisrc/about.asp), a central clearinghouse for information and data related to the Sound that Dr. Lewis is managing at University of Connecticut, in partnership with USGS-Woods Hole and several other agencies. The second database the Marine Geoscience Data System (MGDS; http://www.marine-geo.org/portals/lis/) maintained by the Lamont-Doherty Earth Observatory with funding from the U.S. National Science Foundation, via the Long Island Sound Data Portal. Data uploaded into the LISRC and the MGDS databases are fully accessible to the public, and both databases provide a range of tools for data search and download. In addition, the MGDS database offers tools for data analysis and visualization. Thus, the products of this survey will be publicly accessible, available to future researchers, and securely archived in a long-term (100 year) repository. In particular, the seismic data files are being submitted in the standard SEGY format to the MGDS database. A digital map of survey lines, metadata files, and this report will also be accompanying the data submissions.

The investigators on this project are pursuing further data analysis and interpretation, and it is their intent to submit their results to a peer-reviewed journal for publication.

9. RELATED EFFORTS

An extensive survey of Long Island Sound has started in 2012, thanks to a settlement fund created to map its benthic environment. This LISMaRC project (Long Island Sound Mapping and Research Collaborative) involves the participation of multiple agencies and universities, including the University of Rhode Island and the Lamont-Doherty Earth Observatory. LISMARC is jointly managed by the Long Island Sound Cable Fund Steering Committee, the State of Connecticut Department of Energy and Environmental Protection, the State of New York Department of Environmental Conservation, the Connecticut Sea Grant, the New York Sea Grant, and the Environmental Protection Agency:
longislandsoundstudy.net/wp-content/uploads/2010/02/SCOPE-OF-WORK-Phase1-20120226_finalwobudget.pdf

A pilot area in central Long Island Sound, located between Port Jefferson (NY) and Bridgeport (CT), was selected to test and streamline the approaches to be used with LISMaRC. That pilot area was surveyed in 2012 and 2013. Survey tools included the acquisition of multibeam bathymetry, sidescan sonar imagery, chirp profiling, and gravity cores using three different survey ships. As of writing of this report, phase 2 has started and is focused entirely on the eastern end of the sound; that second phase might also involve the acquisition of a few subbottom lines in spring 2018. While it is hoped that work in the western Long Island Sound will be part of a next phase of the project, it will probably be several years out and not happen before 2020.

We note that the survey tracks for the LISMaRC CHIRP survey have / will have a spacing of 500 m to 1000 m, larger than the 200 m achieved with this project. This spacing would not be sufficient to differentiate between stratigraphic offsets related to tectonic or sedimentary processes. It also would not be sufficient to unambiguously determine fault strike, should any fault be recognized. Nonetheless, any additional seismic data collected in the under-surveyed eastern Long Island Sound, might go a long way in answering key geological questions.

10. ACKNOWLEDGEMENTS

We are indebted to Clifford (Chip) Heil, Brian Cacciopoli, and Monique LaFrance from URI for their professional assistance with survey preparation, strong expertise with data acquisition, and friendly help with post-processing. We are grateful to the U.S. Geological Survey for their financial support of this project, a project that we hope will deliver new geological insight beyond its first year.

11. REFERENCES

Bertoni, R., J. J. Dowling, L. Frankel, Freshwater-lake sediments beneath Block Island Sound, Geology, 5, 631-635, 1977.

Calais, E., A. M. Freed, R. Van Arsdale, and S. Stein, Triggering of New Madrid seismicity by late-Pleistocene erosion, Nature, 466, 608-611, 2010.

Coppersmith, K. J. and R. R. Youngs, Data needs for probabilistic fault displacement hazard analysis. Journal of Geodynamics, 29:3-5, 329-343, 2000.

Cormier, M.H., L. Seeber, C.M.G. McHugh, A. Polonia, M.N. Çagatay, Ö. Emre, L. Gasperini, N. Görür, G. Bortoluzzi, E. Bonatti, WB.F. Ryan, and K.R. Newman, The North Anatolian fault in the Gulf of Izmit (Turkey): Rapid vertical motion in response to minor bends of a non-vertical continental transform, *J. Geophys. Res., 111*, doi:1029/2005JB003633, B04102, 2006.

Dawers, N. H., and L. Seeber, Intraplate faults revealed in crystalline bedrock in the 1983 Goodnow and 1985 Ardsley epicentral areas, New York, Tectonophysics, 186, 115-131, 1991.

DiGiacomo-Cohen, M. L. and J. R. Stone, Maps showing the shape of the marine transgressive surface and the thickness of postglacial sediments in Long Island Sound. U.S. Geological Survey Open-File Report 00-304, CD-ROM: Chapter 1., 2000.

Fenton, C.H., J. Adams, and S. Halchuk, Seismic hazards assessment for radioactive waste disposal sites in regions of low seismic activity. Geotechnical and Geological Engineering, 24, 579-592, 2006.

Frankel, A. D., M. D. Petersen, C. S. Mueller, K. M. Haller, R. L. Wheeler, E. V. Leyendecker, R. L. Wesson, S. C. Harmsen, C. H. Cramer, D. M. Perkins, and K. S. Rukstales, Seismic-hazard maps for the conterminous United States, U.S. Geological Survey, Scientific Investigations Map 2883, 2005.

Hall, L. M., Geology of the White Plains quadrangle New York, New York State Geol. Surv. Open-File Rept. 1g1366, 1981.

Hutchinson, D. R., K. D. Klitgord, and R. S. Detrick, Rift basins of the Long Island platform, Bull. Geol. Soc. Am. 97, 688-702, 1986.

Johnston, A.C., The effect of large ice sheets on earthquake genesis, NATO advanced research workshop on causes and effects of earthquakes at passive margins and in areas of post-glacial rebound on both sides of the North Atlantic (1988), 266, 581-599, 1989.

Johnston, A.C., The stable continental region earthquake database, in The Earthquakes of Stable Continental Regions: Assessment of Large Earthquake Potential, EPRI Rpt. TR-102261, Chapt. 3, pp. 3-1-3-80, J. Schneider (Editor), Electric Power Res. Inst., Palo Alto, 1994.

Kim, B.-H. and H. J. Bokuniewicz, Estimates of sediment fluxes in Long Island Sound, *Estuaries, 14*, 237-247, 1991.

Klitgord, K. D., D. R. Hutchinson, and H. Schouten, U. S. Atlantic continental margin; structural and tectonic framework, in The Geology of North America, The Atlantic Continental Margin, R. E. Sheridan and J. A. Grow (Editors), Vol. I-2, Geological Society America, Boulder, Colorado, 19-55, 1988.

Klose, C. and L. Seeber, Shallow seismicity in stable continental regions, Seismological Research Letters 78, 550-559, 2007.

Lewis, R. S. and J. R. Stone, Late Quaternary stratigraphy and depositional history of the Long Island Sound basin: Connecticut and New York, Journal of Coastal Research, SI11, 1-23, 1991.

Lewis, R.S., and M. DiGiacomo-Cohen, A review of the geological framework of the Long

Island Sound Basin, with some observations relating to postglacial sedimentation, J. Coastal Research, 16 (3), 522-532, 2000.

McHugh, C.M., M.H. Cormier, P. Marchese, Y. Zheng, G. Stewart, V. Acosta, A. Bowman, A. Cortes, L. Leon, M. Rosa, D. Semple, N. Thaker, W. Vargas, L Williams, Late Quaternary Depositional History and Anthropogenic Impacts of Western Long Island Sound, New York, *Fall meeting of the American Geophysical Union, San Francisco, CA*, December 2006.

Merguerian, C., Brittle fault chronology of New York City (NYC), Geological Society of America Abstracts with Programs, 36:2, 73, 2004.

Nordenson, GJP, and G.R. Bell, Seismic design requirements for regions of moderate seismicity, Earthquake Spectra, 16, 205-225, 2000.

Petersen, Mark D., Frankel, Arthur D., Harmsen, Stephen C., Mueller, Charles S., Haller, Kathleen M., Wheeler, Russell L., Wesson, Robert L., Zeng, Yuehua, Boyd, Oliver S., Perkins, David M., Luco, Nicolas, Field, Edward H., Wills, Chris J., and Rukstales, Kenneth S., Documentation for the 2008 Update of the United States National Seismic Hazard Maps: U.S. Geological Survey Open-File Report 2008–1128, 61 p., 2008.

Petersen, M.D., Moschetti, M.P., Powers, P.M., Mueller, C.S., Haller, K.M., Frankel, A.D., Zeng, Yuehua, Rezaeian, Sanaz, Harmsen, S.C., Boyd, O.S., Field, E.H., Chen, Rui, Luco, Nicolas, Wheeler, R.L., Williams, R.A., Olsen, A.H., and Rukstales, K.S., Seismic-hazard maps for the conterminous United States, 2014: U.S. Geological Survey Scientific Investigations Map 3325, 6 sheets, scale 1: 7,000,000, http://dx.doi.org/10.3133/sim3325, 2014.

Polonia, A., L. Gasperini, A. Amorosi, E. Bonatti, G. Bortoluzzi, M.N. Çagatay, L. Capotondi, M.H. Cormier, N. Görür, C.M.G. McHugh, L. Seeber, Holocene slip rate of the North Anatolian Fault beneath the Sea of Marmara, *Earth Planet. Sci. Lett., 227*, 411-426, 2004.

Poppe, L. J., H. J. Knebel, B. A. Seekins and M. E. Hastings, Map showing the distribution of surficial sediments in Long Island Sound. Reston, VA, U.S. Geological Survey Open-file Report 00-304, 2000a.

Poppe L. J., S. J. Williams, M. S. Moser, N. A. Forfinski, H. F. Stewart and E. F. Doran, Quaternary Geology and Sedimentary Processes in the Vicinity of Six Mile Reef, Eastern Long Island Sound, Journal of Coastal Research, 24: 1, 255-266, 2000b.

Poppe, L. J., V. F. Paskevich, R. S. Lewis and M. L. DiGiacomo-Cohen, Geological framework data from Long Island Sound, 1981-1990: a digital data release: U.S. Geological Survey Open-File Report 02-002, DVD-ROM, 2002.

Poppe, L. J., S. J. Williams, M. S. Moser, N. A. Forfinski, H. F. Sterwart and E. f. Doran, Quaternary geology and sedimentary processes in the vicinity of Six Mile Reef, eastern Long Island Sound, Journal of Coastal Research 24, 255-266, 2008.

Ratcliffe, N. M., W. C. Burton, R. M. D'Angelo, and J. K. Costain, Low-angle extensional faulting, reactivated mylonites, and seismic reflection geometry of the Newark basin margin in eastern Pennsylvania, Geology, 14, 766-770, 1986.

Seeber, L. and J.G. Armbruster, Low-Displacement seismogenic faults and nonstationary seismicity in the Eastern United States, in Annals of the New York, 1989.

Seeber, L., and N. Dawers, Characterization of an intraplate seismogenic fault in the Manhattan prong, Westchester Co. N.Y., Seism. Res. Lett. 60, 71-78, 1989.

Seeber, L. and J.G. Armbruster, The NCEER-91 Earthquake Catalog: Improved Intensity-Based Magnitudes and Recurrence Relations for U.S. Earthquakes East of New Madrid, Technical Report NCEER-91-0021, pp. 98, 1991.

Seeber, L., J. G. Armbruster, W.-Y. Kim, N. Barstow, and C. Scharnberger, The 1994 Cacoosing Valley earthquakes near Reading, Pennsylvania: a shallow rupture triggered by quarry unloading, J. Geophys. Res., 103, 24505-24521, 1998.

Seeber, L., The New York City Seismic Zone in the context of Rocks and Seismogenesis in Stable Continental Regions, Field Trip Guide, Annual Meeting of the Seismological Society of America - Eastern Section, October 2009.

Stein, S., and S. Mazzotti, Continental Intraplate Earthquakes: Science, Hazard, and Policy Issues, GSA Special Paper 425, 402 pages, 2007.

Stein, S., and M. Liu, Long aftershock sequences within continents and implications for earthquake hazard assessment, Nature 462:5, 87-89, 2009.

Stone, B. D. and H. W. Borns, Pleistocene glacial and interglacial stratigraphy of new England, Long Island, and adjacent Georges Bank and Gulf of Maine. Quaternary Science reviews, 5, 39-52, 1986.

Stone, J. R., J. P. Schafer, E. H. London, M. L. DiGiancomo-Cohen, R. S. Lewis and W. B. Thompson, Quaternary geologic map of Connecticut and Long Island Sound basin, Scientific Investigations Map 2784, U.S. Geological Survey, 2005.

Sykes, L. R., J. G. Armbruster, W.-Y. Kim, and L. Seeber, Observations and Tectonic Setting of Historic and Instrumentally Located Earthquakes in the Greater New York City-Philadelphia Area, Bulletin of the Seismological Society of America, 98:4, 1696-1719, 2008.

Tantala, M. W., G. J. P. Nordenson, G. Deodatis, and K. Jacob, Earthquake loss estimation for the New York City Metropolitan Region, Soil Dyn. Earth. Engi., 28, 812-835, 2008.

Vargas, W., M.H. Cormier, C.M. McHugh, High Resolution Geophysical Survey of Western Long Island Sound Offshore New York: A Seafloor Morphology Shaped by Glacial Features, Tidal Currents, and Human Activity, Joint Assembly of the American Geophysical Union, Acapulco, Mexico, *Eos Trans. AGU, 88(23*), Abstract OS23B-10, May 2007.

Appendix A
Summary List of CHIRP profiles

Line name (during acquisition)	Line name (after acquisition)	Date	Average course (N°E)	Start time (GMT)	Start latitude / longitude	End time (GMT)	End latitude / longitude	Comments
Sonarwiz acquisition laptop: time is EDT (GMT -4). However, system time in Sonarwiz software is GMT. Hypack laptop for navigation: time is 1 hour slow: GMT-5.								
NewRochelle2016-20160719_074624-CH1	100a	19-Jul-16	52°	11:46:24	40.90086°N -73.74530°W	12:17:36	40.91571°N -73.71989°W	63 ms rep. rate, 5 ms pulse, 6 dB gain
NewRochelle2016-20160719_081736-CH1	100b	19-Jul-16	52°	12:17:36	40.91571°N -73.71988°W	13:04:28	40.93995°N -73.67801°W	Sunny, mid 80's °F, wind NW @ 10 knots. Incoming tide makes W to E lines slower. E to W, tow speed is 4.0 knots with good data quality. Low tide was at 5:30am, local time.
Turn-NewRochelle2016-20160719_090429-CH1	100_turn	19-Jul-16						
NewRochelle2016-20160719_090639-CH1	101	19-Jul-16	232°	13:06:39	40.94028°N -73.67946°W	13:16:14	40.93419°N -73.69098°W	Line 101 is spaced 100 m north of line 100a - 100b
Turn-NewRochelle2016-20160719_091614-CH1	101_turn	19-Jul-16						Angling to next line over, as we decided to space lines at 200m rather than 100m. If time permits, we will acquire additional lines in between in order to achieve 100 m spacing.
NewRochelle2016-20160719_091754-CH1	102	19-Jul-16	232°	13:17:54	40.93357°N -73.69316°W	13:55:54	40.90931°N -73.73488°W	Off Mamaroneck
Turn-NewRochelle2016-20160719_095554-CH1	102_turn	19-Jul-16						
NewRochelle2016-20160719_100007-CH1	103	19-Jul-16	52°	14:00:07	40.91186°N -73.73441°W	14:33:17	40.93034°N -73.70279°W	Off Mamaroneck
Turn-NewRochelle2016-20160719_103317-CH1	103_turn	19-Jul-16						
NewRochelle2016-20160719_103549-CH1	104	19-Jul-16	232°	14:35:49	40.93100°N -73.70514°W	15:02:27	40.91450°N -73.73414°W	Off Mamaroneck
Turn-NewRochelle2016-20160719_110227-CH1	104_turn	19-Jul-16						

Appendix A
Summary List of CHIRP profiles

Line name (during acquisition)	Line name (after acquisition)	Date	Average course (N°E)	Start time (GMT)	Start latitude / longitude	End time (GMT)	End latitude / longitude	Comments
NewRochelle2016-20160719_110839-CH1	105	19-Jul-16	52°	15:08:39	40.91869°N -73.73023°W	15:32:01	40.93287°N -73.70603°W	Off Mamaroneck
Turn-NewRochelle2016-20160719_113201-CH1	105_turn	19-Jul-16						
NewRochelle2016-20160719_113513-CH1	106	19-Jul-16	232°	15:35:13	40.93486°N -73.70609°W	16:00:43	40.92021°N -73.73186°W	Off Mamaroneck
Turn-NewRochelle2016-20160719_120044-CH1	106_turn	19-Jul-16						
NewRochelle2016-20160719_120338-CH1	107	19-Jul-16	52°	16:03:38	40.92251°N -73.73130°W	16:24:59	40.93604°N -73.70914°W	Off Mamaroneck
Turn-NewRochelle2016-20160719_122459-CH1	107_turn	19-Jul-16						
NewRochelle2016-20160719_122738-CH1	108_tieline	19-Jul-16	189°	16:27:39	40.93573°N -73.71084°W	16:45:44	40.92009°N -73.71498°W	Off Mamaroneck. Had to adjust heading to avoid sailing class; had to end tie-line earlier than wanted because of sailing class.
Turn-NewRochelle2016-20160719_124544-CH1	108_turn	19-Jul-16		16:45:44	40.9201°N -73.71498°W	17:08:54	40.91951°N -73.73423°W	Long transit west to Larchmont area; log that transit as a turn.
NewRochelle2016-20160719_130854-CH1	109	19-Jul-16	232°	17:08:54	40.91951°N -73.73423°W	17:31:53	40.90603°N -73.75511°W	Off Larchmont. Line blocked by boats, turn onto a tie-line.
Turn-NewRochelle2016-20160719_133154-CH1	110_tieline	19-Jul-16	134°	17:31:54	40.90603°N -73.75510°W	17:40:00	40.89983°N -73.74690°W	acquiring tie line through location of next 5 profiles (111 to 115); logged as a turn
Turn-NewRochelle2016-20160719_134001-CH1	110_turn	19-Jul-16						

Appendix A
Summary List of CHIRP profiles

Line name (during acquisition)	Line name (after acquisition)	Date	Average course (N°E)	Start time (GMT)	Start latitude / longitude	End time (GMT)	End latitude / longitude	Comments
NewRochelle2016-20160719_135013-CH1	111	19-Jul-16	52°	17:50:14	40.89631°N -73.75624°W	18:08:39	40.90771°N -73.73831°W	Off New Rochelle (Echo bay). Possible fault offset at seafloor? Near 40°54'10.8"N 73°44'30.93"W. Profile crosses sewer line indicated on nautical chart; it shows as swath of no penetration, somewhat like a shallow gas front
Turn-NewRochelle2016-20160719_140839-CH1	111_turn	19-Jul-16						
NewRochelle2016-20160719_141055-CH1	112	19-Jul-16	232°	18:10:55	40.90855°N -73.74004°W	18:30:41	40.89789°N -73.75802°W	Off New Rochelle. On lines 111 to 115, the sewer line indicated on the nautical chart corresponds to a flat, strong, shallow reflector, with an appearance similar to that of gas-charged sediments.
Turn-NewRochelle2016-20160719_143041-CH1	112_turn	19-Jul-16						
NewRochelle2016-20160719_143219-CH1	113	19-Jul-16	52°	18:42:19	40.89721°N -73.75716°W	18:49:33	40.90816°N -73.73924°W	Off New Rochelle. Line 13 is located between lines 111 and 112, 100 m from either one.
Turn-NewRochelle2016-20160719_144934-CH1	113_turn	19-Jul-16						
NewRochelle2016-20160719_145416-CH1	114	19-Jul-16	232°	18:54:16	40.90891°N -73.74344°W	19:12:57	40.89924°N -73.75960°W	Off New Rochelle.
Turn-NewRochelle2016-20160719_151258-CH1	114_turn	19-Jul-16						
NewRochelle2016-20160719_151558-CH1	115	19-Jul-16	52°	19:15:58	40.90007°N -73.76199°W	19:35:32	40.91296°N -73.74095°W	Off New Rochelle.
Turn-NewRochelle2016-20160719_153532-CH1	115_turn	19-Jul-16						
July 20, 2017 Averaging ~3.7 knot								
NewRochelle2016-20160720_082512-CH1	200_loop	20-Jul-16						Eastchester Bay

Appendix A
Summary List of CHIRP profiles

Line name (during acquisition)	Line name (after acquisition)	Date	Average course (N°E)	Start time (GMT)	Start latitude / longitude	End time (GMT)	End latitude / longitude	Comments
NewRochelle2016-20160720_082841-CH1	201	20-Jul-16	~210°	12:28:41	40.83536°N -73.78589°W	12:47:35	40.81913°N -73.79873°W	Eastchester Bay. Mostly gas-charged sediments, but peentration reachs ~35 m in a few places.
Turn-NewRochelle2016-20160720_084735-CH1	201_turn	20-Jul-16						Eastchester Bay
NewRochelle2016-20160720_085001-CH1	202	20-Jul-16	~30°	12:50:01	40.81807°N -73.79699°W	13:13:33	40.83551°N -73.78289°W	Eastchester Bay
NewRochelle2016-20160720_093205-CH1	203	20-Jul-16	~17°	13:32:05	40.85669°N -73.78004°W	13:47:12	40.87048°N -73.77379°W	City Island to Davids Island. Calm, Winds N @ 5-10 knot becoming W-SW at 5-10 knots. Partly cloudy, mid-to upper 80's°F. Redeployed CHIRP after quick transit to area between City Island and Davids Island
Turn-NewRochelle2016-20160720_094712-CH1	203_turn	20-Jul-16						drive around Middle Reef, start new line soon after.
NewRochelle2016-20160720_095015-CH1	204	20-Jul-16	~17°	13:50:15	40.87306°N -73.77261°W	13:55:46	40.87839°N -73.77024°W	Middle Reef to Davids Island
Turn-NewRochelle2016-20160720_095546-CH1	204_turn	20-Jul-16						
NewRochelle2016-20160720_095738-CH1	205	20-Jul-16	~197°	13:57:38	40.87875°N -73.77229°W	14:18:00	40.85785°N -73.78274°W	Davids Island to City Island
Turn-NewRochelle2016-20160720_101800-CH1	205_turn	20-Jul-16						
NewRochelle2016-20160720_101929-CH1	206	20-Jul-16	~17°	14:19:29	40.85904°N -73.78324°W	14:42:08	40.87973°N -73.77456°W	City Island to Davids Island.
Turn-NewRochelle2016-20160720_104208-CH1	206_turn	20-Jul-16						
NewRochelle2016-20160720_104621-CH1	207_tieline	20-Jul-16	116°-120°	14:46:22	40.87877°N -73.77633°W	15:14:03	40.85978°N -73.76047°W	South of Davids Island

Appendix A
Summary List of CHIRP profiles

Line name (during acquisition)	Line name (after acquisition)	Date	Average course (N°E)	Start time (GMT)	Start latitude / longitude	End time (GMT)	End latitude / longitude	Comments
NewRochelle2016-20160720_111404-CH1	207_turn	20-Jul-16	~207°	15:04:04	40.85976°N -73.76048°W	15:18:16	40.85844°N -73.76376°W	***switch to 125 ms repetition rate with 10 ms pulse, due to deeper bottom in navigation channel
NewRochelle2016-20160720_111816-CH1	208	20-Jul-16	~27°	15:18:16	40.85844°N -73.76375°W	15:45:48	40.88275°N -73.74682°W	In navigation channel; Hart Island to west of Execution Rocks. Profile crosses two pipelines.
Turn-NewRochelle2016-20160720_114549-CH1	208_turn	20-Jul-16						
NewRochelle2016-20160720_114851-CH1	209	20-Jul-16	~207°	15:48:51	40.88277°N -73.74950°W	16:13:09	40.85880°N -73.76621°W	West of Execution Rocks to Hart Island
Turn-NewRochelle2016-20160720_121309-CH1	209a_turn	20-Jul-16						
NewRochelle2016-20160720_121414-CH1	209b_turn	20-Jul-16		16:14:14	40.85935°N -73.76738°W	16:15:11	40.86021°N -73.76781°W	
NewRochelle2016-20160720_121511-CH1	210	20-Jul-16	~27°	16:15:11	40.86021°N -73.76781°W	16:33:47	40.87546°N -73.75729°W	***switch back to 63 ms repetition rate, 5 ms pulse. Slight excursion for anchored boat. Hart Island to Pea Island.
Turn-NewRochelle2016-20160720_123347-CH1	210_turn	20-Jul-16						
NewRochelle2016-20160720_123654-CH1	211	20-Jul-16	~207°	16:36:54	40.87411°N -73.76060°W	16:43:41	40.86788°N -73.76529°W	Pea Island to Hart Island.
Turn-NewRochelle2016-20160720_124341-CH1	211_turn	20-Jul-16						
NewRochelle2016-20160720_124549-CH1	212	20-Jul-16	~27°	16:45:49	40.86938°N -73.76675°W	16:52:33	40.87537°N -73.76298°W	East Nonations to Pea Island. Ending line slightly early - moorings
Turn-NewRochelle2016-20160720_125233-CH1	212_turn	20-Jul-16						

Appendix A
Summary List of CHIRP profiles

Line name (during acquisition)	Line name (after acquisition)	Date	Average course (N°E)	Start time (GMT)	Start latitude / longitude	End time (GMT)	End latitude / longitude	Comments
NewRochelle2016-20160720_125424-CH1	213	20-Jul-16	~207°	16:54:24	40.87597°N -73.76488°W	17:08:16	40.86294°N -73.77411°W	Pea Island to Hart Island. Gassy sediments in general, excep tfor a fe windows with good penetration
Turn-NewRochelle2016-20160720_130816-CH1	213_turn	20-Jul-16						13:10 - pull CHIRP to transit north of Davids Island
NewRochelle2016-20160720_133048-CH1	214	20-Jul-16	~23°	17:30:48	40.88800°N -73.75250°W	17:48:04	40.90639°N -73.74094°W	Crosses cable area marked on nautical chart: It shows as a swath of no penetration (like a gas-front)
Turn-NewRochelle2016-20160720_134804-CH1	214_turn	20-Jul-16						
NewRochelle2016-20160720_135130-CH1	215	20-Jul-16	~203°	17:51:30	40.90456°N -73.74478°W	18:06:00	40.88917°N -73.75456°W	Off New Rochelle. Cross cable area again.
Turn-NewRochelle2016-20160720_140600-CH1	215_turn	20-Jul-15						
NewRochelle2016-20160720_140744-CH1	216	20-Jul-16	~23°	18:07:44	40.89015°N -73.75623°W	18:15:01	40.89811°N -73.75141°W	Off New Rochelle.
Turn-NewRochelle2016-20160720_141501-CH1	216_turn	20-Jul-16						
NewRochelle2016-20160720_141843-CH1	217	20-Jul-16	~203°	18:18:48	40.89626°N -73.75512°W	18:26:34	40.88825°N -73.76028°W	Off new Rochelle
Turn-NewRochelle2016-20160720_142634-CH1	217_turn	20-Jul-16						
NewRochelle2016-20160720_142830-CH1	218	20-Jul-16	~23°	18:28:31	40.88911°N -73.76230°W	18:33:09	40.89380°N -73.76045°W	Off New Rochelle
Turn-NewRochelle2016-20160720_143309-CH1	218_turn	20-Jul-16						
NewRochelle2016-20160720_143420-CH1	219	20-Jul-16	~203°	18:34:20	40.89424°N -73.76172°W	18:39:15	40.88952°N -73.76477°W	Off New Rochelle

Appendix A
Summary List of CHIRP profiles

Line name (during acquisition)	Line name (after acquisition)	Date	Average course (N°E)	Start time (GMT)	Start latitude / longitude	End time (GMT)	End latitude / longitude	Comments
Turn-NewRochelle2016-20160720_143915-CH1	219_turn	20-Jul-16						
NewRochelle2016-20160720_144200-CH1	220	20-Jul-16	~23°	18:42:00	40.88960°N -73.76700°W	18:50:44	40.89950°N -73.76111°W	Off New Rochelle
Turn-NewRochelle2016-20160720_145044-CH1	220b	20-Jul-16		18:50:44	40.89951°N -73.76110°W	18:59:23	40.89302°N -73.76486°W	Off new Rochelle
NewRochelle2016-20160720_145923-CH1	221_tieline	20-Jul-16	~92°	18:59:23	40.89302°N -73.76485°W	19:09:38	40.89170°N -73.74928°W	Off New Rochelle
Turn-NewRochelle2016-20160720_150938-CH1	222	20-Jul-16	~16°	19:09:38	40.89170°N -73.74928°W	19:17:37	40.90000°N -73.74298°W	Off New Rochelle
NewRochelle2016-20160720_151737-CH1	223	20-Jul-16	~53°	19:17:37	40.90000°N -73.74297°W	19:31:53	40.91072°N -73.72460°W	Off Larchmont. Have to swerve around a sailboat
Turn-NewRochelle2016-20160720_153153-CH1	223_turn	20-Jul-16						
NewRochelle2016-20160720_153403-CH1	224	20-Jul-16	~233°	19:34:03	40.90915°N -73.72378°W	19:52:30	40.89826°N -73.74197°W	Off Larchmont
Turn-NewRochelle2016-20160720_155230-CH1	224_turn	20-Jul-16						
NewRochelle2016-20160720_155443-CH1	225	20-Jul-16	~53°	19:54:43	40.89721°N -73.74007°W	20:10:11	40.90887°N -73.71984°W	Off Larchmont

Appendix B

The following pages display each CHIRP profile as a page-size figure.

The vertical exaggeration has been adjusted for each profile in order to maximize the use of the page. The horizontal axis is labeled in meters, and the vertical axis is in millisecond, with horizontal grid lines every 20 ms.
Profiles are located in Figures 8 and 9.

Line 100a

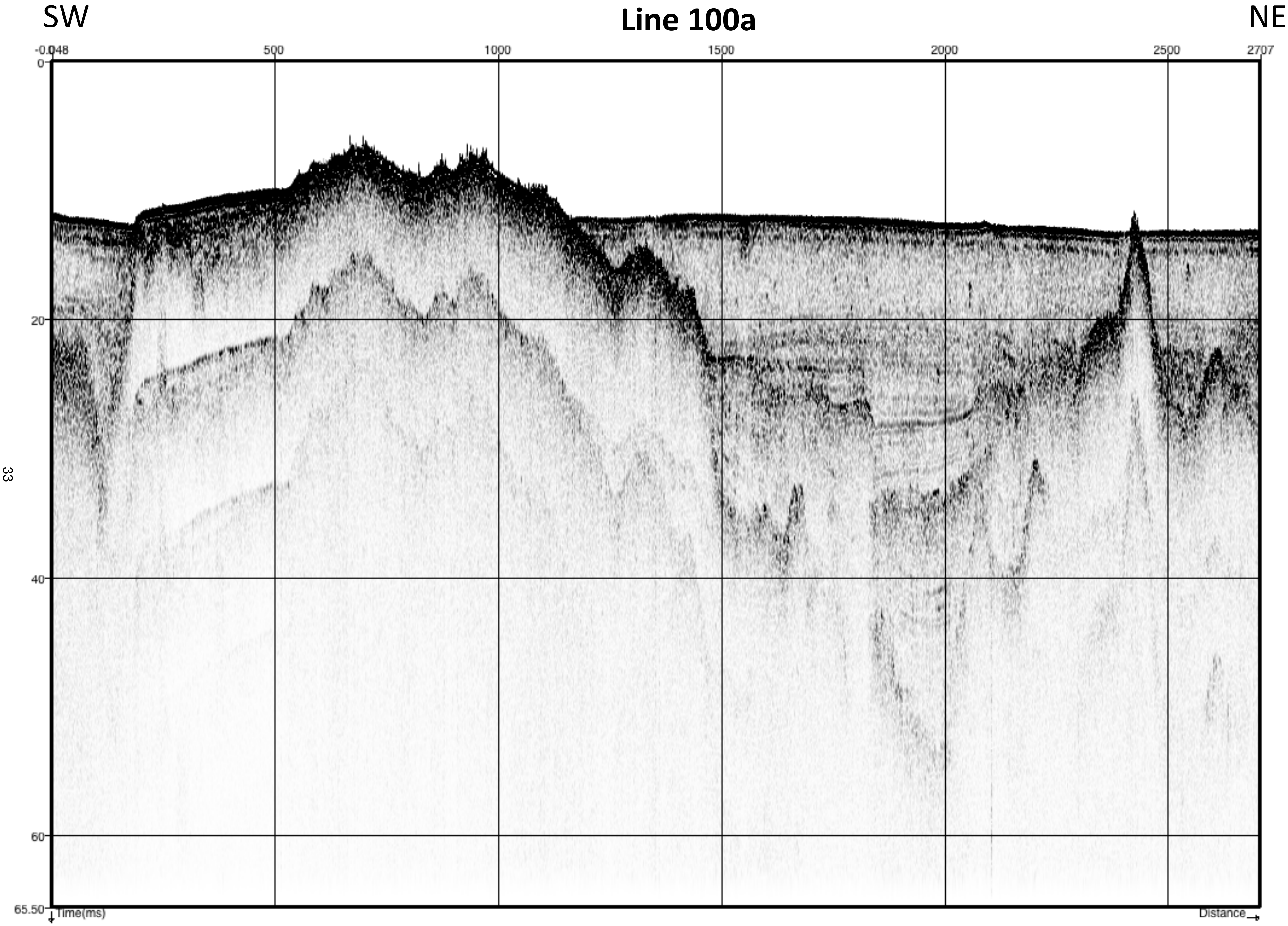

SW
NE
-0.048
500
1000
1500
2000
2500
2707
0
20
40
60
65.50
Time(ms)
Distance

Line 100b

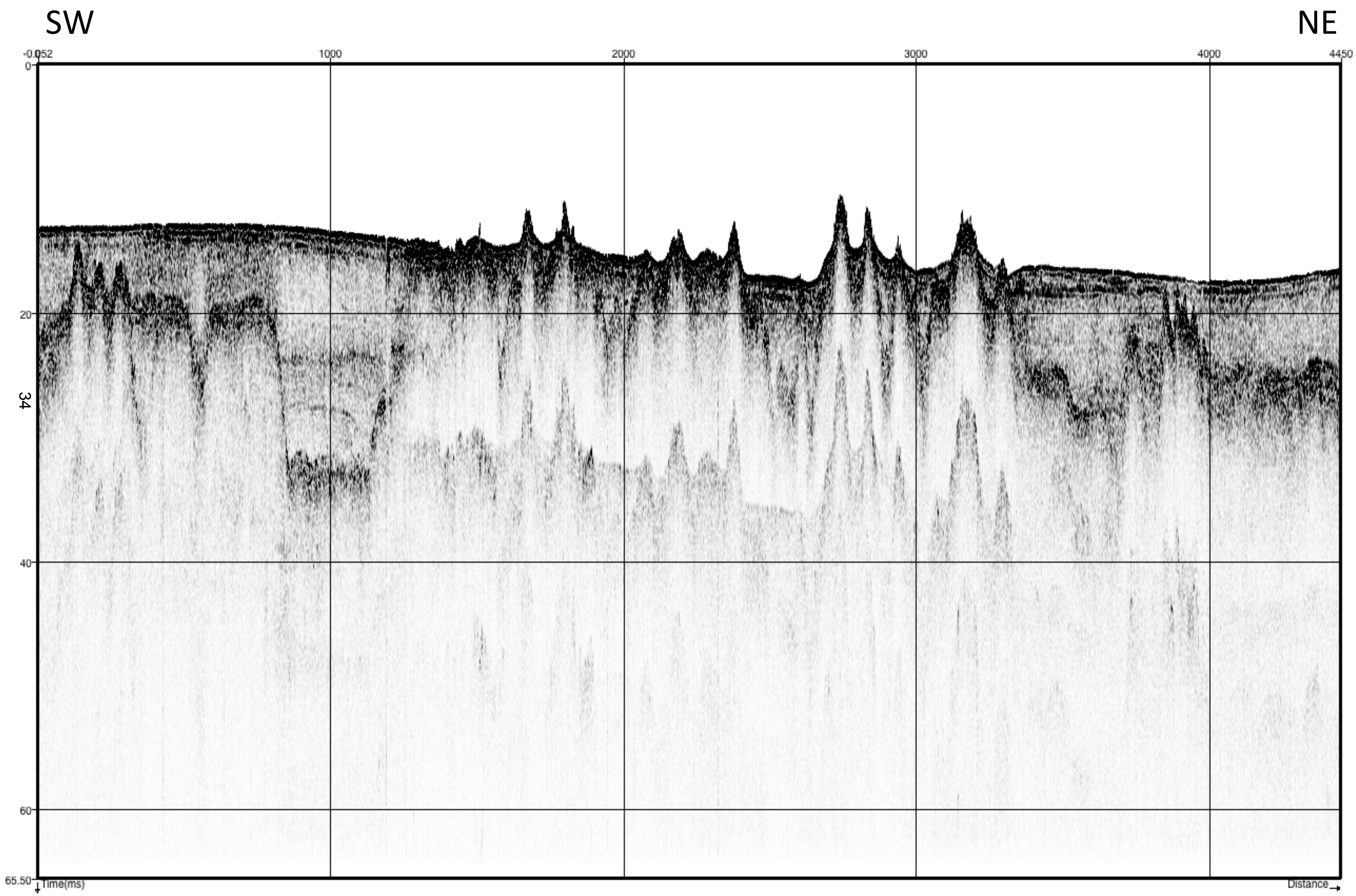

SW
NE
-0.052
1000
2000
3000
4000
4450
0
20
40
60
65.50
Time(ms)
Distance

SW

Line 101

NE

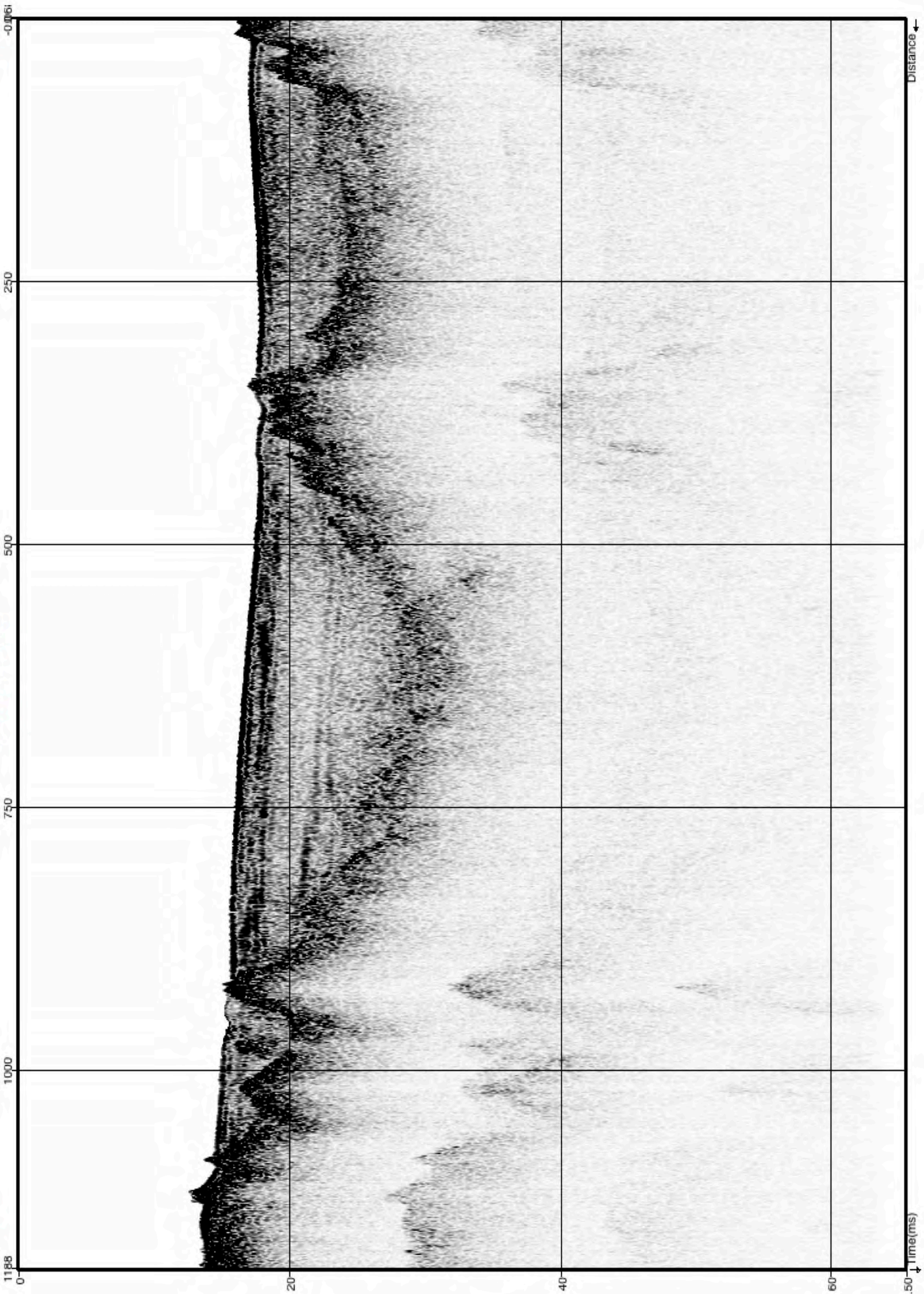

Line 102

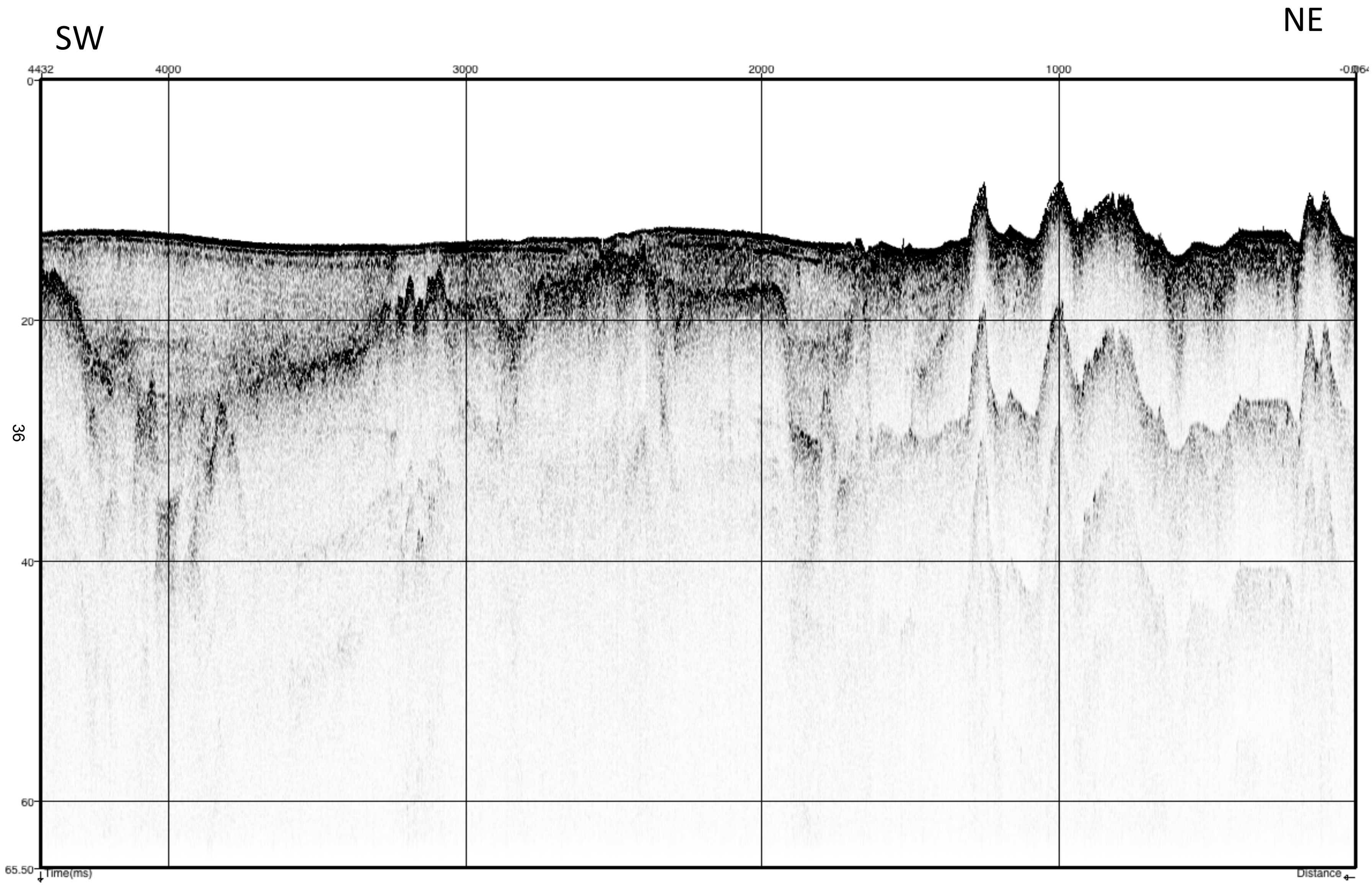

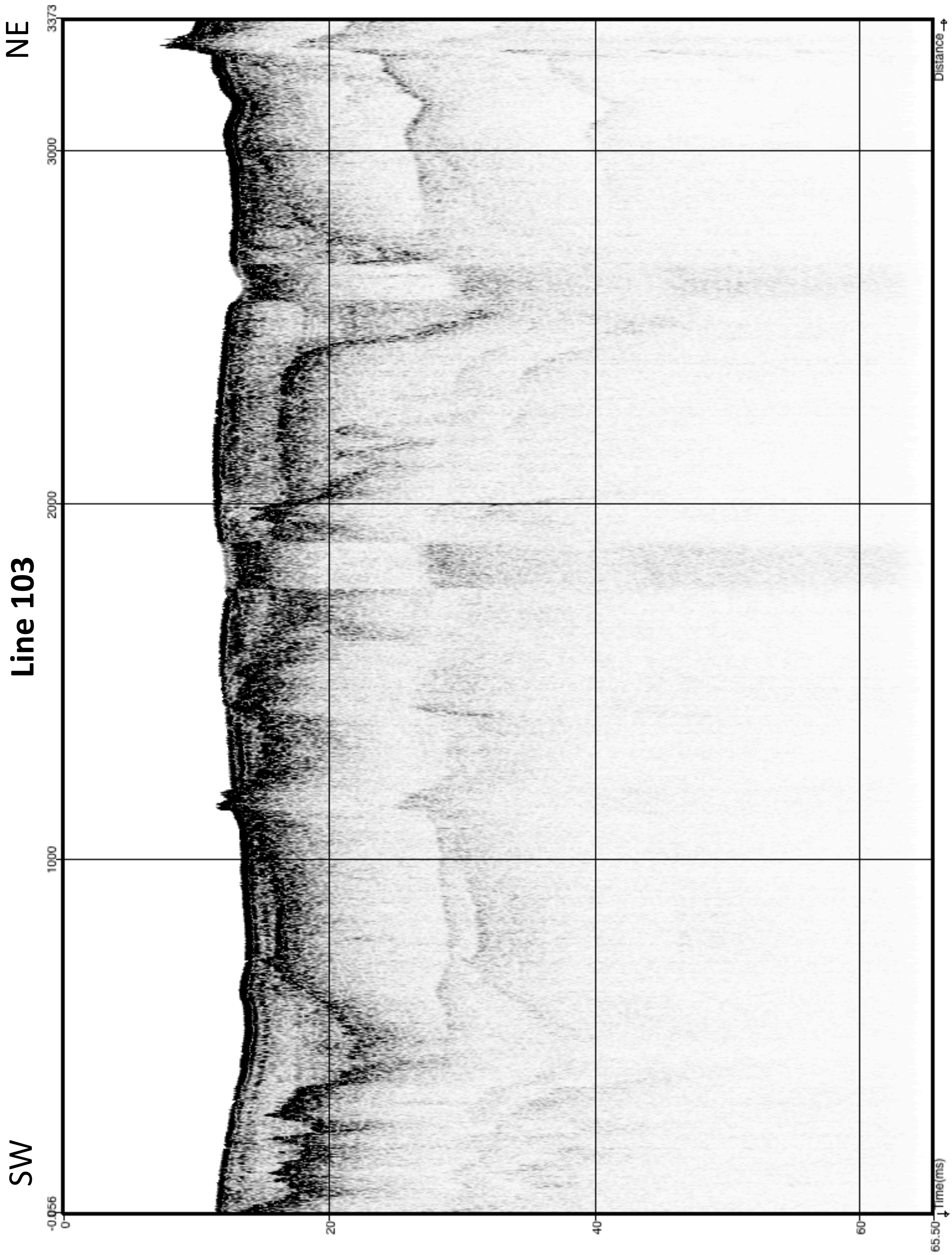
Line 103
SW
NE
Distance
Time(ms)
-0.056
0
1000
2000
3000
3373
20
40
60
65.50

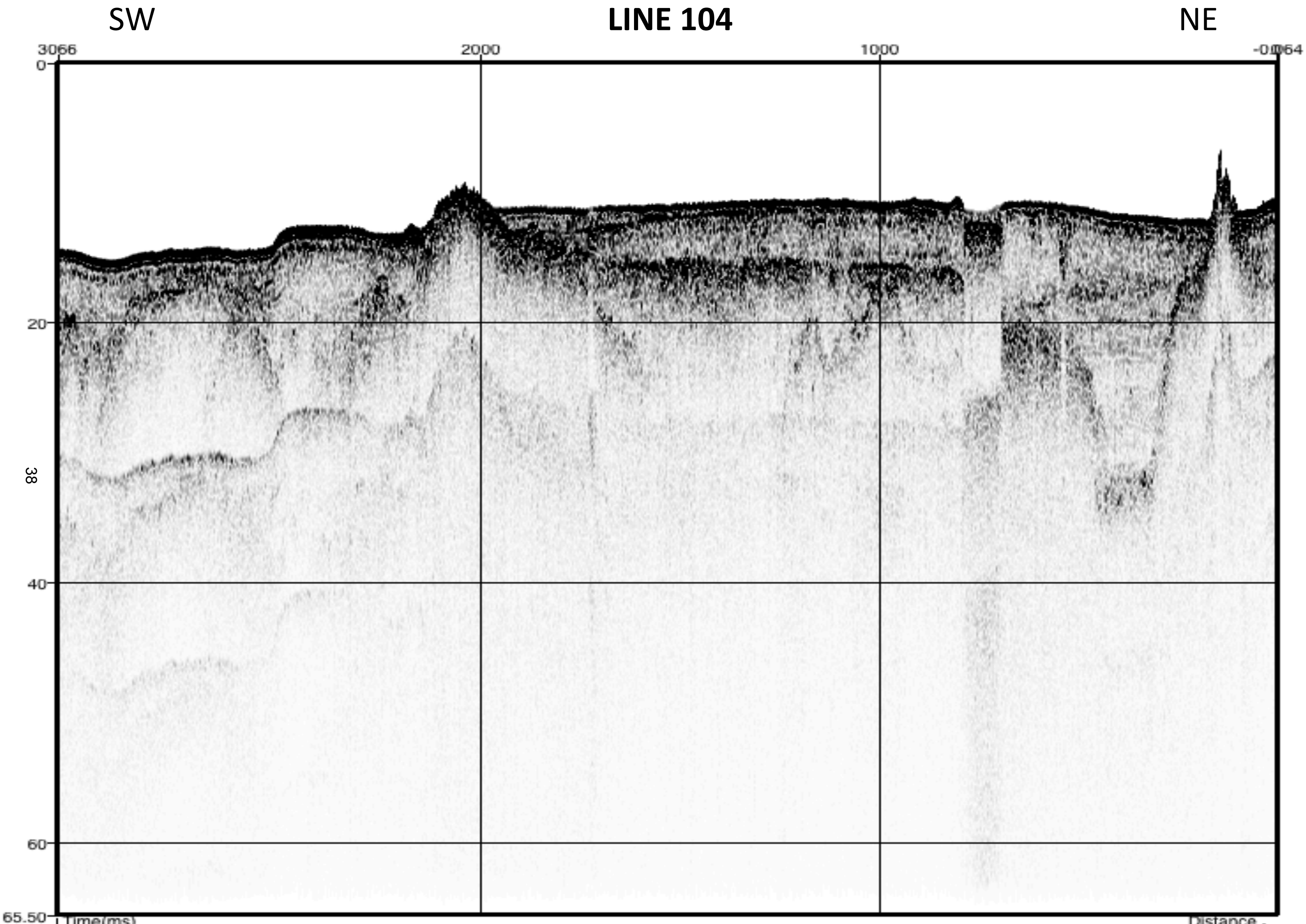
SW
LINE 104
NE
3066
2000
1000
-0.064
0
20
40
60
65.50
Time(ms)
Distance

SW **Line 105** NE

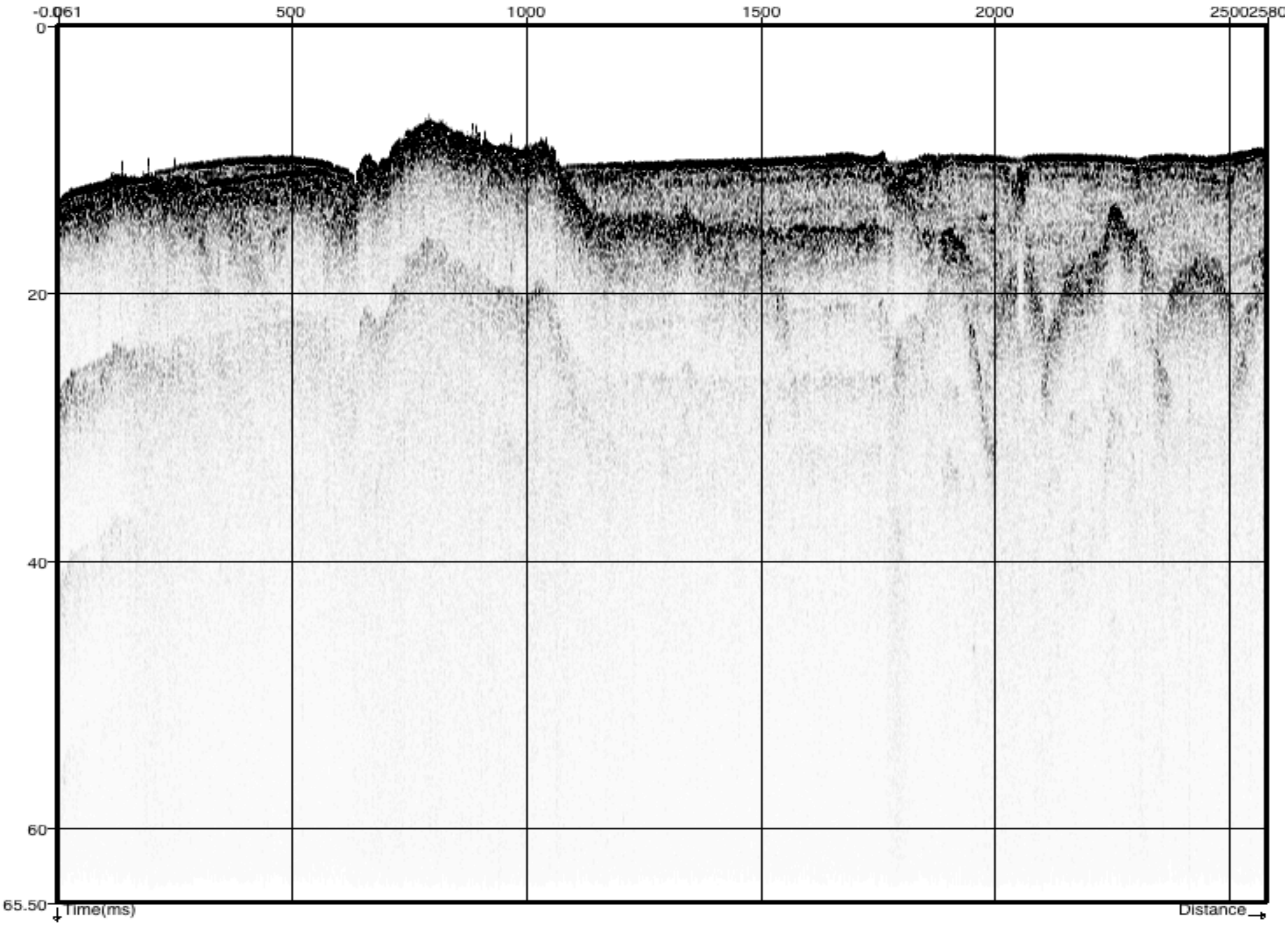

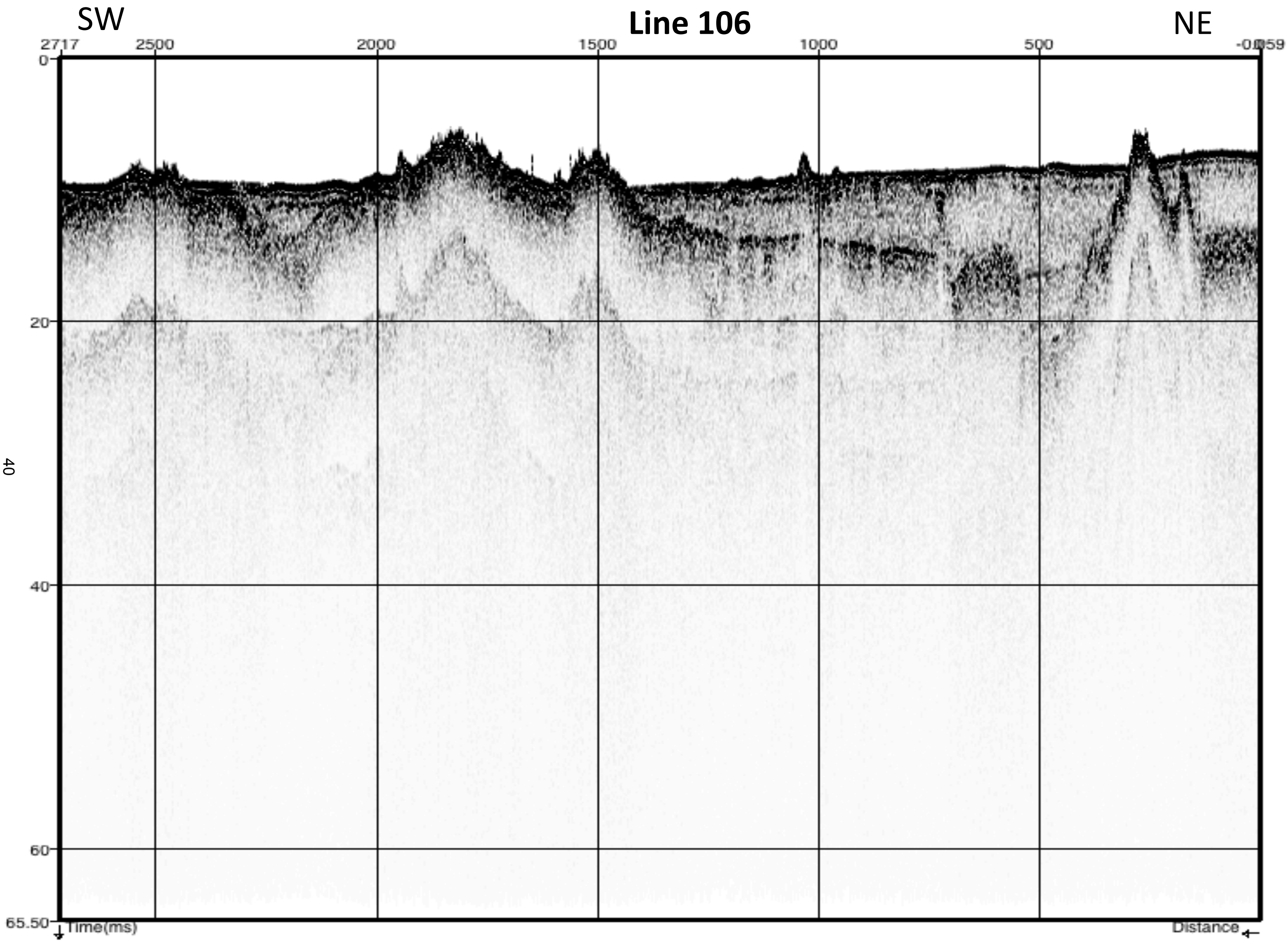
SW
Line 106
NE
2717
2500
2000
1500
1000
500
0
20
40
60
65.50
Time(ms)
Distance

Line 107

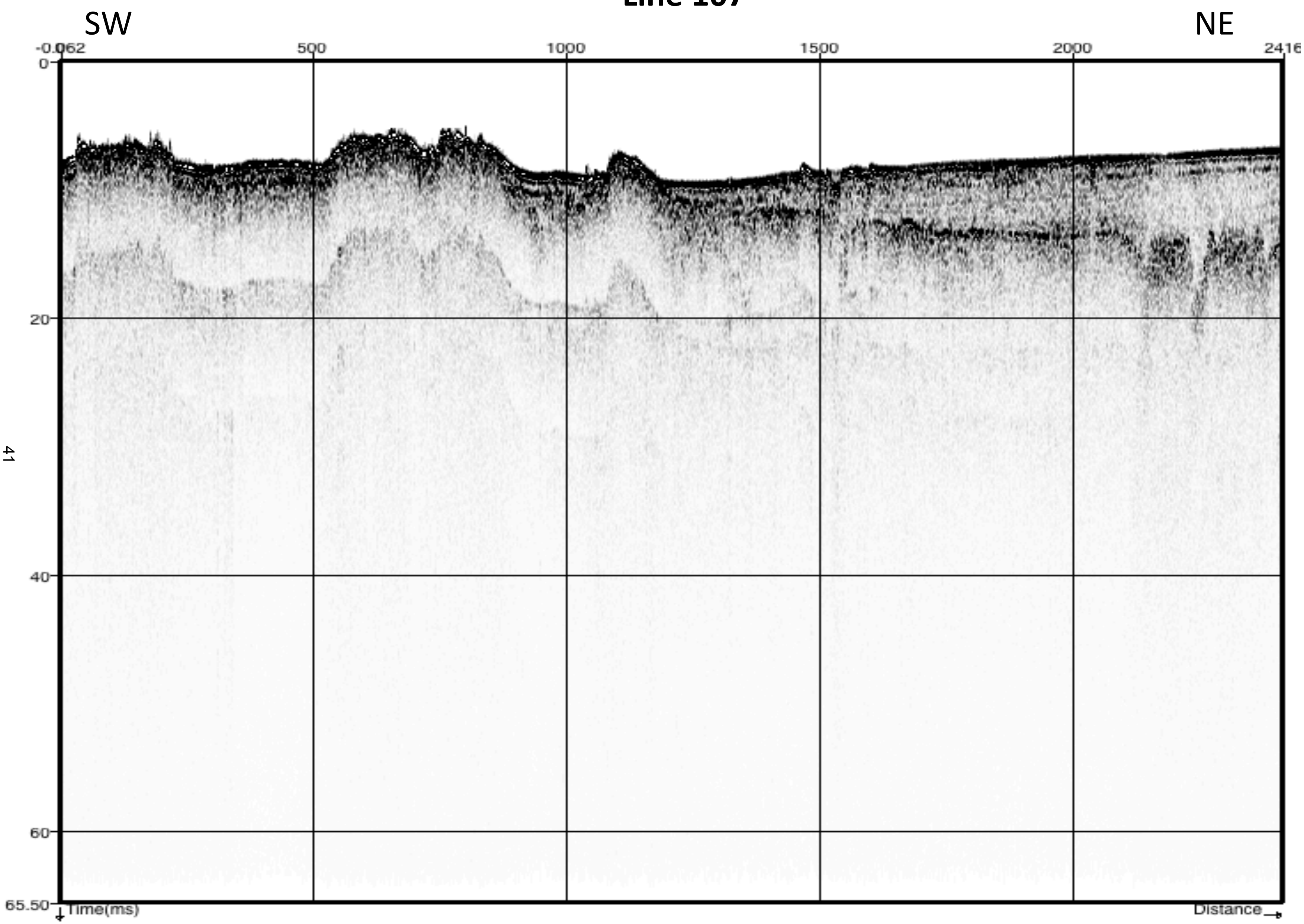

SW
NE
-0.062
500
1000
1500
2000
2416
0
20
40
60
65.50
Time(ms)
Distance

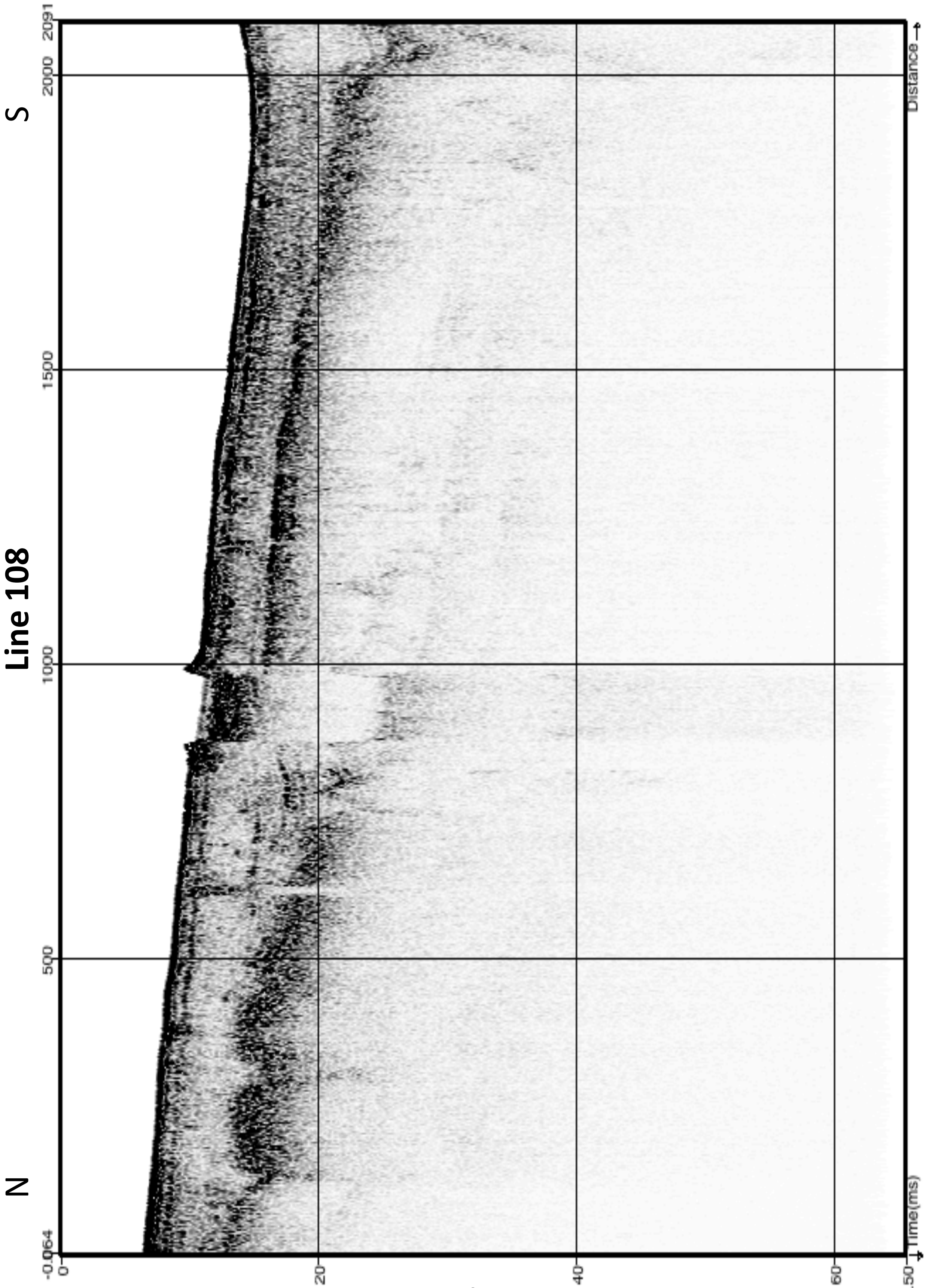
N
Line 108
S
Distance
Time(ms)
-0.064
500
1000
1500
2000
2091
0
20
40
60
65.50

Line 108_turn (various course changes)

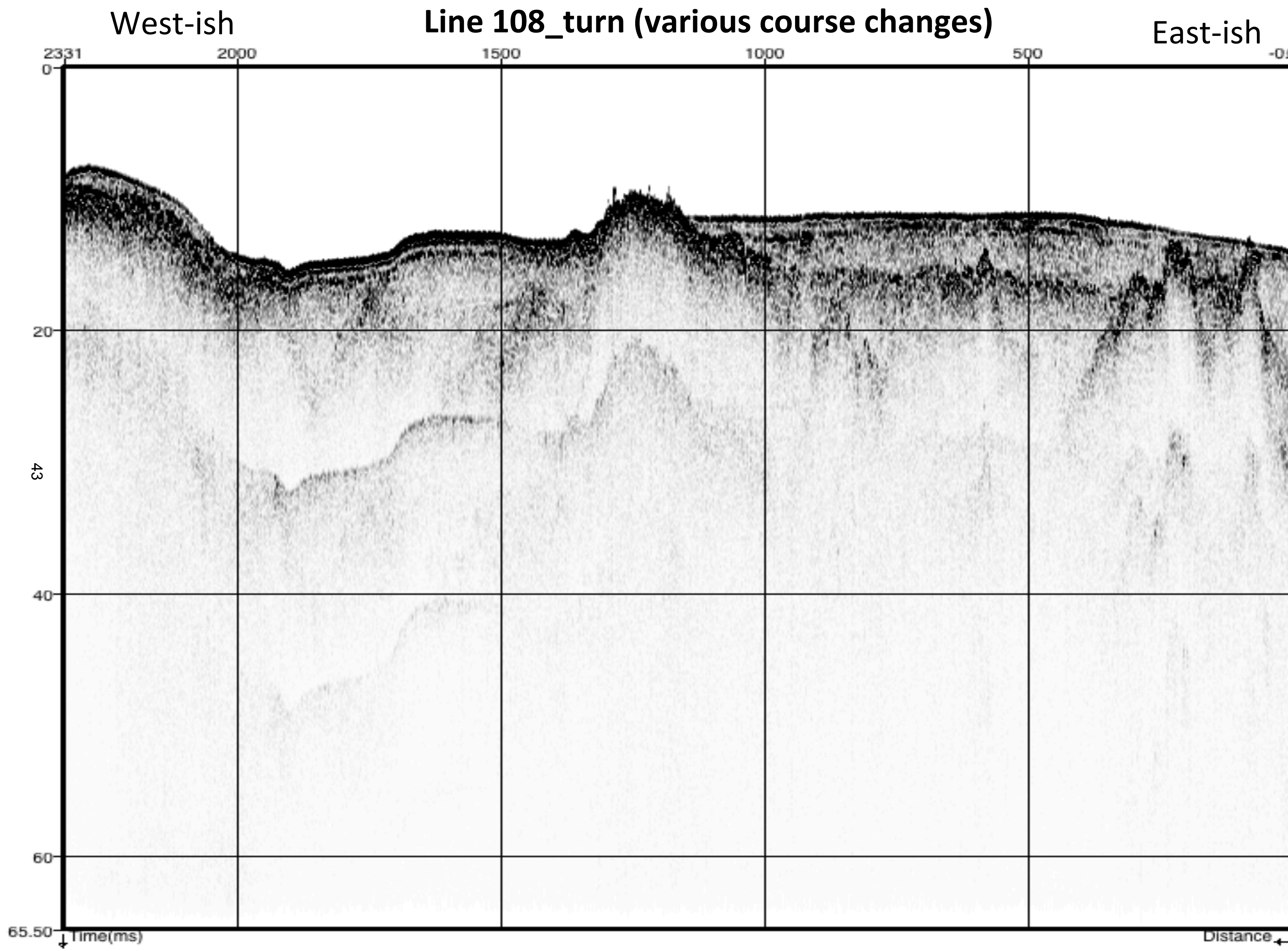

Line 109

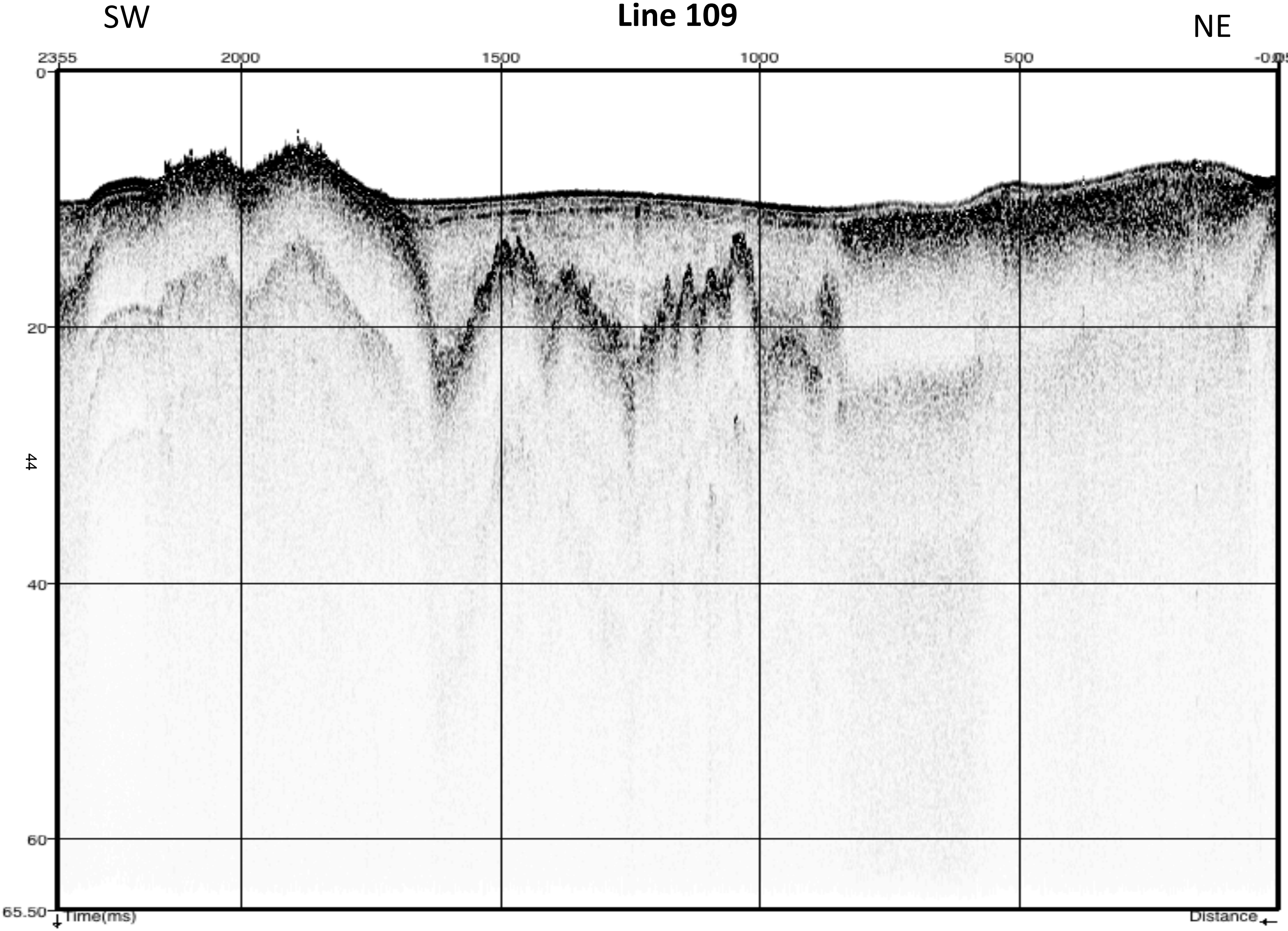
SW
NE
2355
2000
1500
1000
500
-0.05
0
20
40
60
65.50
Time(ms)
Distance

Line 110 - tieline

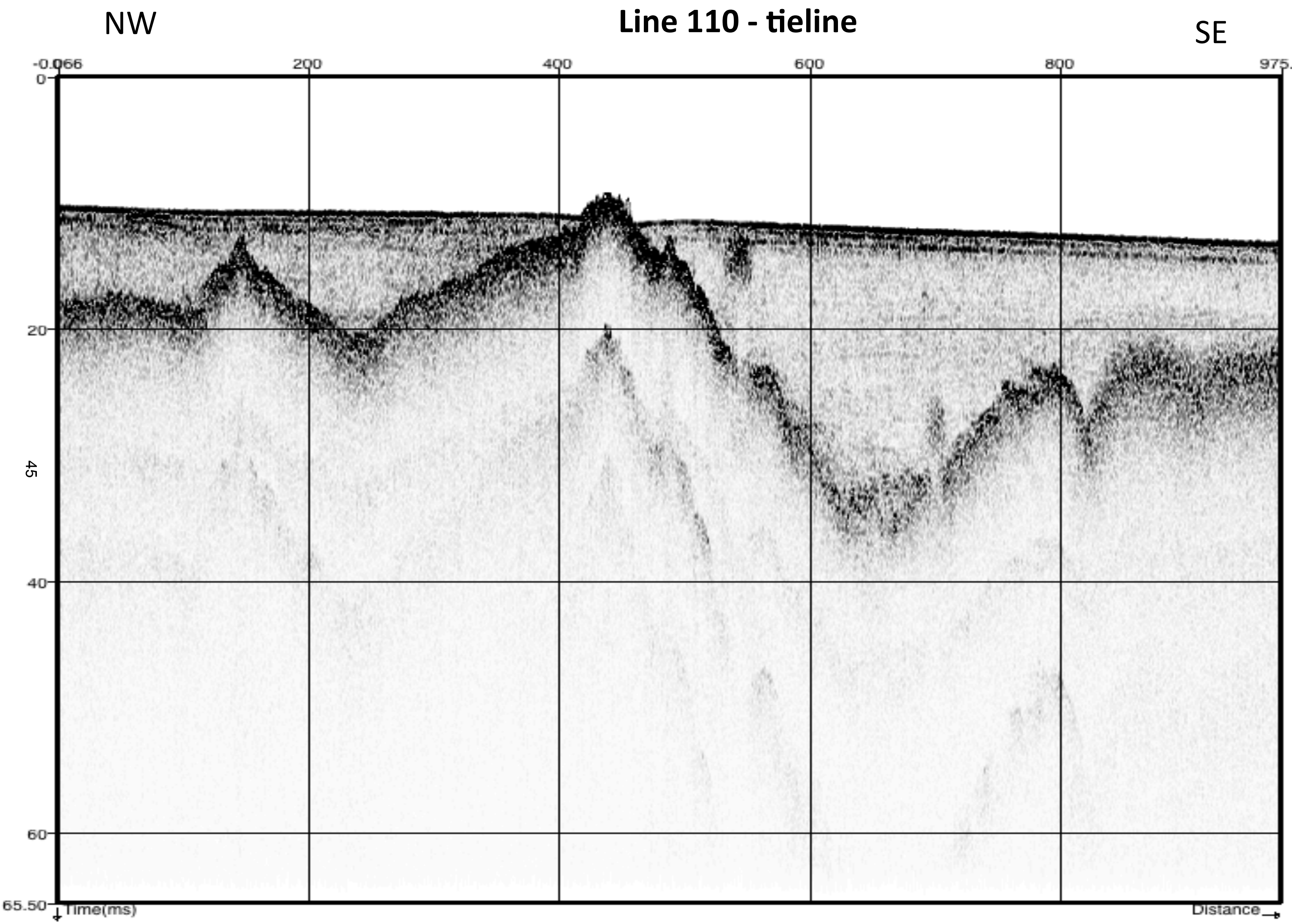

Line 110_turn

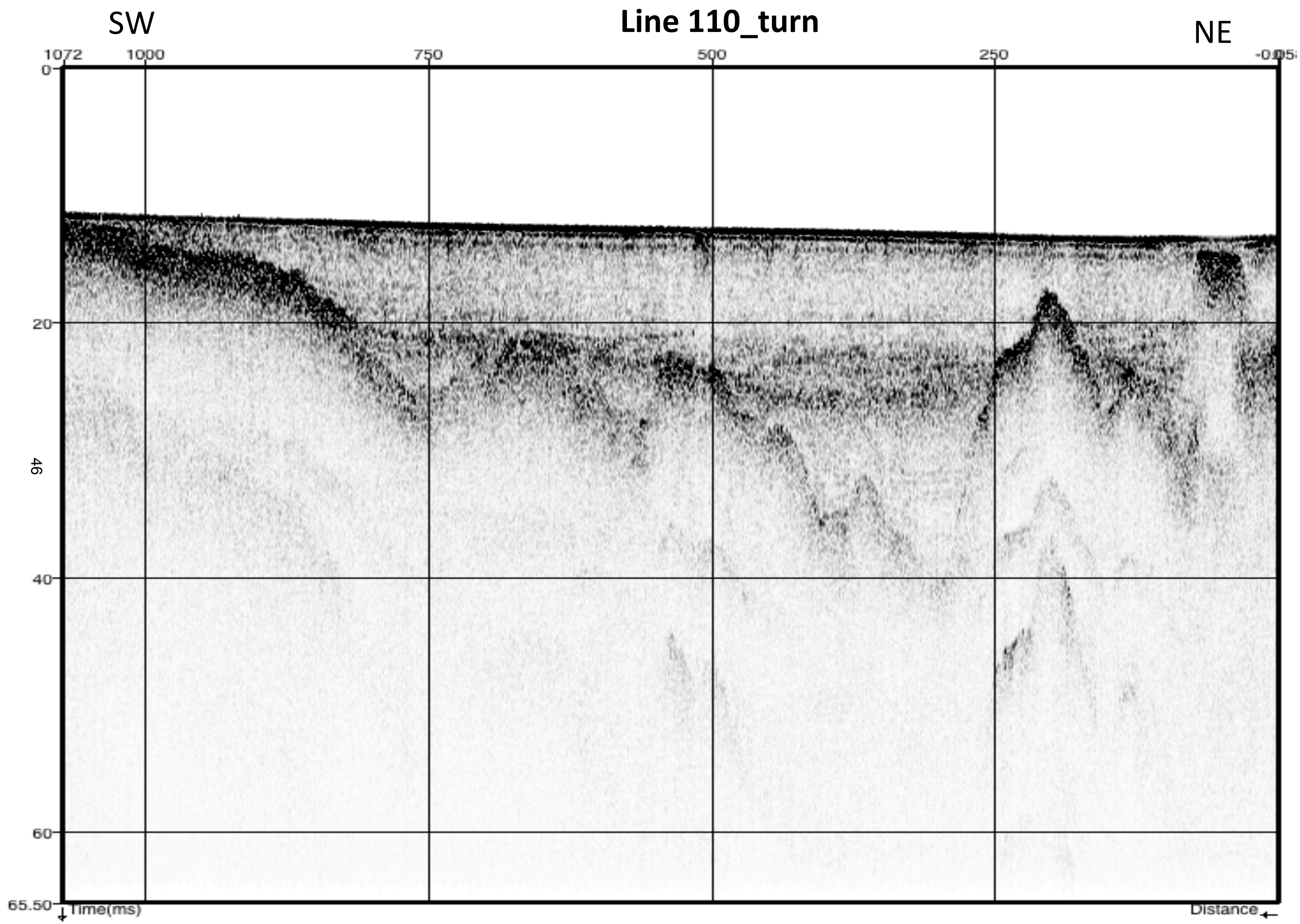

Line 111

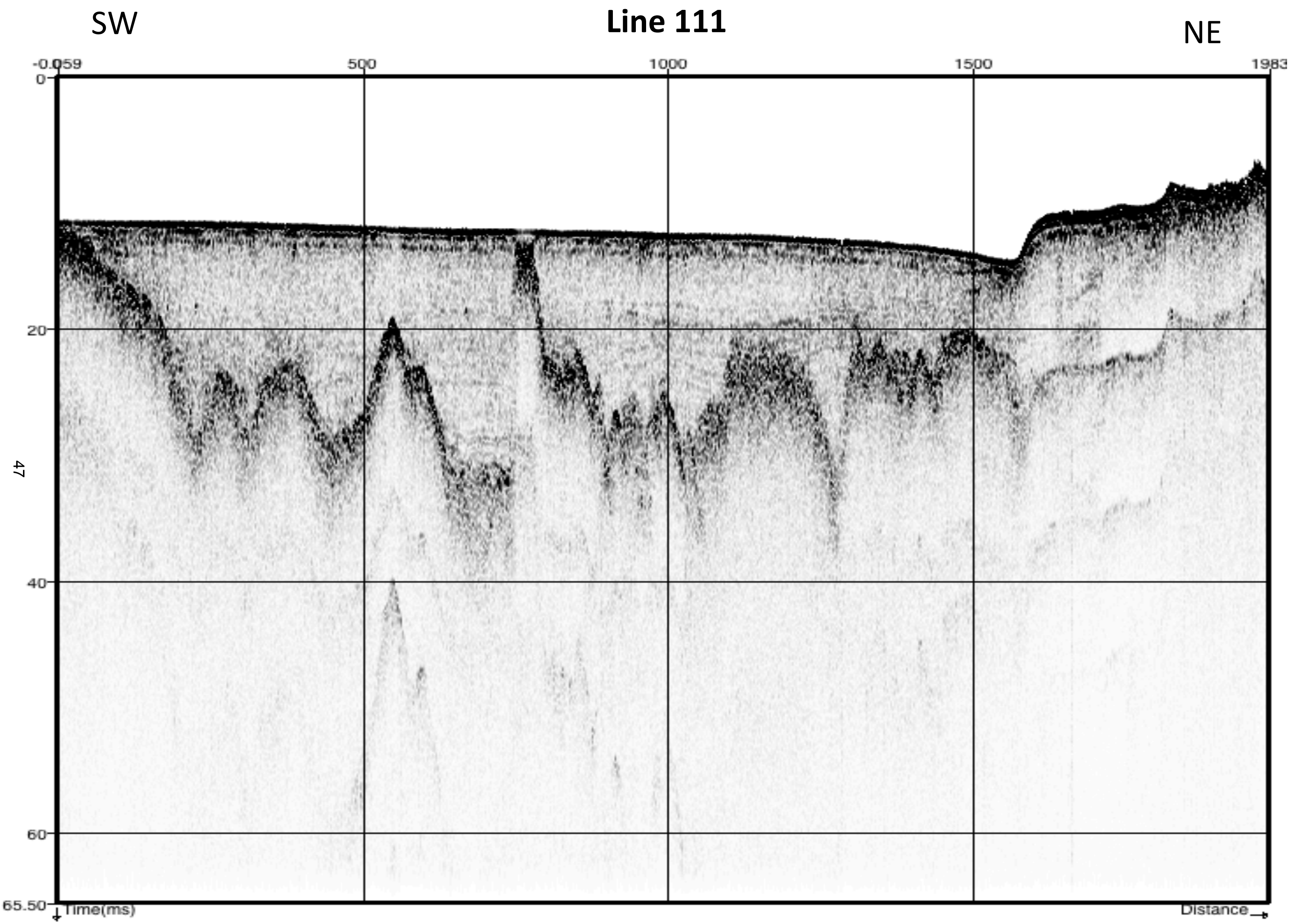

Line 112

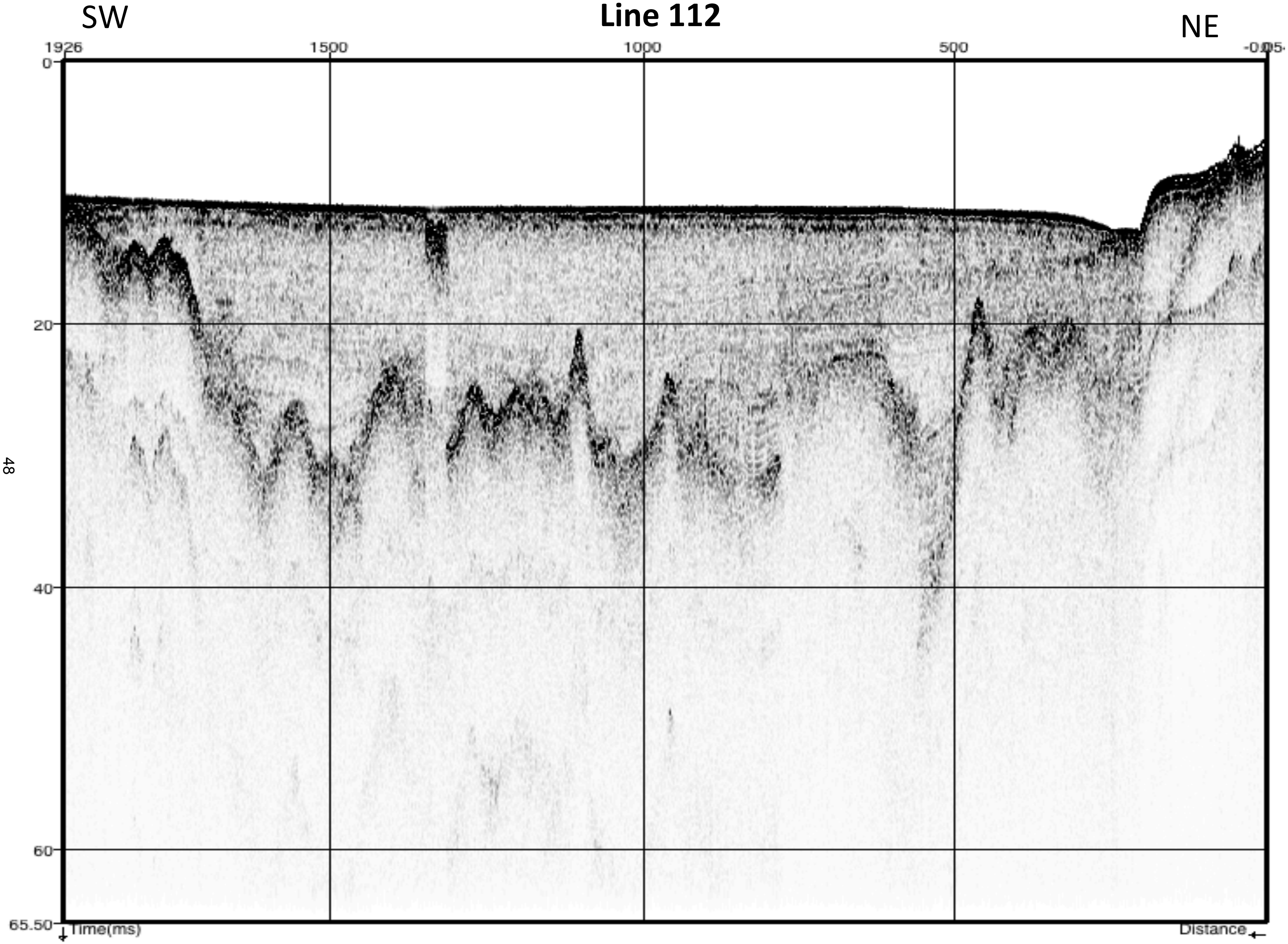

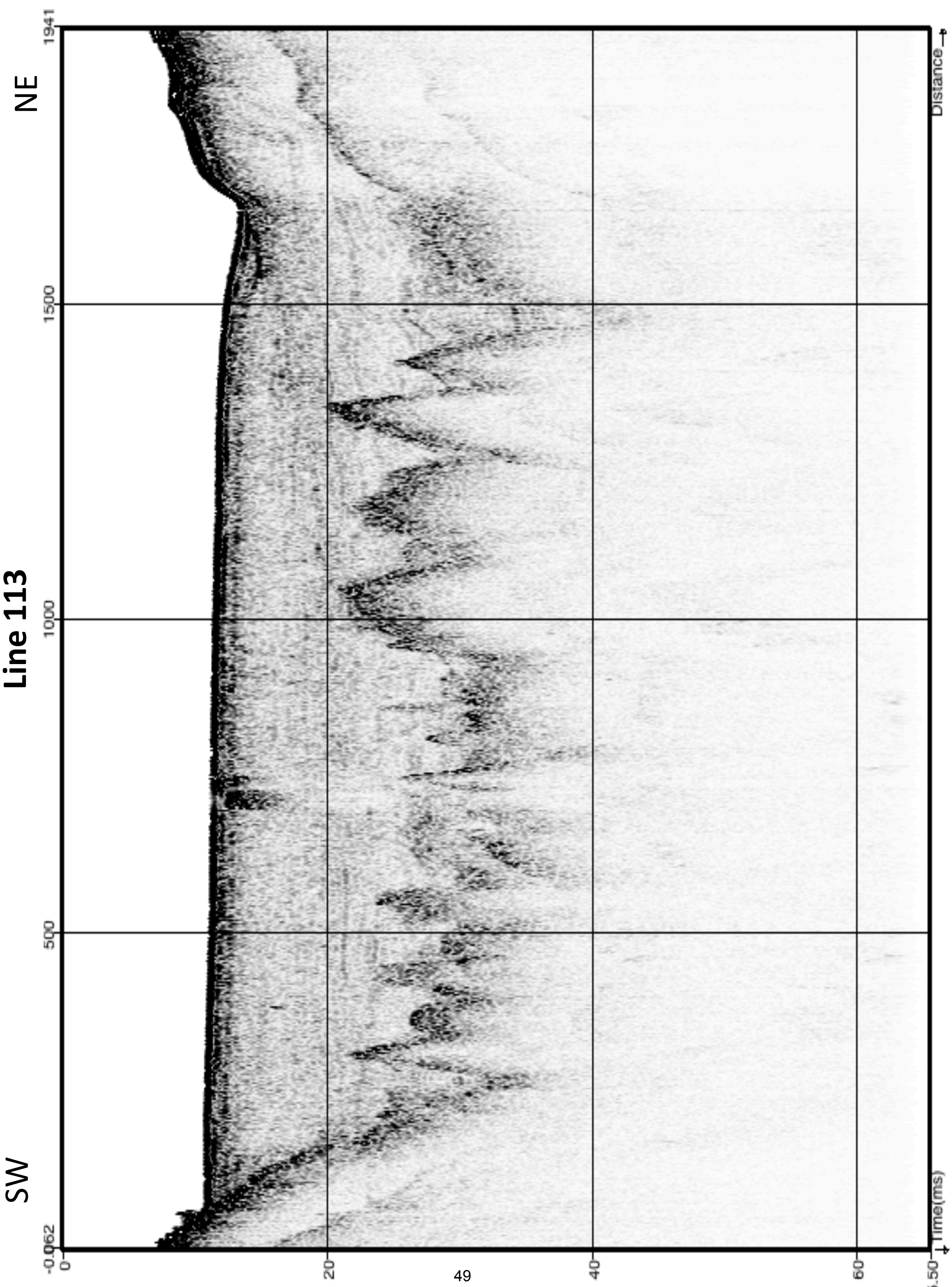

SW
Line 113
NE
-0.062
500
1000
1500
1941
Distance
Time(ms)
0
20
40
60
65.50

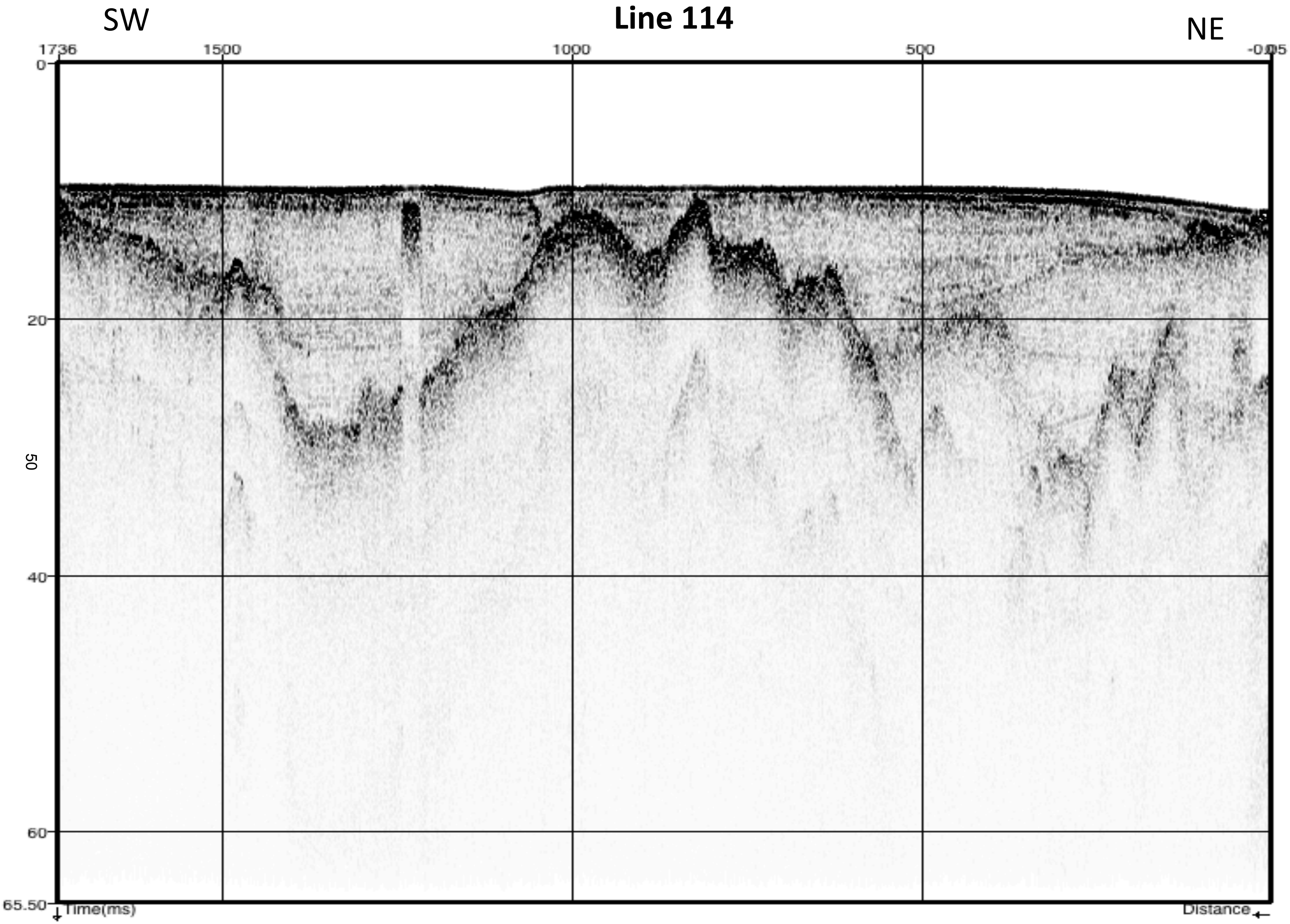
SW
Line 114
NE
1736
1500
1000
500
-0.05
0
20
40
60
65.50
Time(ms)
Distance

Line 115

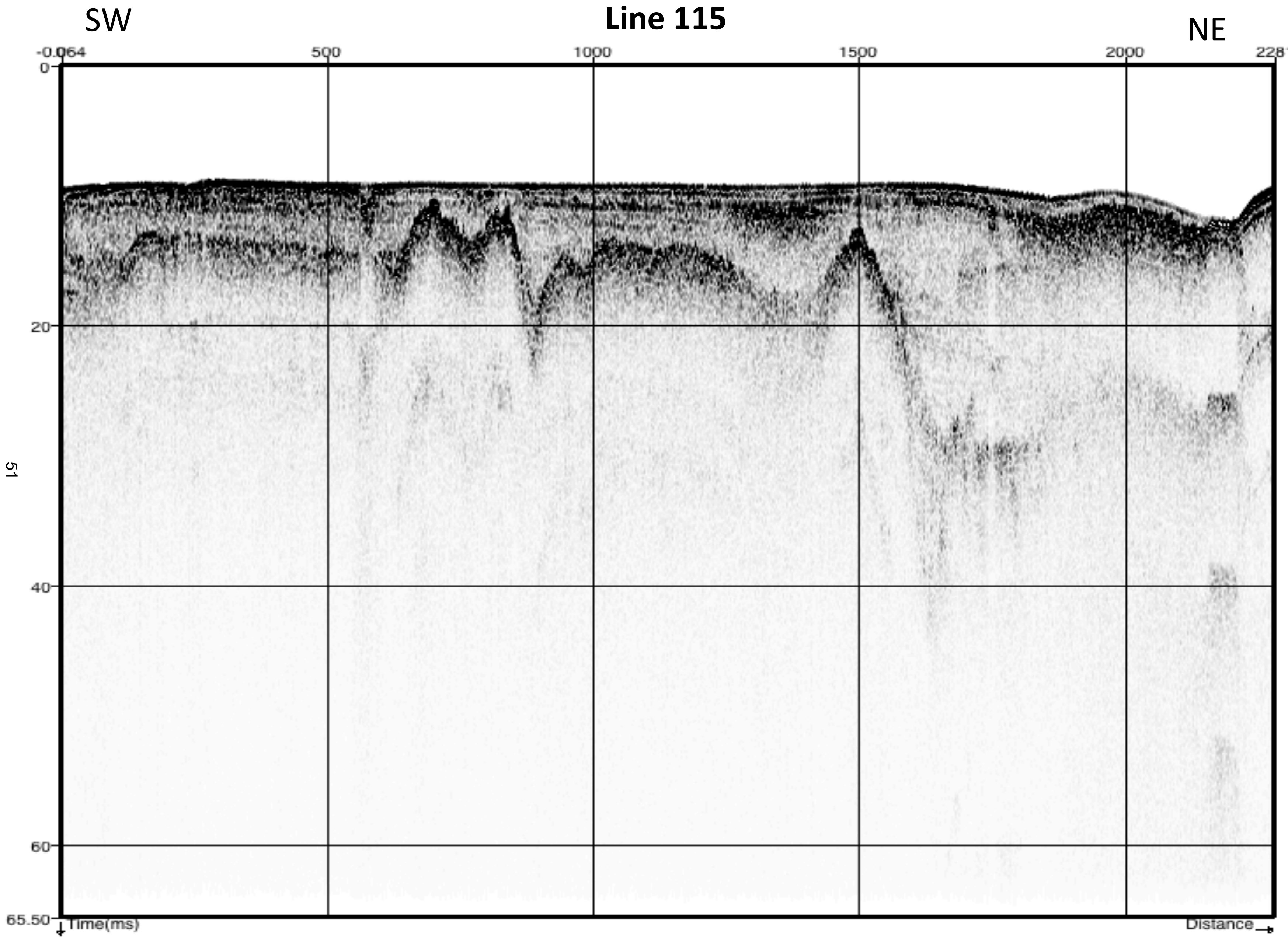

SW
NE
-0.064
500
1000
1500
2000
2281
0
20
40
60
65.50
Time(ms)
Distance

Line 201

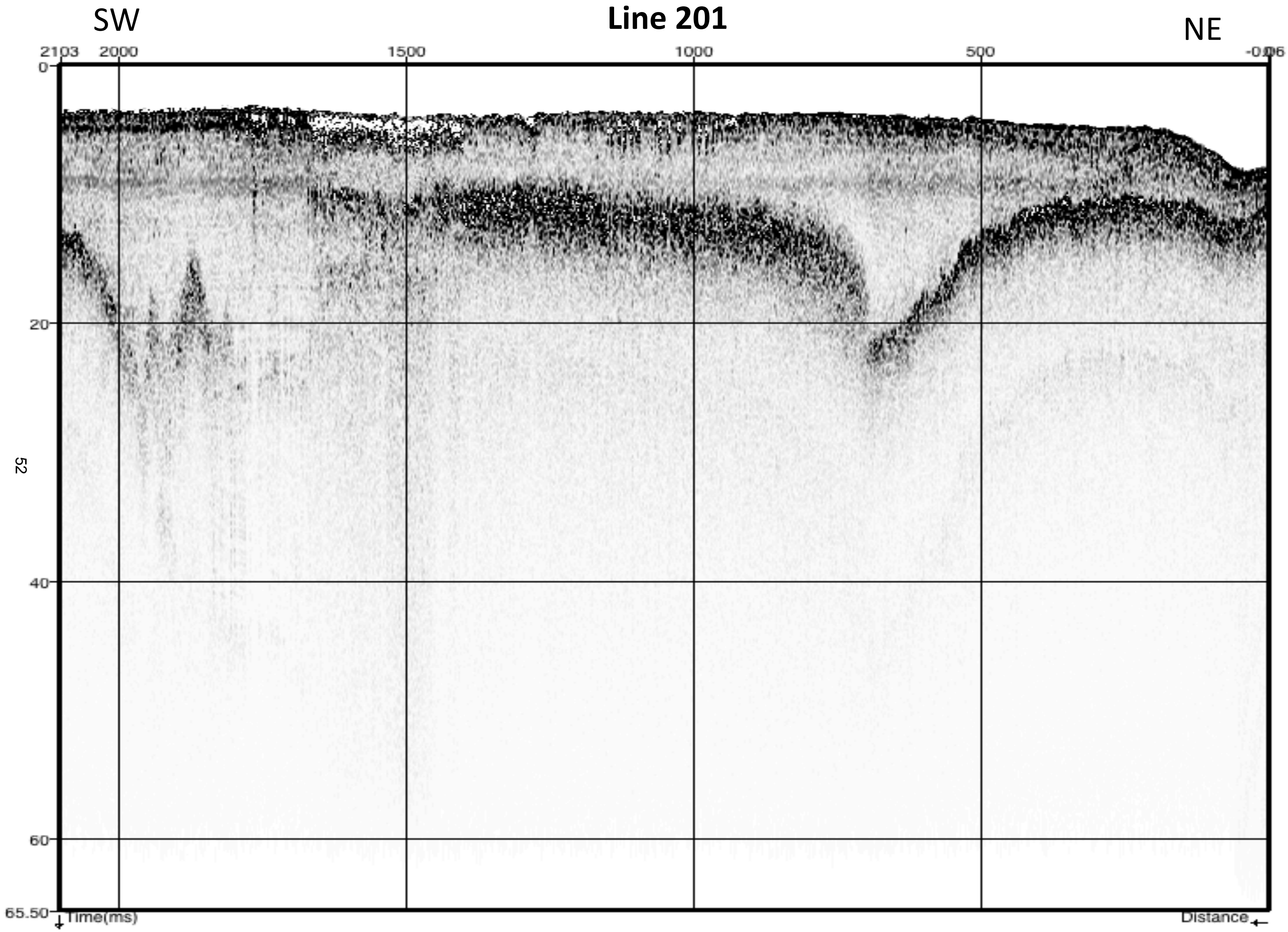
SW
NE
2103
2000
1500
1000
500
-0.06
0
20
40
60
65.50
Time(ms)
Distance

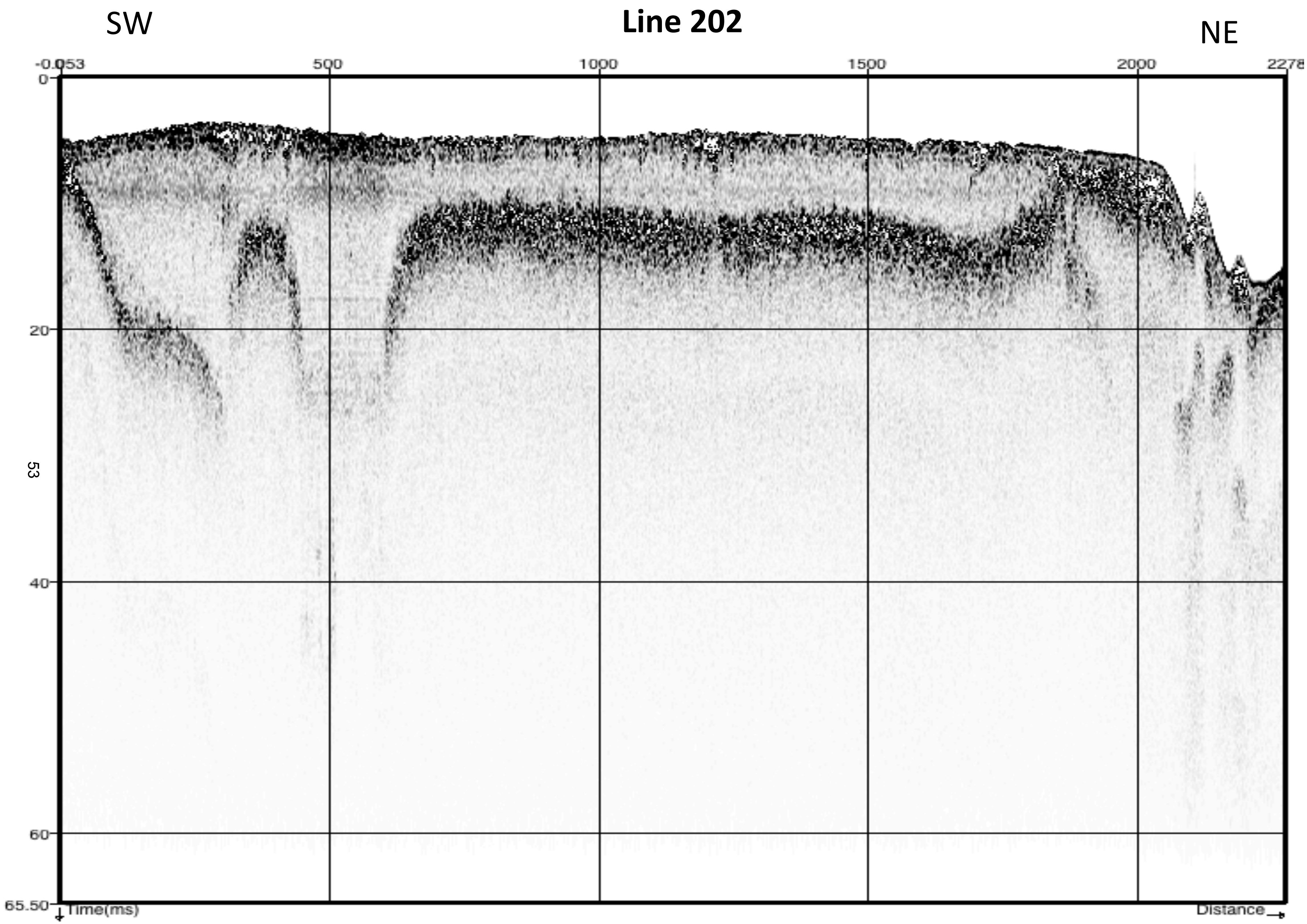
SW
Line 202
NE
-0.053
500
1000
1500
2000
2278
0
20
40
60
65.50
Time(ms)
Distance

Line 203

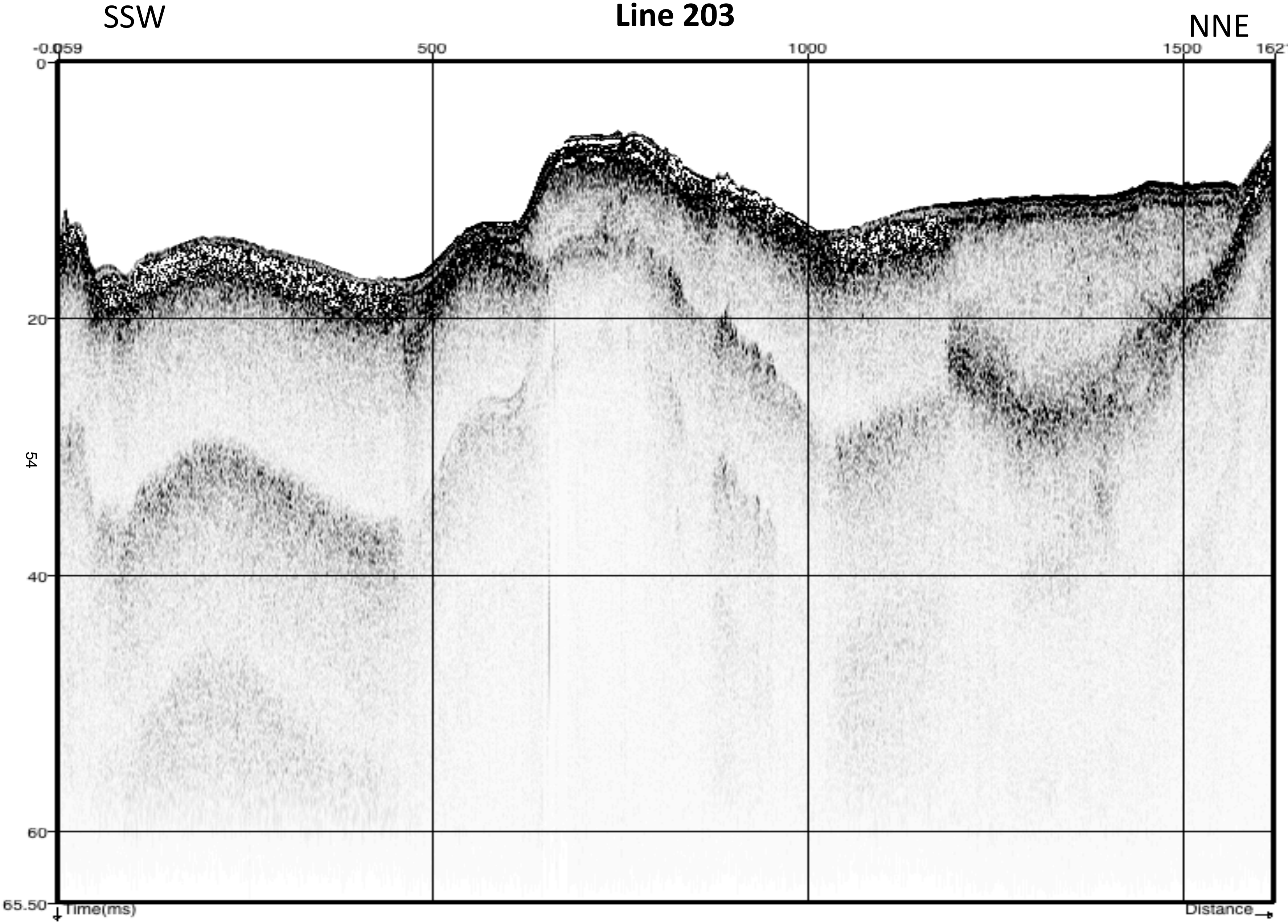
SSW
NNE
-0.059
500
1000
1500
1621
0
20
40
60
65.50
Time(ms)
Distance

Line 204

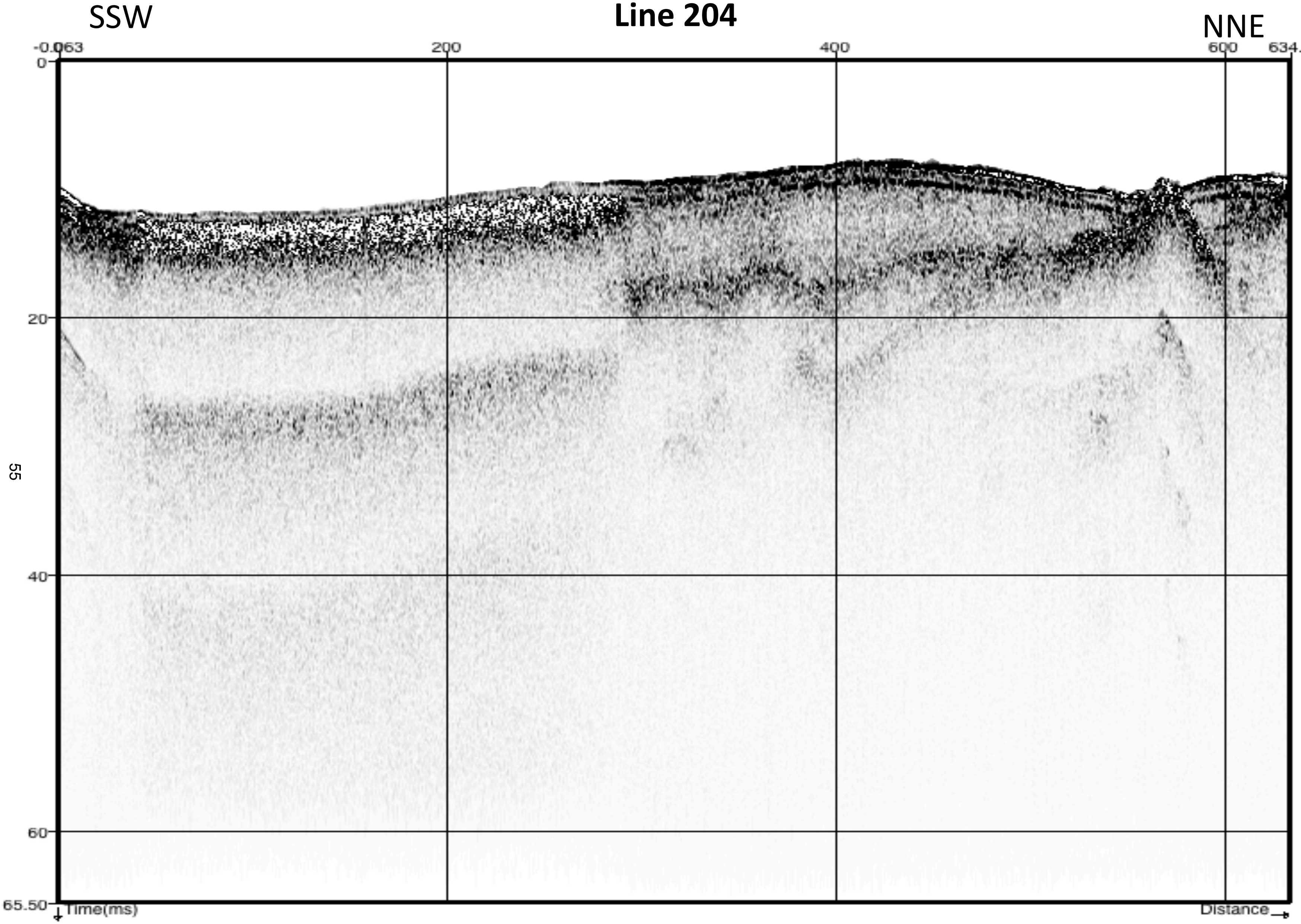

Line 205

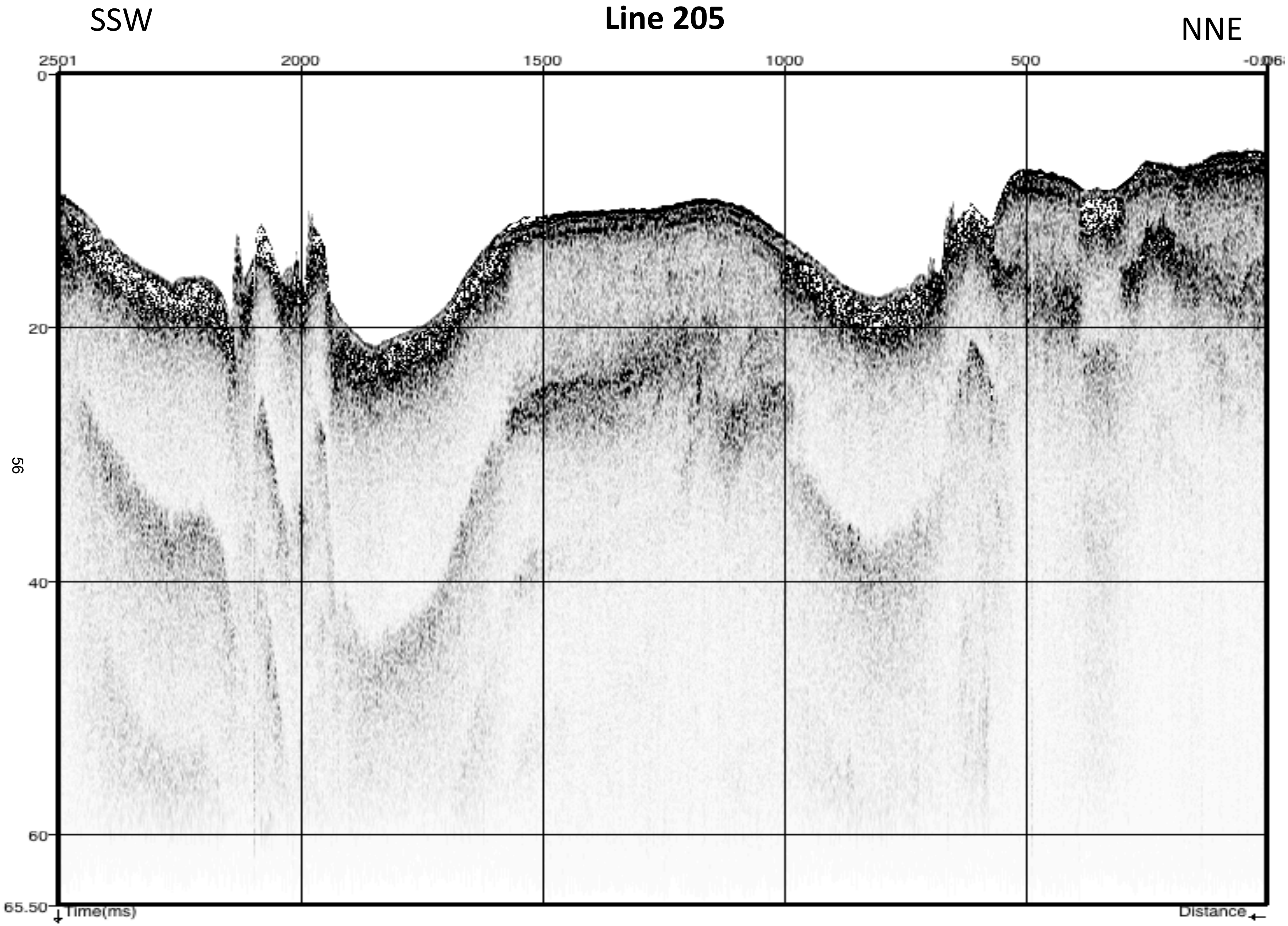
SSW
NNE
2501
2000
1500
1000
500
0
20
40
60
65.50
Time(ms)
Distance

Line 206

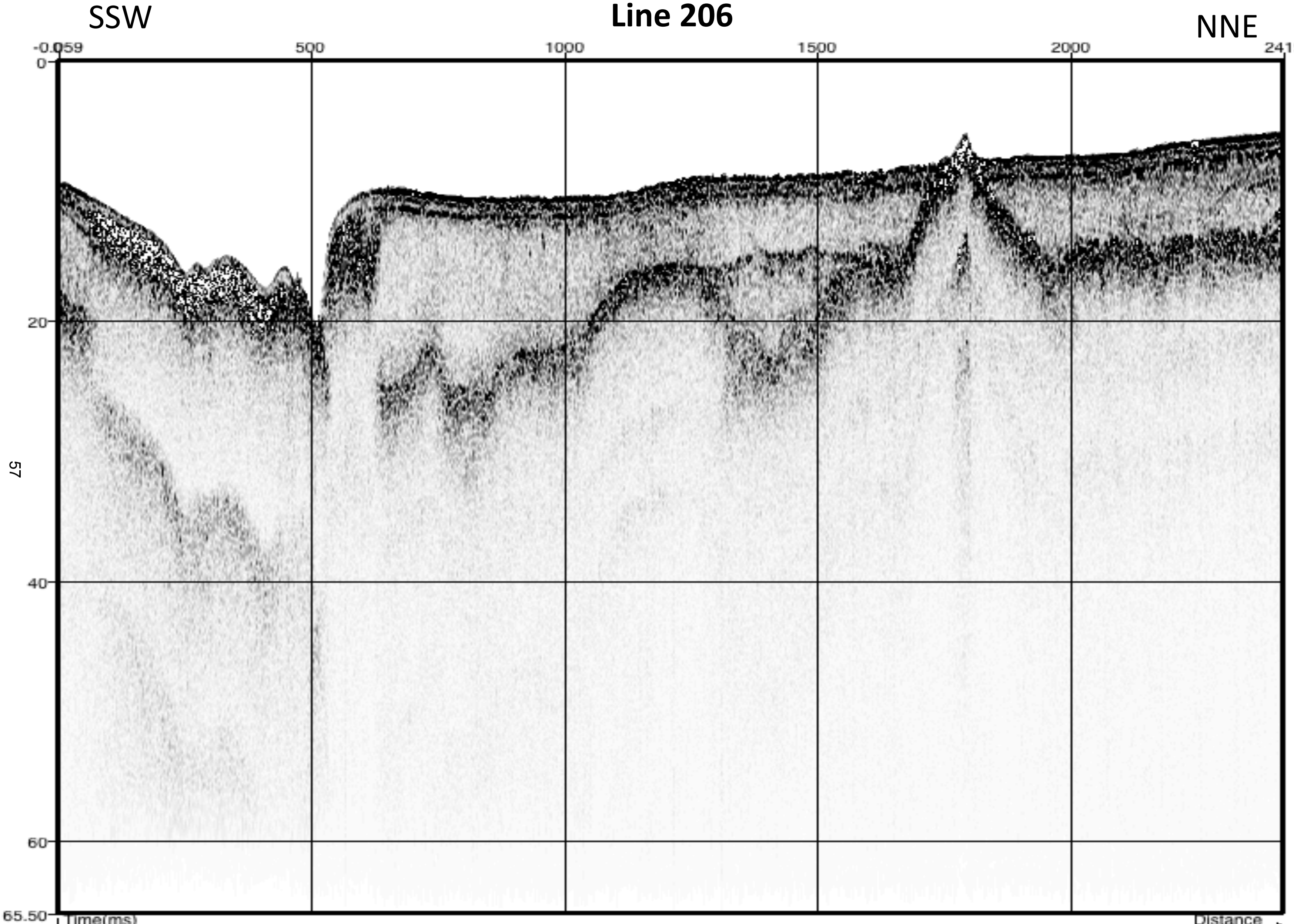
SSW
NNE
-0.059
500
1000
1500
2000
2419
0
20
40
60
65.50
Time(ms)
Distance

NW **Line 207, tie line and turn (course changes)** SE and then SSW

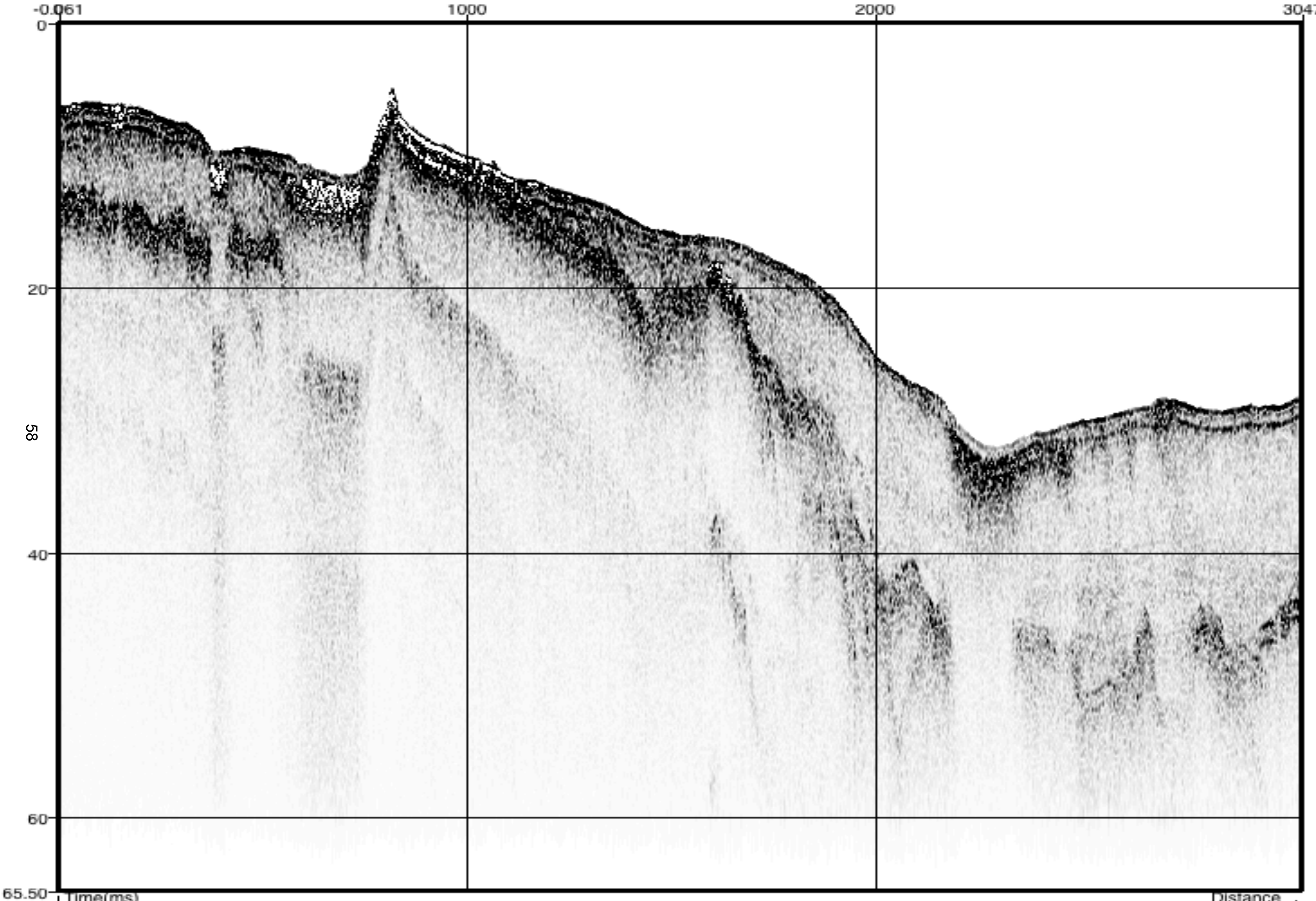

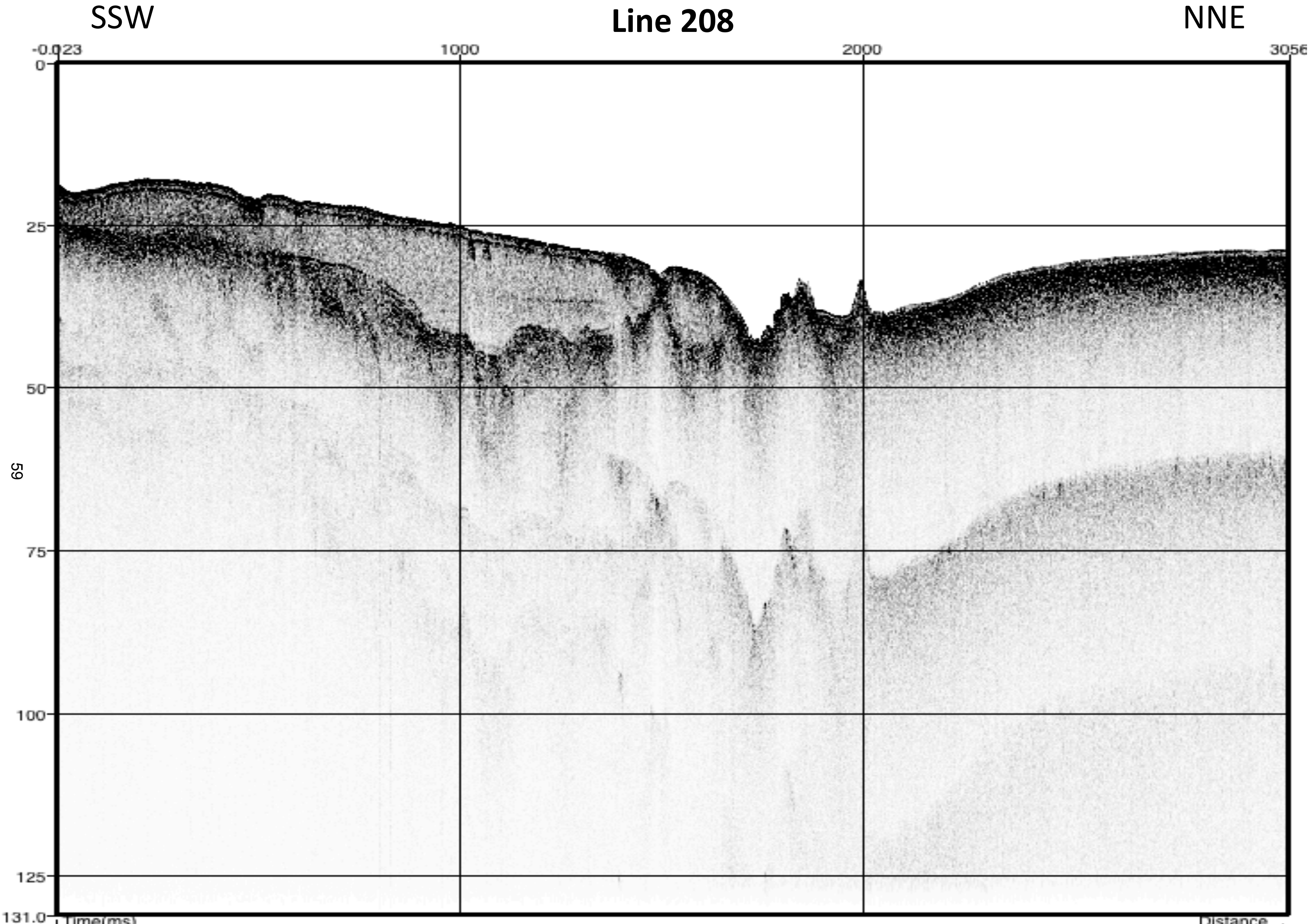
SSW
Line 208
NNE
-0.023
1000
2000
3056
0
25
50
75
100
125
131.0
Time(ms)
Distance

Line 209

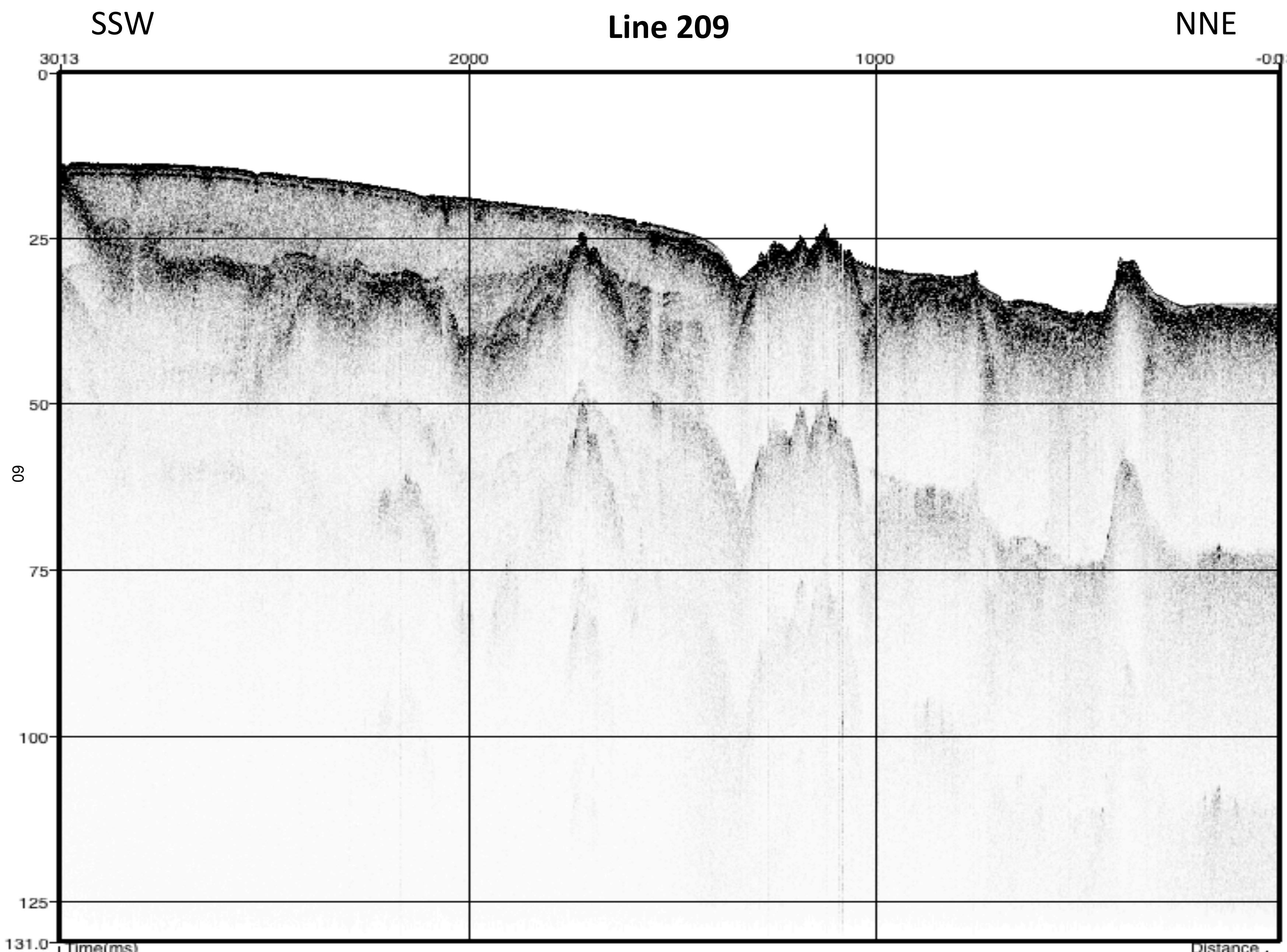

SSW
NNE
3013
2000
1000
-0.03
0
25
50
75
100
125
131.0
Time(ms)
Distance

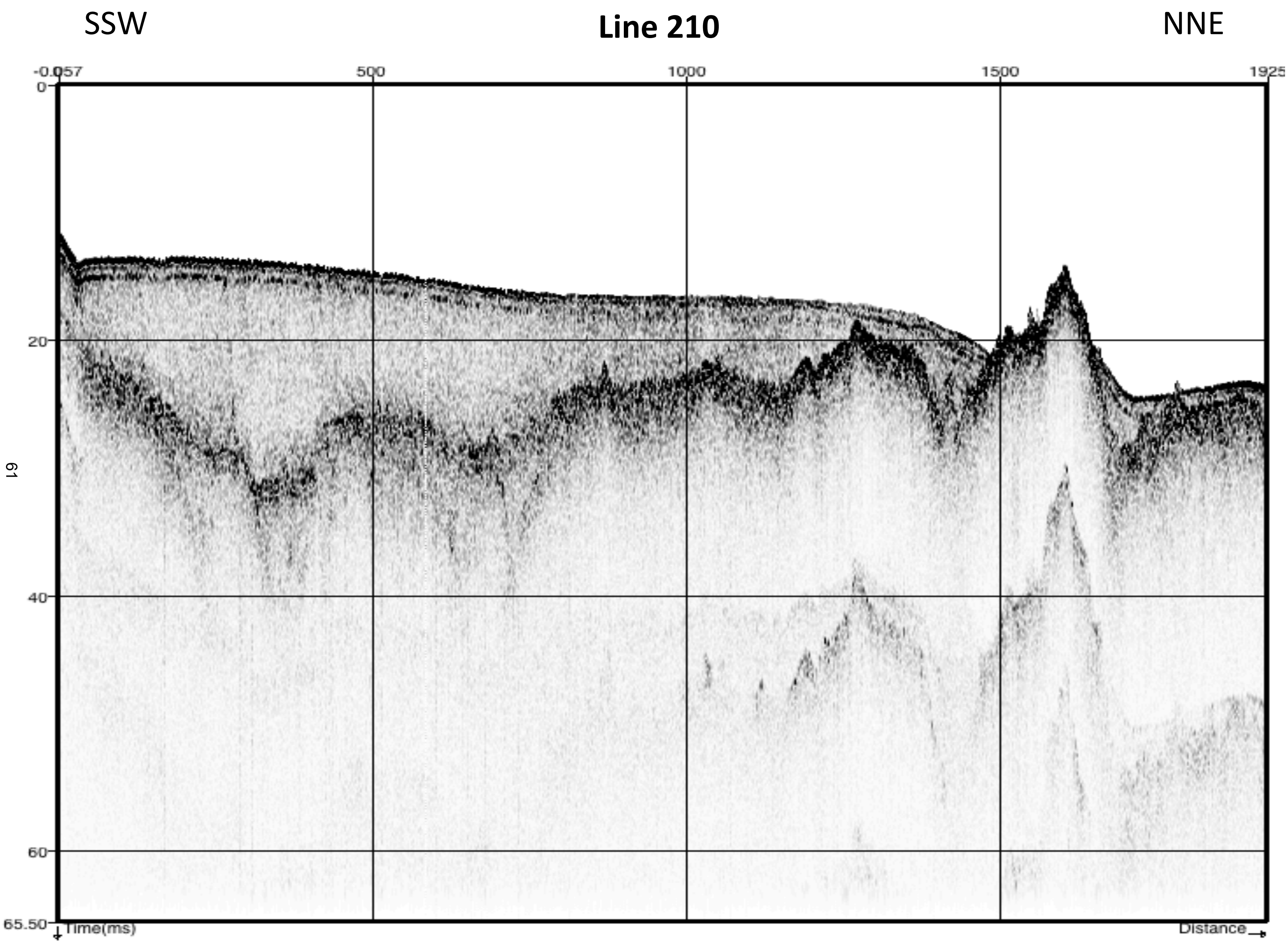
SSW
Line 210
NNE
-0.057
500
1000
1500
1925
0
20
40
60
65.50
Time(ms)
Distance

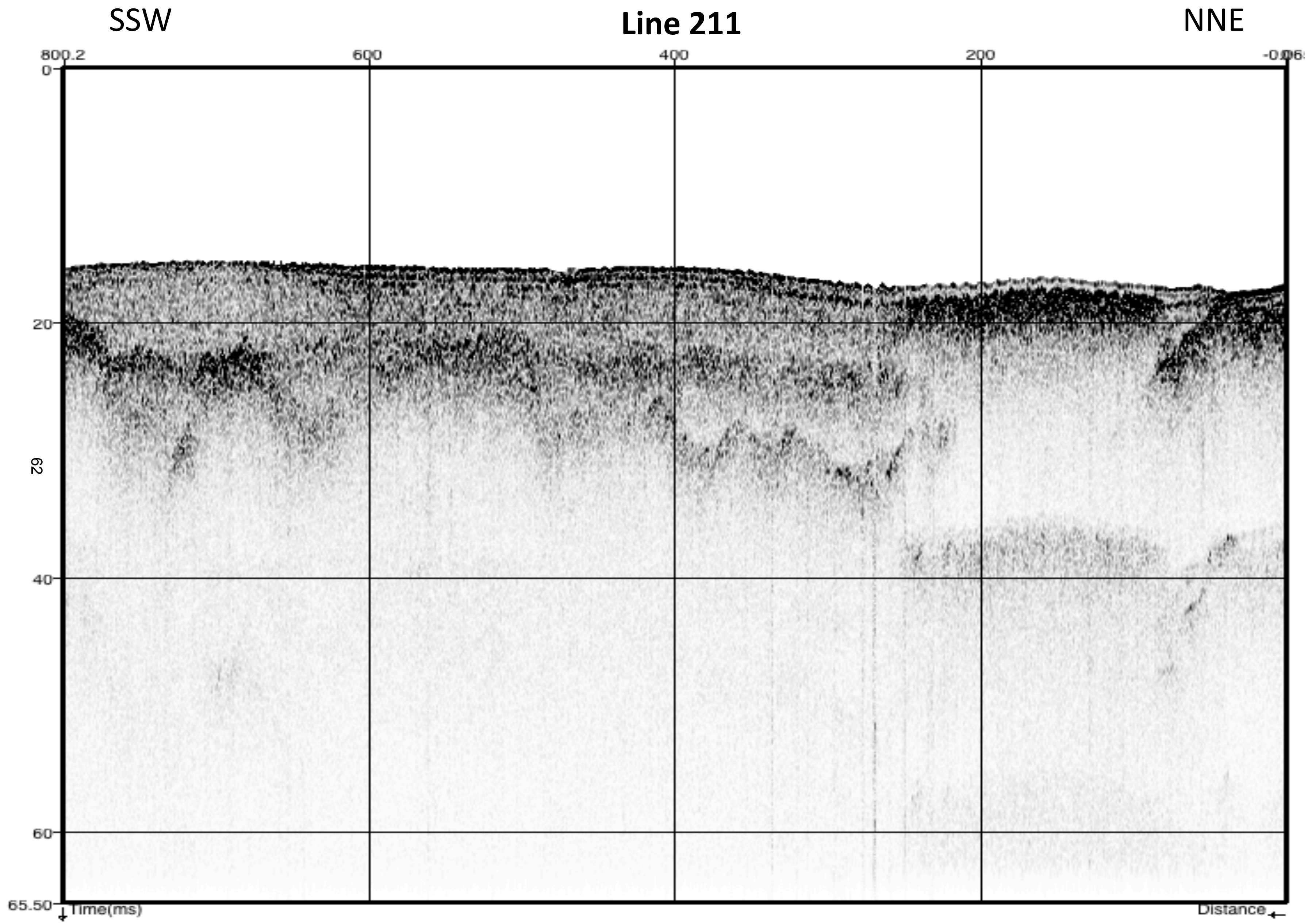

SSW
Line 211
NNE
800.2
600
400
200
-0.06
0
20
40
60
65.50
Time(ms)
Distance

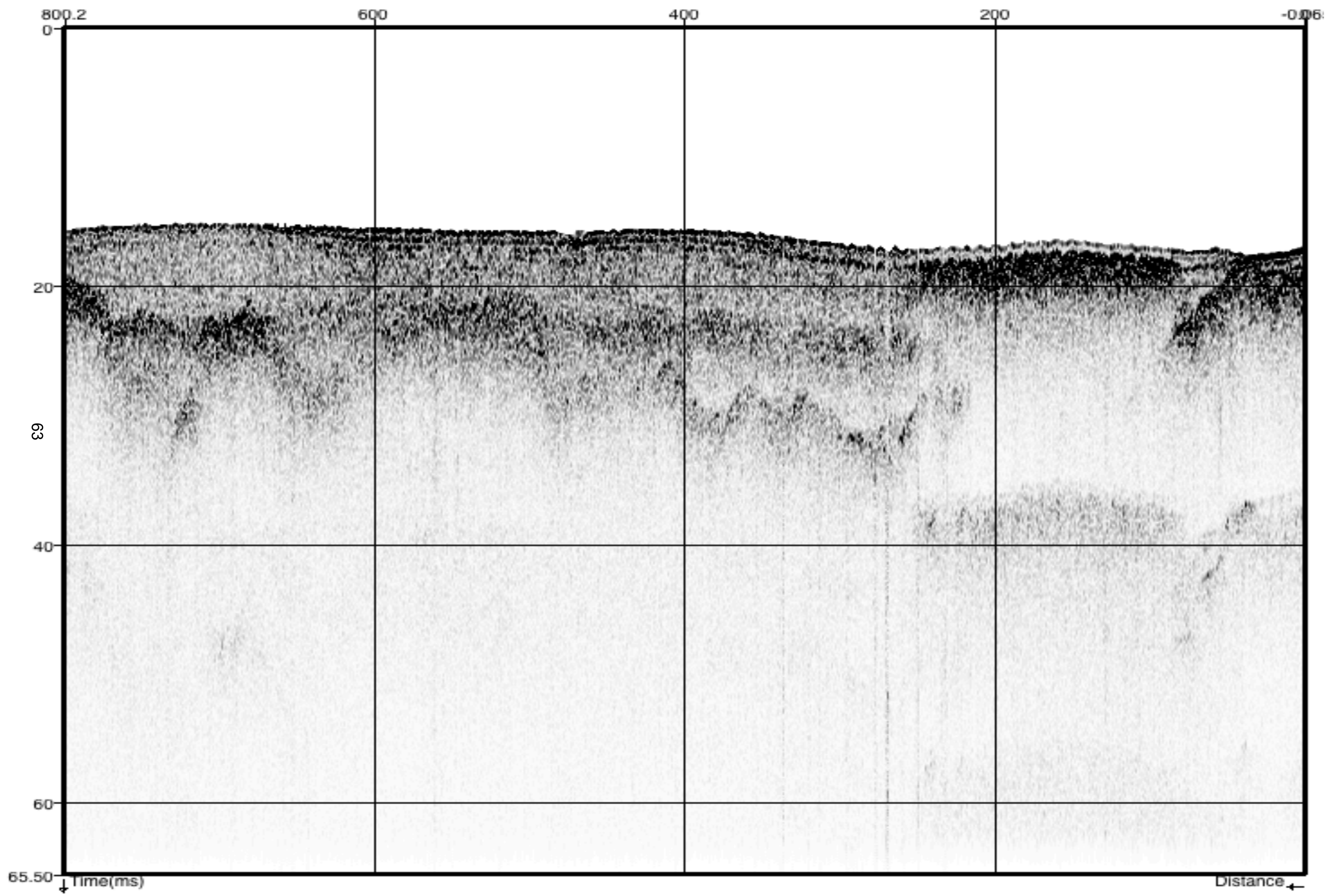
SSW
Line 211
NNE
800.2
600
400
200
0
20
40
60
65.50
Time(ms)
Distance

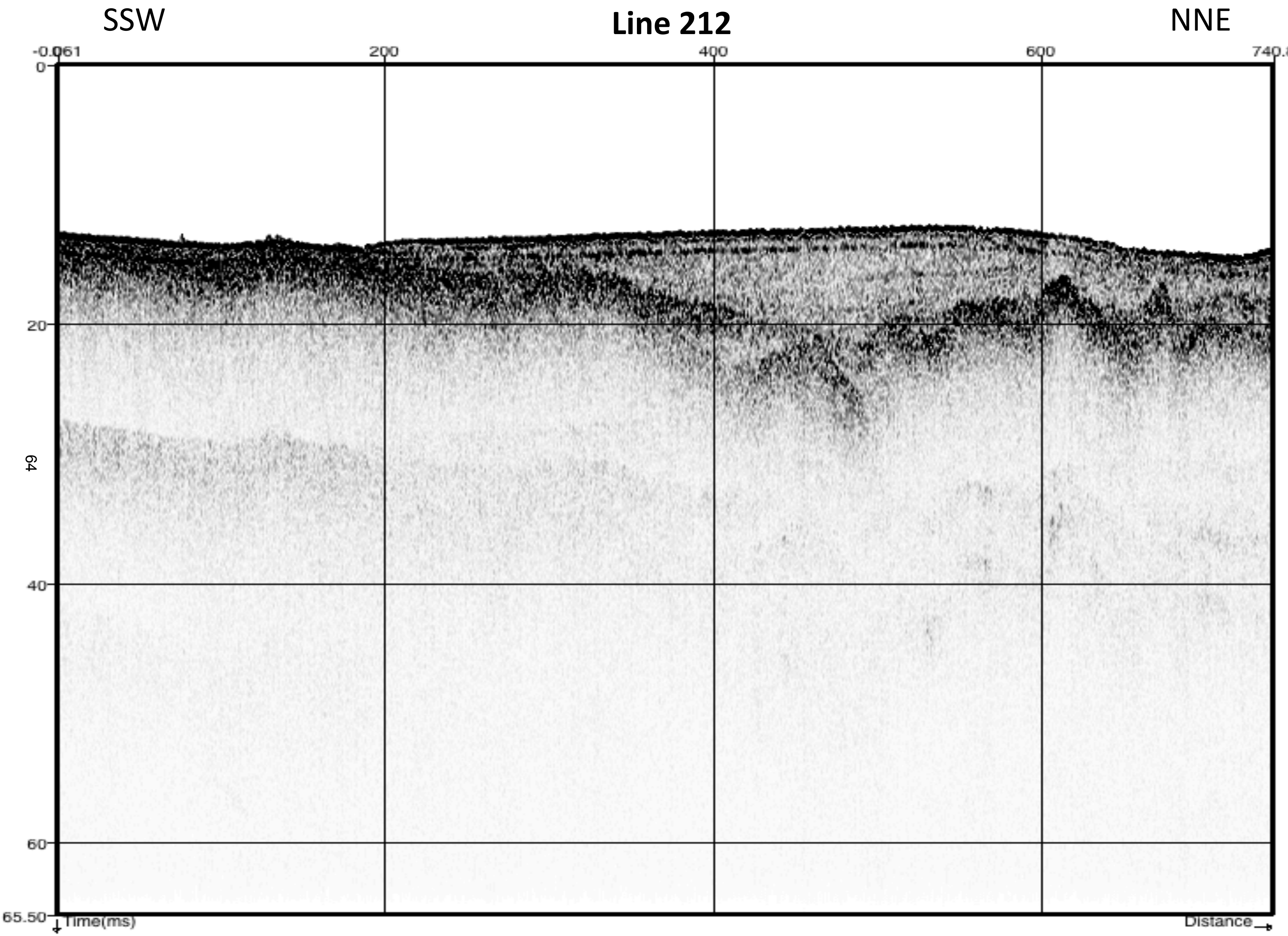
SSW
Line 212
NNE
-0.061
200
400
600
740.8
0
20
40
60
65.50
Time(ms)
Distance

Line 213

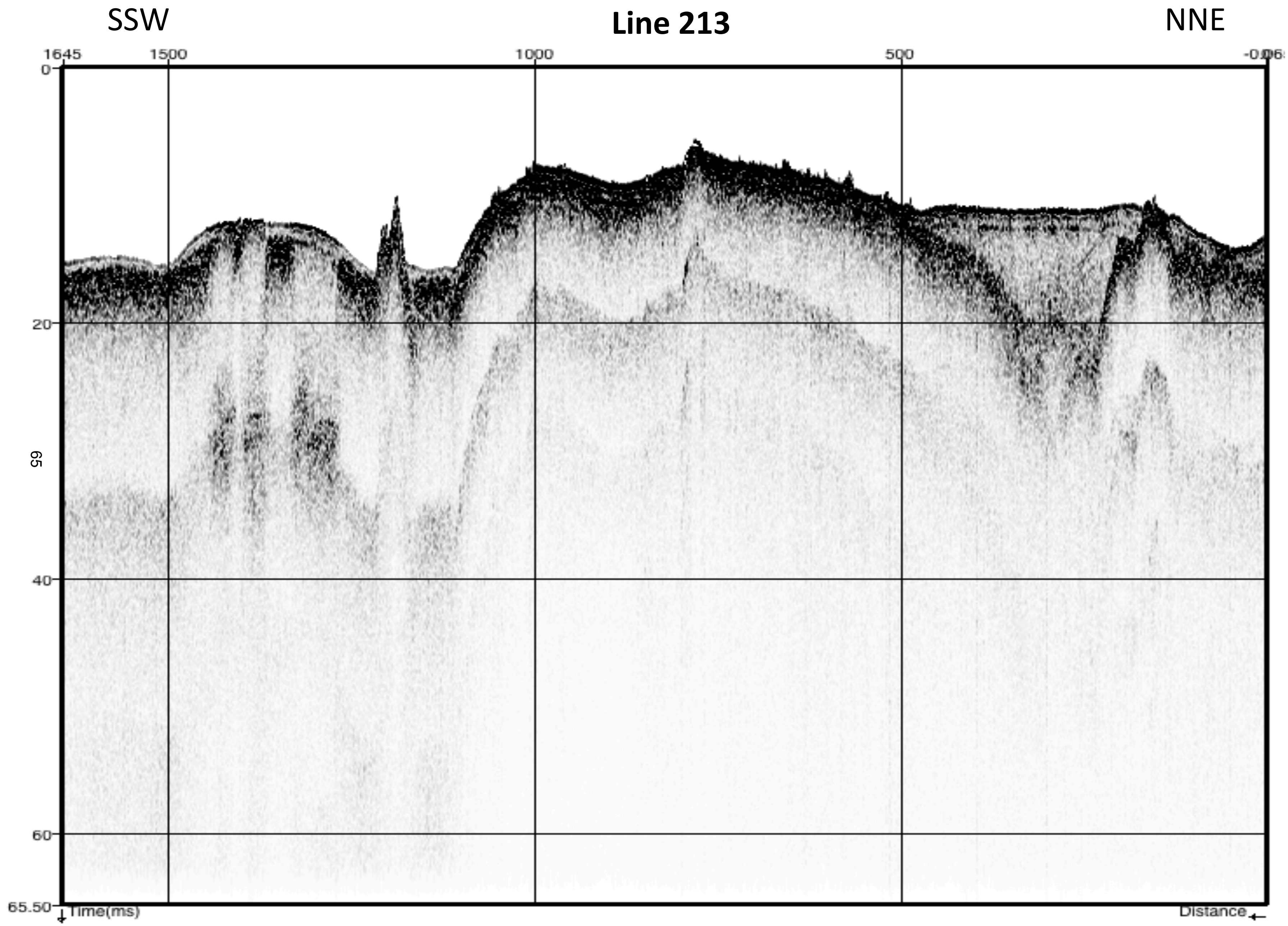

Line 214

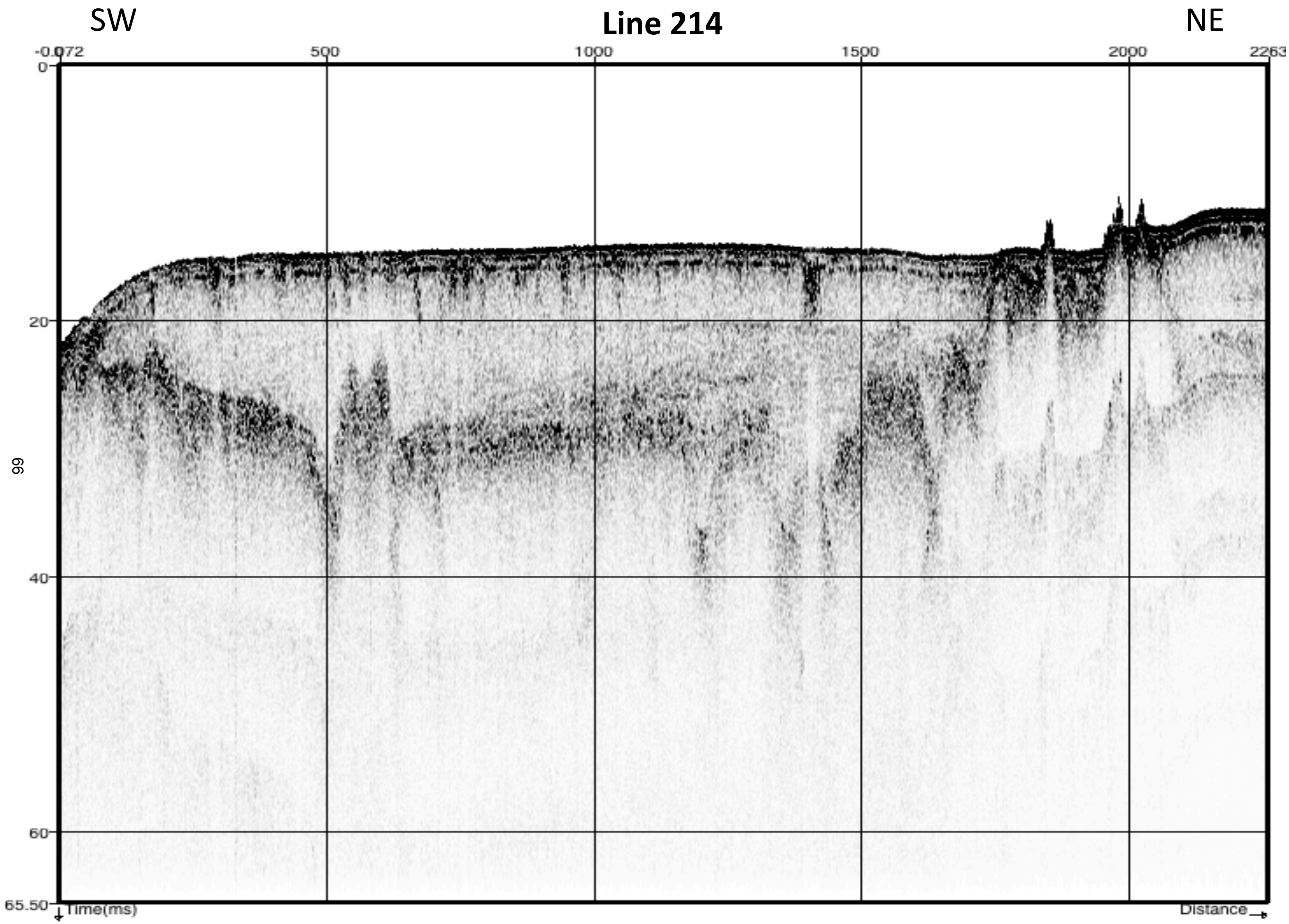

SW
NE
-0.072
500
1000
1500
2000
2263
0
20
40
60
65.50
Time(ms)
Distance

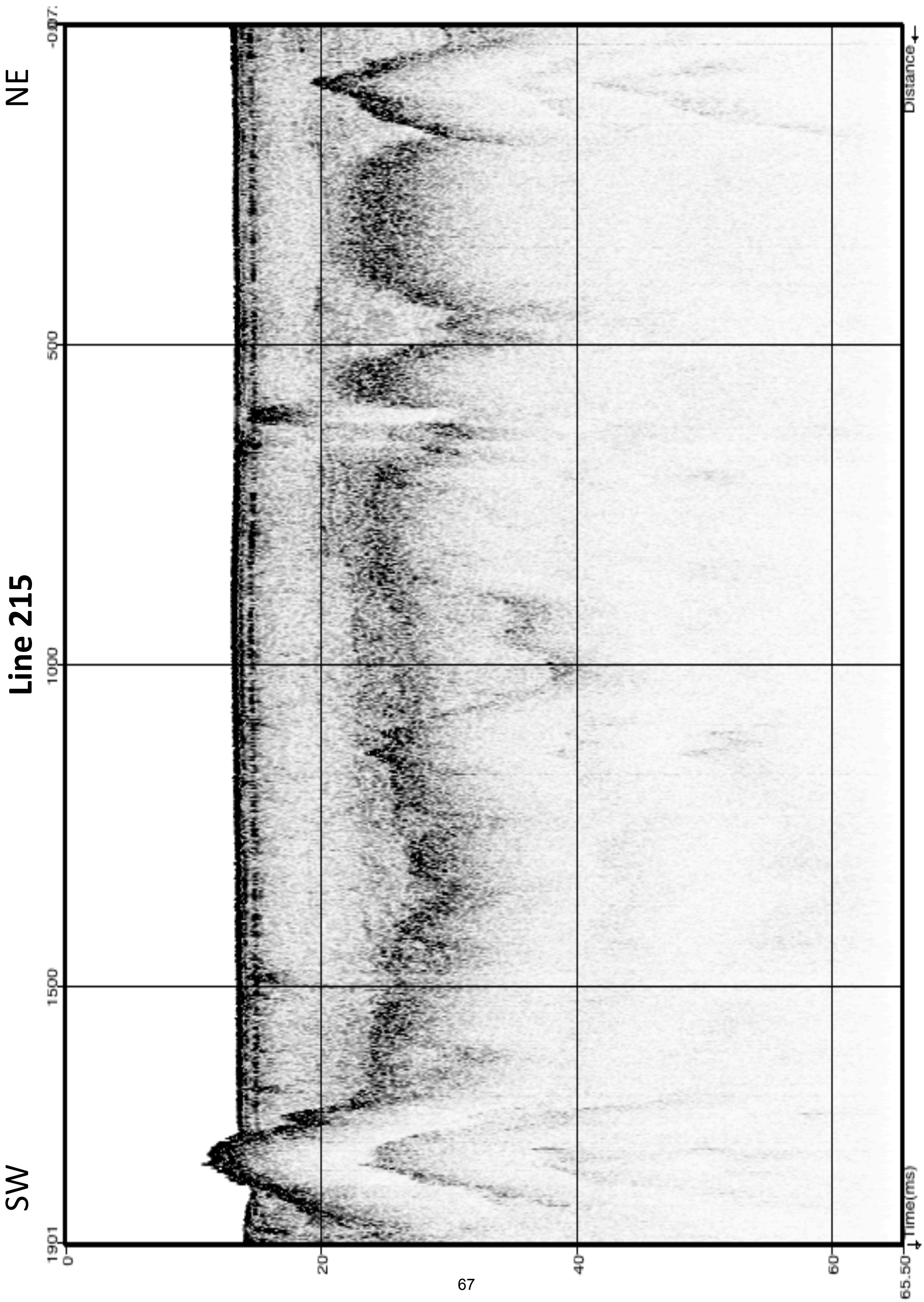
NE
Line 215
SW
Distance
Time(ms)
-0.07
500
1000
1500
1901
0
20
40
60
65.50

SW **Line 216** NE

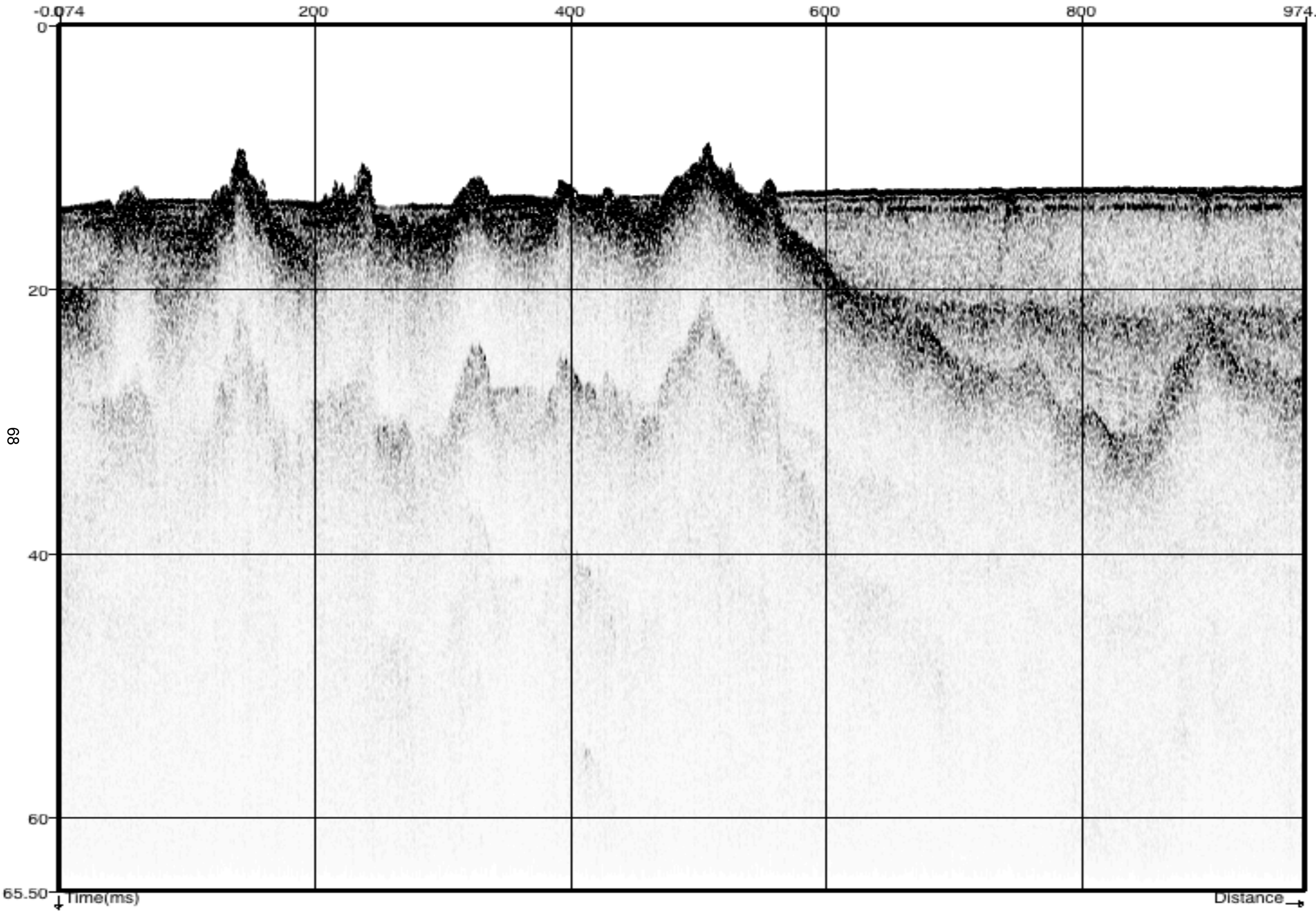

Line 217

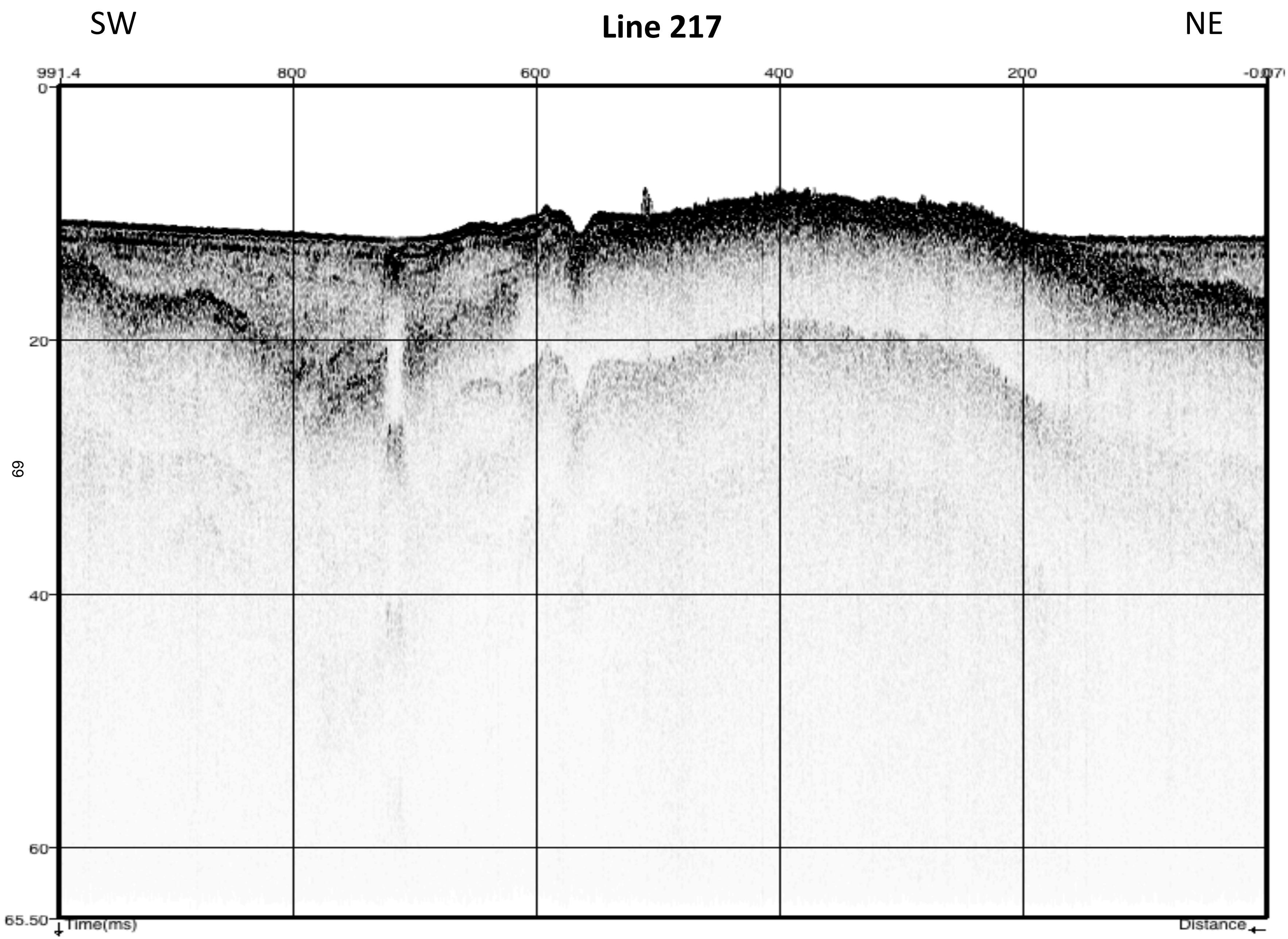

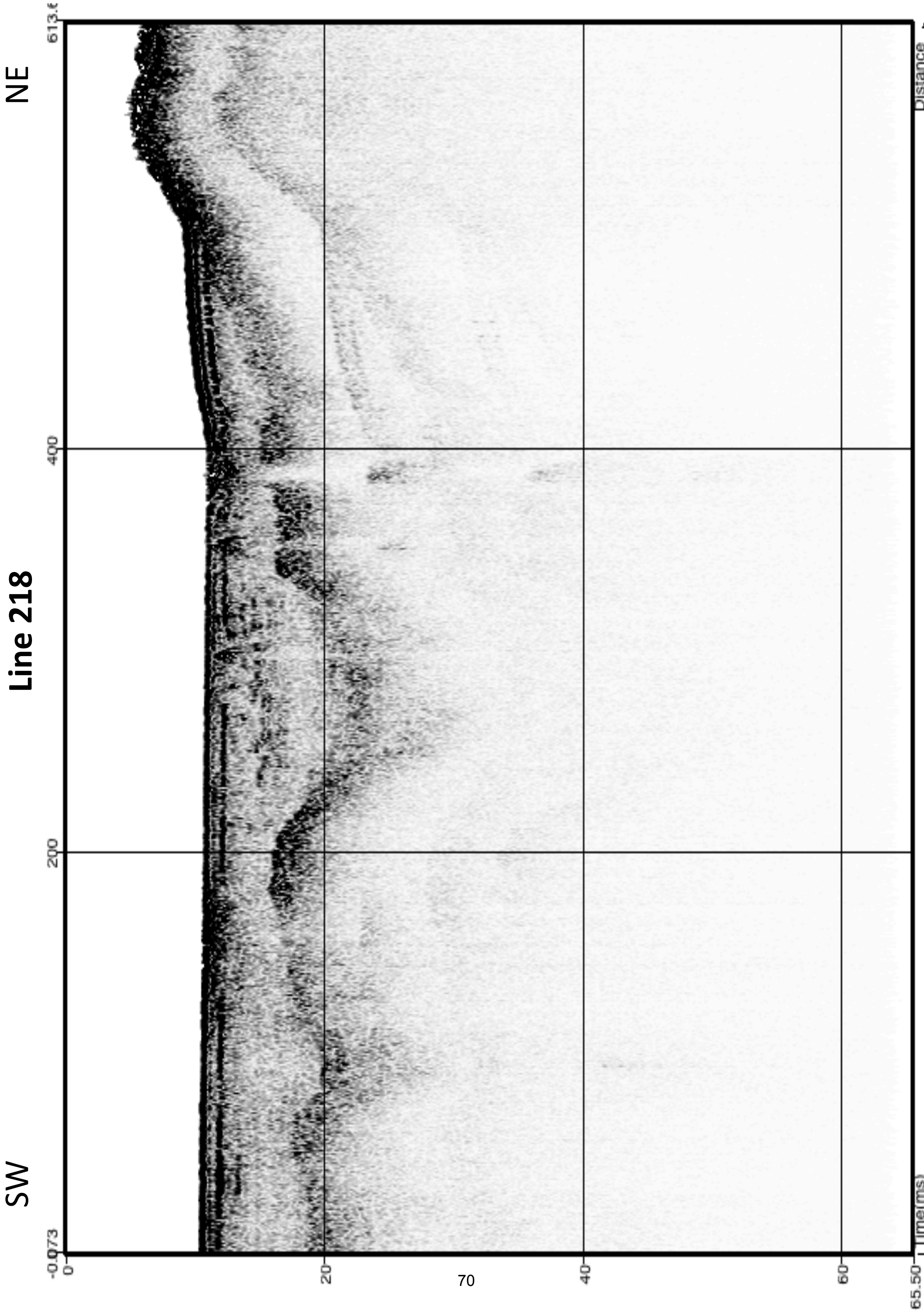
Line 218
SW
NE
Distance
Time(ms)
200
400
20
40
60
65.50

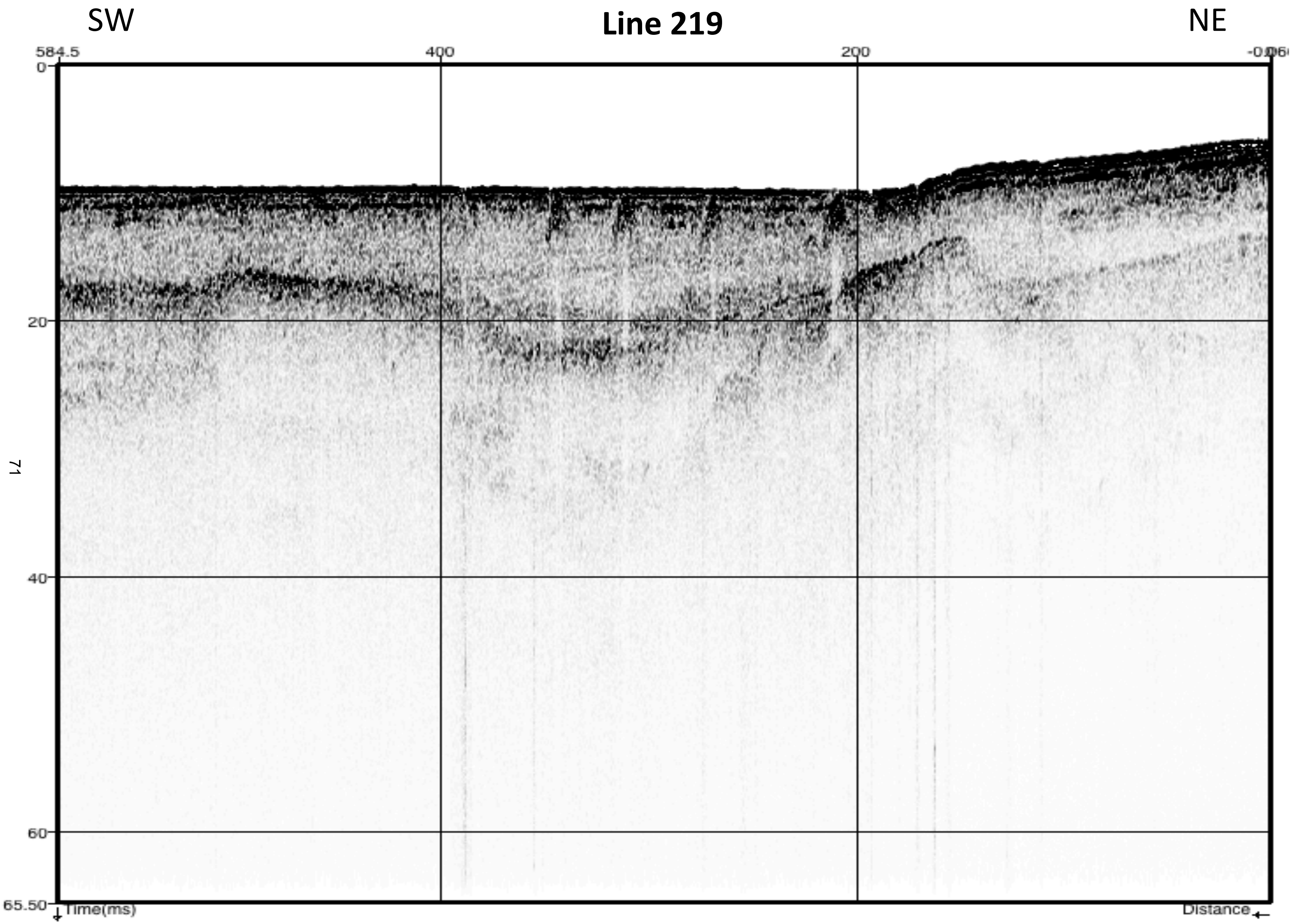
SW
Line 219
NE
584.5
400
200
-0.06
0
20
40
60
65.50
Time(ms)
Distance

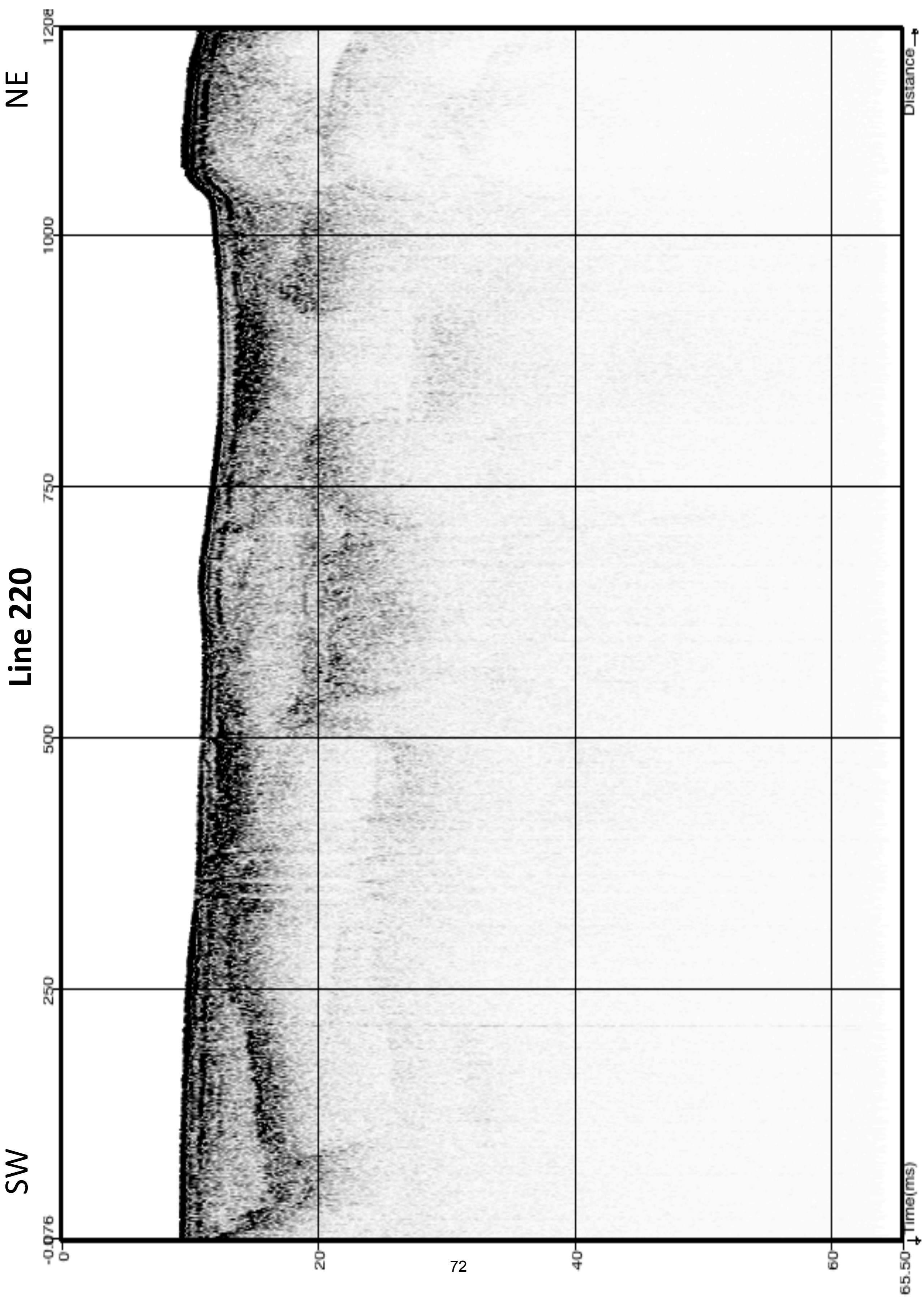
Line 220
SW
NE
Distance
Time(ms)
-0.076
250
500
750
1000
1208
0
20
40
60
65.50

Line 220b

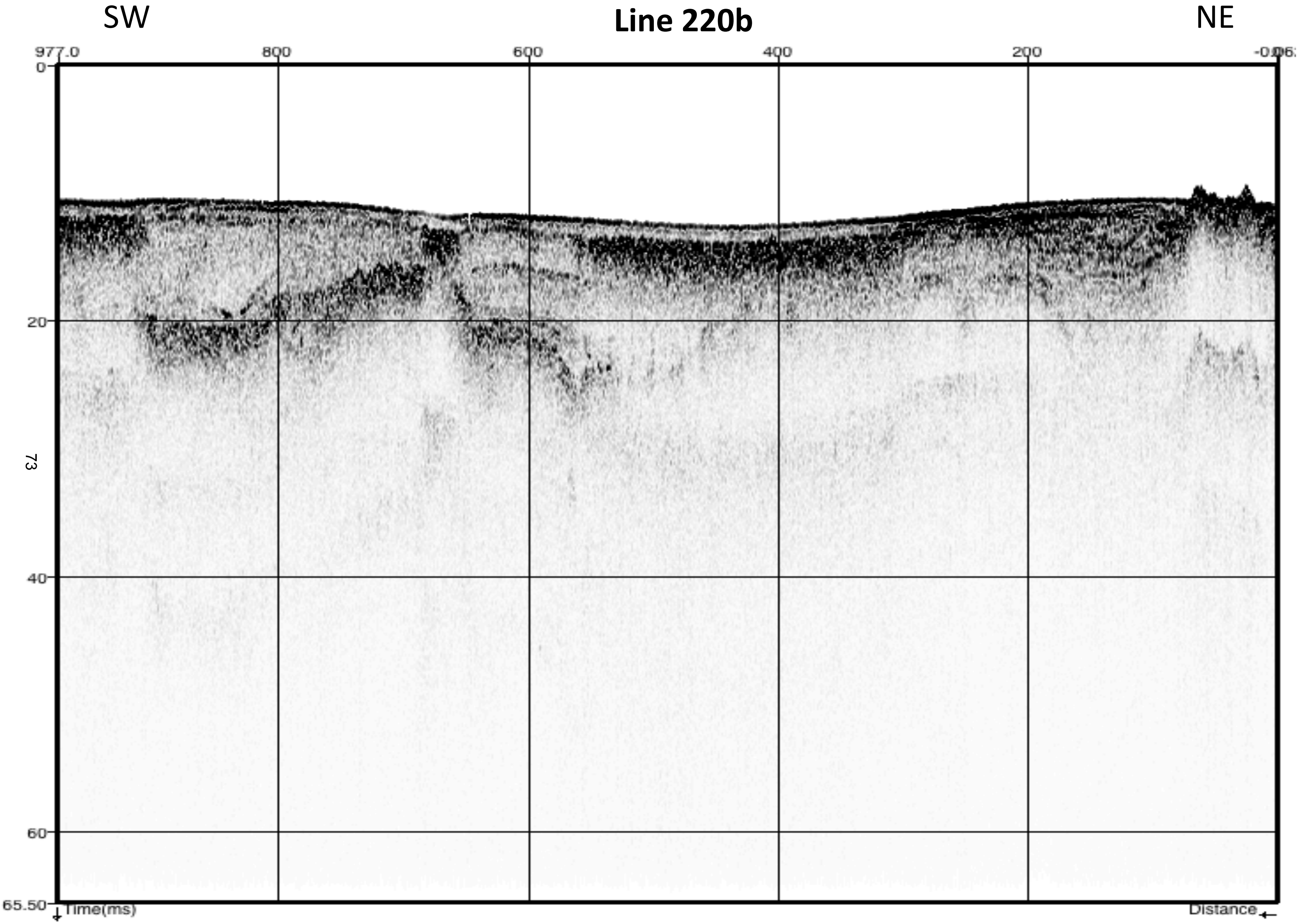

Line 221, tie line

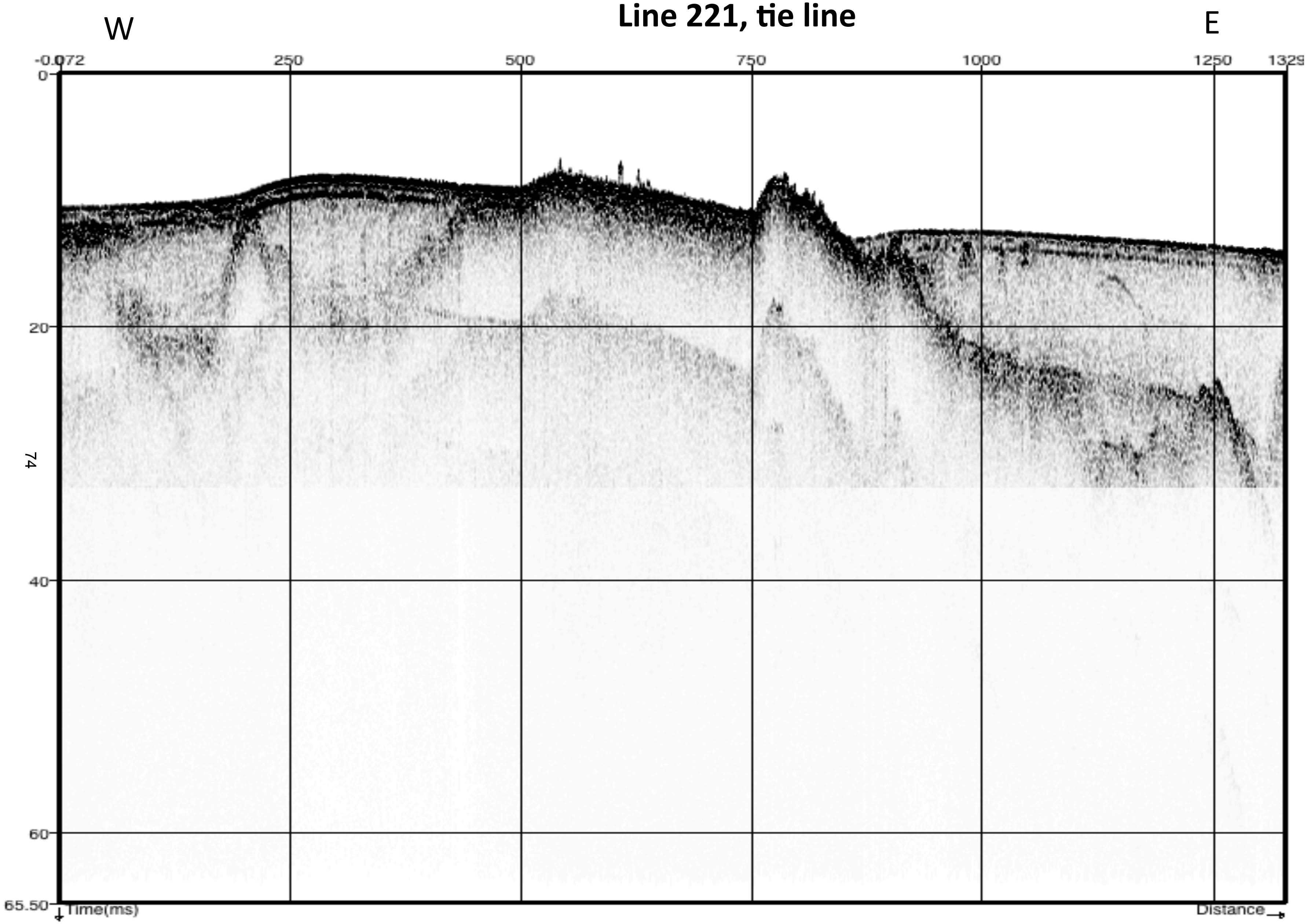

Line 222

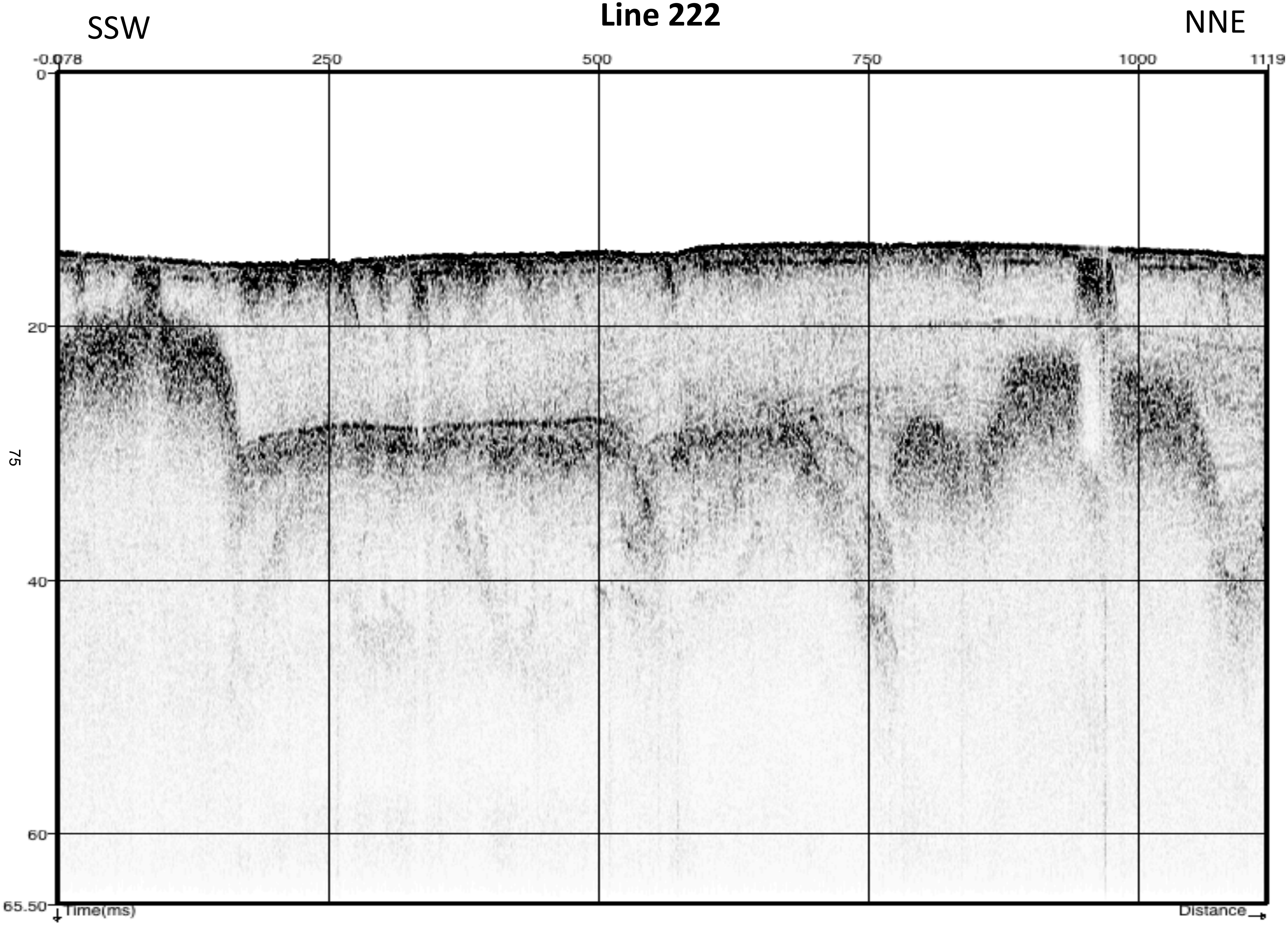
SSW
NNE
-0.078
250
500
750
1000
1119
0
20
40
60
65.50
Time(ms)
Distance

Line 223

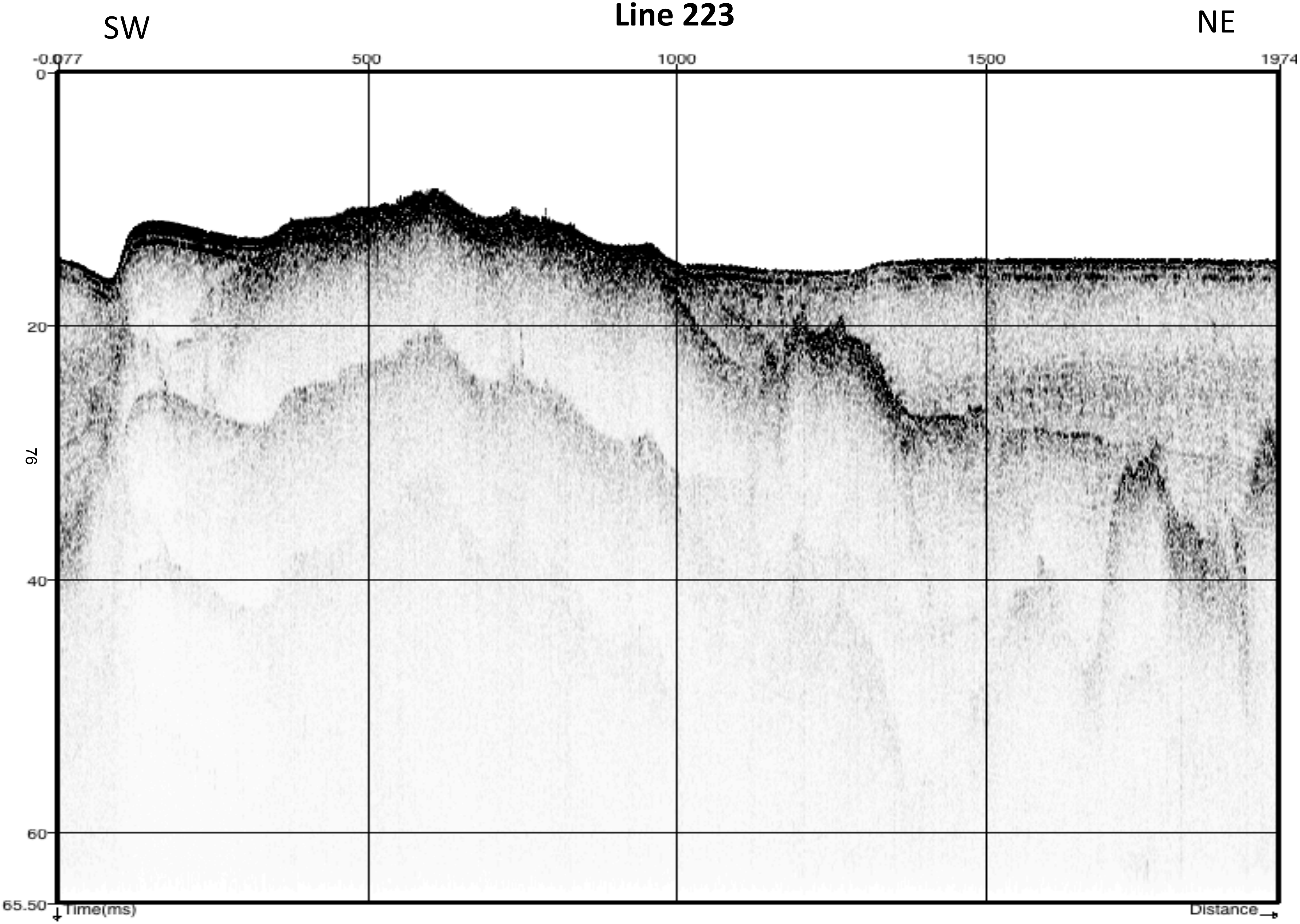

Line 224

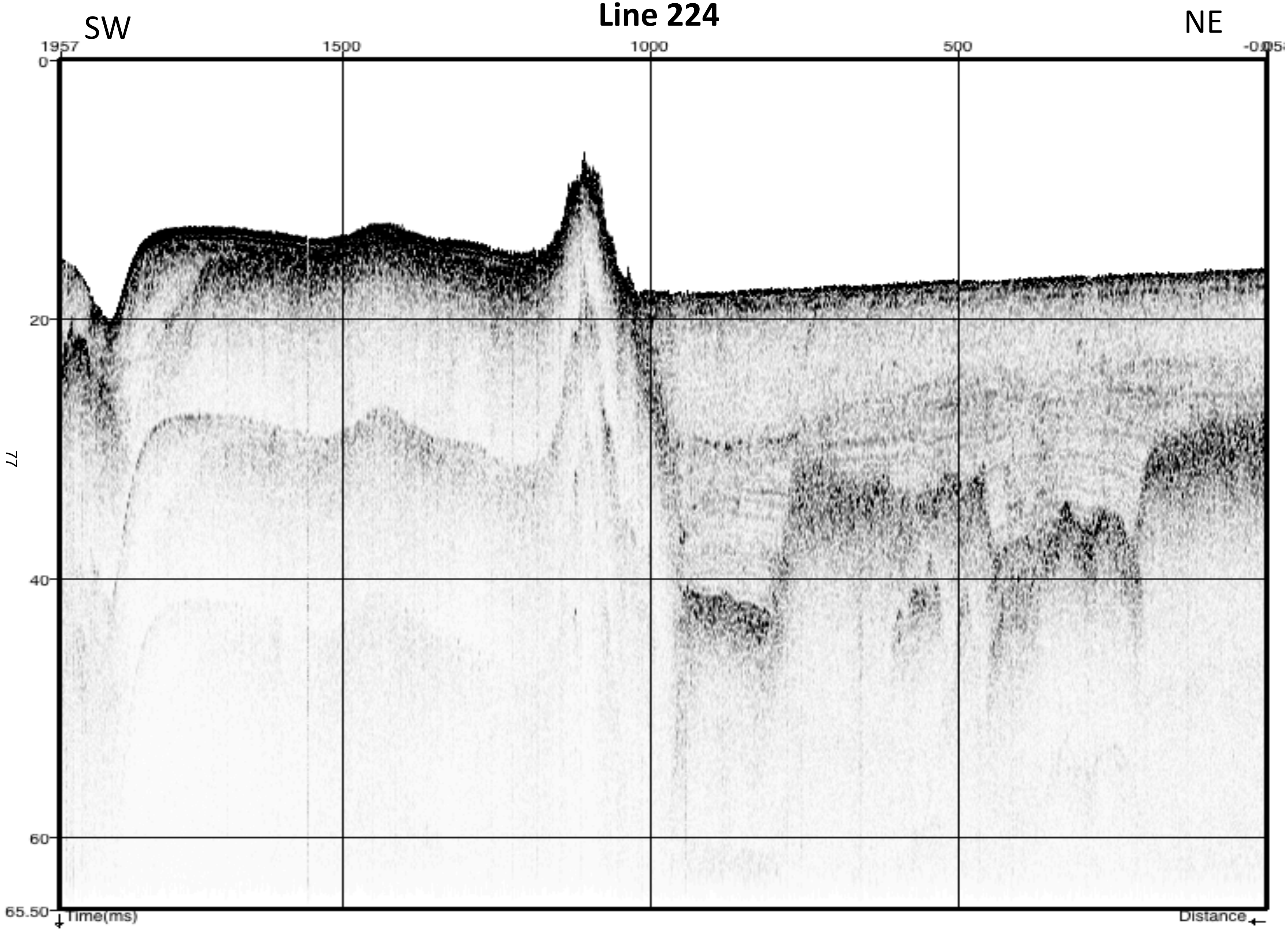

Line 225

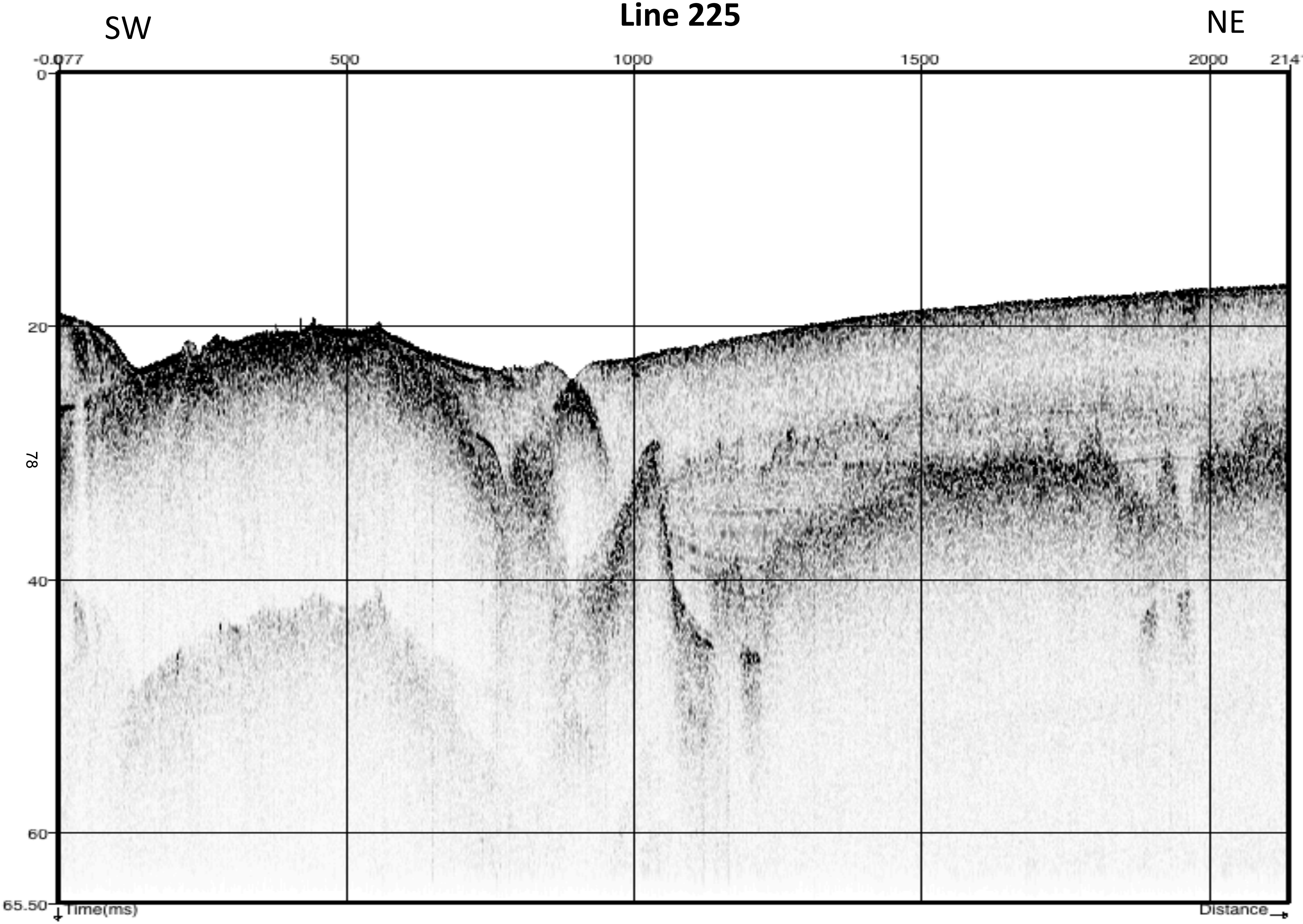

SW
NE
-0.077
500
1000
1500
2000
2141
0
20
40
60
65.50
Time(ms)
Distance